Rate Adaptation, Power Control, and Diversity Combining in Wireless Systems

Anders Milde Gjendemsjø

A Dissertation Submitted in Partial Fulfillment
of the Requirements for the Degree of

Philosophiae Doctor

Department of Electronics and Telecommunications
Norwegian University of Science and Technology

2007

Abstract

The present dissertation consists of a collection of six papers preceded by an introduction. The papers investigate the design and performance analysis of communication systems operating over wireless fading channels.

Wireless communication systems carry great expectations for future services. They are expected to give users both reliable high data rate transmission and the freedom of mobility. However, due to the limited available spectral resources and the random nature of the wireless channel, these systems also constitute formidable challenges to the designer. This thesis explores some modern analysis and design tools that can help overcome these challenges to meet the great expectations.

Specifically, the thesis is concerned with adaptive transmission schemes for both single link and multi-link communication systems. Key adaptive techniques investigated are those of: i) *Adaptive modulation*, increasing the spectral efficiency by adapting the signal constellation to the channel state, ii) *power control*, providing a flexible tool for exploiting the degrees of freedom offered by the wireless channel, e.g., by throughput enhancing power allocation for single-link transmission, or to provide battery savings at the mobile unit and interference management for multi-link scenarios, and iii) (adaptive) *diversity combining*, improving and stabilizing link quality by utilizing multiple independent signal paths for communication.

Preface

This dissertation is submitted in partial fulfilment of the requirements for the degree of Philosophiae Doctor (PhD) at the Department of Electronics and Telecommunications, Norwegian University of Science and Technology (NTNU). The studies have been carried out in the period from August 2004 to August 2007. The work includes the equivalent of half a year of full-time course studies and twelve months of teaching duties. The latter included being a teaching assistant in several graduate courses, as well as being an advisor for students working on their master theses or term projects. Also, I have been project leader for the NTNU Alumni project at the Department of Electronics and Telecommunications, in addition to vice-chairing the IEEE NTNU Student Branch. My advisors have been Prof. Geir E. Øien at the Department of Electronics and Telecommunications, NTNU, and Dr. Pål Orten at Thrane & Thrane Norge AS.

As a PhD student, I had the pleasure of two research stays abroad. First, from August to October 2005, I was part of the MAESTRO team headed by Dr. Phillipe Nain at the Institut National de Recherche en Informatique et en Automatique (INRIA), Sophia Antipolis, France. During the same period I also collaborated with Prof. David Gesbert at Institut Eurécom, Sophia Antipolis, France. Secondly, from April to May 2007, I visited the Laboratory for Advanced Wireless Communications Research headed by Prof. Hong-Chuan Yang, at the University of Victoria, Victoria, Canada.

The work included in this thesis has been funded in part by the Co-optimised Ubiquitous Broadband Access Networks (CUBAN) project under the IKT-2010 programme within the Research Council of Norway (NFR), and in part by the Department of Electronics and Telecommunications, NTNU; whereas the teaching assistantship has been funded by the Department of Electronics and Telecommunications, NTNU. The stay in France was funded by NTNU, TOTAL E&P Norway, and the EU FP6 Network of Excellence NEWCOM, while the stay in Canada was funded by the CUBAN project.

Acknowledgements

First of all I would like to thank Prof. Geir E. Øien for having been such an outstanding supervisor during the three years I have been working with this thesis. He is one of those few possessing the unbeatable combination of academic excellence and superior social skills, creating a fantastic environment for PhD students. The writing of this dissertation would certainly not have been possible without him.

Through Prof. Øien I was introduced to the world-class researchers Profs. Mohamed-Slim Alouini, David Gesbert, and Hong-Chuan Yang. With most of the papers included in this thesis benefiting from their excellent ideas and guidance, it is clear that I have gained immensely from the collaboration with them. For this I am very thankful. My co-supervisor Dr. Pål Orten is thanked for his excellent inputs during the work with this thesis.

I would also like to thank Dr. Phillipe Nain and Prof. Hong-Chuan Yang for allowing me to be part of their research group at INRIA and the University of Victoria, respectively. The stays abroad have been very fruitful both scientifically and socially.

I am grateful to have been part of the Signal Processing group at the Department of Electronics and Telecommunications, providing me with excellent colleagues and the not-to-be-missed events of wine-meetings, food-meetings, and the legendary Christmas party. From the group, I would like to thank fellow graduate students, Pål Anders "Bænditt" Floor, Dr. Sébastien de la Kethulle de Ryhove, Rodrigo de Miguel de Juan for both scientific discussions and social events, and Prof. Nils Holte for some very interesting lunch room discussions. Dr. Vegard Hassel is thanked for reviewing the introduction of this thesis, and for, together with his wife Tove Irene, creating a very nice household in 19, Rue de Rivoli during the autumn of 2005.

I would also like to express my gratitude to my parents Åse and Tom, for all their warm support, and always being there for me. Finally, I am enormously thankful to my wife Guri for all her love, support and patience. Together with our beautiful daughter Live, she means the world to me.

Bergen, October 2007
Anders Milde Gjendemsjø

Contents

Abbreviations

3G	3rd generation
3G-LTE	3rd generation - long term evolution
3GPP	3rd generation partnership project
ACK	Acknowledge character
ACM	Adaptive coded modulation
AMDC	Adaptive modulation and diversity combining
ARQ	Automatic repeat-request
ART	Average reliable throughput
ASE	Average spectral efficiency
AWGN	Additive white Gaussian noise
BER	Bit error rate
BES	Bandwidth-efficient AMDC scheme
BPC	Binary power control
BS	Base station
BW	Bandwidth
cdf	Cumulative distribution function
CDMA	Code division multiple access
CPU	Central processing unit
CSI	Channel state information
CSIR	CSI at the receiver

CSIT	CSI at the transmitter
dB	Decibel
DVB-S2	Digital video broadcasting - satellite version 2
FDMA	Frequency division multiple access
FEC	Forward error correction
GSC	Generalized selection combining
GP	1. Geometric programming 2. Geometric program
GSM	Global system for mobile communications
iid	Independent identically distributed
IEEE	Institute of Electrical and Electronics Engineers
IP	Internet protocol
LOS	Line of sight
MAC	Medium access control
MASA	Maximum average spectral efficiency for adaptive coded modulation
MRC	Maximum ratio combining
MS-GSC	Minimum selection - GSC
NACK	Negative acknowledge character
NP	Non-deterministic polynomial time
OFDM	Orthogonal frequency division multiplexing
OFDMA	Orthogonal frequency division multiple access
OPRA	Optimal power and rate adaptation
ORA	Optimal rate adaptation
pdf	Probability density function
PES	Processing-power efficient AMDC scheme
QAM	Quadrature amplitude modulation
QoS	Quality of service

RF	Radio frequency
SC	Selection combining
SE	Spectral efficiency
SNIR	Signal to noise and interference ratio
SNR	Signal to noise ratio
SP	1. Signomial programming 2. Signomial program
TDMA	Time division multiple access
UMTS	Universal mobile telecommunications system
UT	User terminal
WiMAX	Worldwide interoperability for microwave access

Part I

Introduction

Introduction[1]

The announced convergence between mobile and data access internet-based services, initiated in systems such as WiMAX [2; 3] and 3G-LTE [4], poses extraordinary challenges to the designers of future generation wireless networks who must cope with the scarcity of the spectral resource in areas with heavy user demand. It is widely admitted that, at the heart of this challenge, lies the ability to exploit the available resources as efficiently as possible in all dimensions allowed, e.g., time, frequencies, codes, power, and beams.

Traditionally, resource planning for wireless communication systems has been based on the philosophy of voice-centric networks. That is, a traditional design is aimed at allowing the users to operate under a common received signal quality level, compatible with the receiver's sensitivity or operating point. This point represents the level of signal quality needed to operate on the link, below which the call may be dropped, at the access points and the user terminals. Consequently, most communication control algorithms are designed to reach a link quality target simultaneously for all user terminals. This approach ensures a performance necessary for connection oriented voice calls [5–8].

The concept of a modem's operating point is however becoming by far less relevant in modern networks designed for data-dominated traffic, as these networks typically feature adaptive coding and modulation protocols capable of adjusting the transmission rate to a wide range of channel conditions. Even if the number of coding rates remains limited in practice due to memory and complexity constraints, the strategy of optimizing the spectral resource for a desired worst case scenario and relying on advanced modem design alone for optimizing performance under this channel state level, is losing some relevance. This in turn shows the limitation of the traditional approach when it comes to network wide optimization of performance. For best-effort data access (e.g., e-mail, web browsing, multimedia messaging) the *network capacity*, defined as the sum of simultaneous

[1]The first few paragraphs and Section 5 of this Introduction are in part based on [1].

transmit-receive link capacities, appears as a more meaningful metric, although additional constraints may be needed to include specific scenarios with quality of service (QoS)-driven traffic data (e.g., voice over IP) into the resource optimization problem.

Now, focusing on designing high-capacity wireless systems, be it a point-to-point or multiple-link system, an obvious question is at what maximum (sum) rate communication can occur, and information still be recovered with an arbitrary low probability of error. This maximum rate is known from information theory as the *channel capacity* [9], and the problem of deriving this capacity for various channels have received significant interest over the last 40-50 years; see e.g., [10] and the references therein. The knowledge of the theoretical capacity, i.e., the upper performance bounds, can be of great help during the design process. One major benefit is being able to give an upper bound on the achievable performance, yielding a benchmark against which the performance of a proposed system can be evaluated.

The upper bounds on the achievable network performance are derived with little or no concern for complexity and implementation issues. A classical example is Shannon's formula for the channel capacity of an additive white Gaussian noise (AWGN) channel under an average power constraint, which is derived assuming infinitely long codewords [11]. However, in practice theoretical constructions such as infinitely long codewords, zero delay, or perfect channel state information can not be applied, and then an interesting line of work is to do performance analysis under the constraint that one or more transmission system components can be realized in practice.

As an example, in resource allocation for wireless networks, certain quantities entering the problem may be continuous-valued, e.g., the transmit power levels [12; 13], or the beamforming coefficients if multiple antennas are used [14]. Then, a potentially interesting tool in modifying the system design consists of discretizing the optimization space so as to reduce the number of potential solutions to search over, and also to reduce the feedback rate needed to communicate overhead data between network nodes. In the case of power control, discretization can be carried out prior to optimization, as a way to greatly simplify the power level search procedure. Remarkably, as will be shown in this thesis, the discretization of power control, even to its extreme of binary on/off control, can be shown to yield optimal results in a number of cases. As such it constitutes a promising tool in designing future multi-link networks.

In most cases however, the promised theoretically optimal performance can not be achieved using practical techniques. The key question is then,

how much of the original performance can be achieved under a less complex system design. One illustration of this is using adaptive coded modulation over a single link channel, for which the channel capacity using continuous power control and infinitely many code rates under perfect channel state information was derived in the classic paper by Goldsmith and Varaiya [15]. This paper sparked a significant interest in the field of adaptive transmission techniques, and several authors have investigated the effect of relaxing idealized assumptions. One example is considering the impact of imperfect channel state information, e.g., obtained by means of channel prediction [16–18]. A large portion of this thesis is dedicated to performance analysis of wireless communication systems under one or more practical constraints, one particular example being pursuing the work of [15] by considering the impact of limiting the number of transmission rates to be finite.

The main theme of this thesis is adaptive techniques, collectively referred to as link adaptation and adaptive (dynamic) resource allocation, specifically those of adaptive modulation, dynamic power control and adaptive diversity combining. Based on a collection of six papers, in this thesis adaptive schemes for both single-link and multiple link-scenarios are proposed and analyzed. In the following, we will give a short introduction to link adaptation (and dynamic resource allocation), succeeded by a presentation of the underpinning ideas and techniques of which the papers in this thesis are based on. This is followed by a summary of the included papers and their contributions, and a brief description of three additional papers to which the author also contributed, but which are not formally included in this thesis. Finally, some suggestions for further research are given.

1 Link Adaptation

Link adaptation, where the basic idea is to track and take advantage of the time-varying characteristics of the wireless channel, is a promising design principle for achieving a high throughput in communication systems [19; 20]. Indeed, today adaptive schemes are already implemented in wireless systems such as Digital Video Broadcasting - Satellite Version 2 (DVB-S2) [21; 22].

According to the channel conditions, it is possible to vary e.g., the modulation constellation size and the channel coding scheme (rate), enabling a rate-adaptive transmission scheme termed *adaptive coded modulation* (ACM) [15; 23–26]. ACM schemes increase the *average spectral efficiency*

(ASE) measured in information bits/s/Hz, while still conserving link reliability, by transmitting with as high as possible information rate when the channel quality is good, and with lower rates as the channel quality is reduced. Furthermore, if the number of constellations are finite, additional throughput gains can be achieved by introducing power control [27].

Throughout this thesis we will frequently make the assumption that the wireless channel under consideration is a slowly-varying and frequency-flat fading channel. That is, the channel coherence time T_c is larger than the symbol duration time T_s, and the transmitted signal bandwidth is significantly smaller than the coherence bandwidth [28]. (This can also model e.g., an orthogonal frequency division multiplexing (OFDM) subchannel in a wideband system.) Under these assumptions we will find it convenient to use a block-fading channel model, where the fading is flat, constant on each block, and independent, identically distributed (iid) across blocks [29]. Then, the channel can subsequently be approximated by an AWGN channel within the length of a codeword [30; 31]. Hence, an adaptive system can be designed by using codes that guarantee desired QoS requirements (e.g., bit error rate) within a range of signal-to-noise-ratios (SNRs) on an AWGN channel. Based on a prediction of the channel, the highest spectral efficiency (SE) code satisfying the QoS constraints is always selected.

Equipped with N different signal constellations, adaptive modulation schemes are designed typically by partitioning the range $[0, \infty)$ of SNRs γ into $N+1$ nonoverlapping regions which are defined by the constellation switching thresholds $\{\gamma_{\mathrm{T}_n}\}_{n=1}^{N}$, as illustrated in Fig. 1[2]. Signal constellation n, with spectral efficiency R_n, is selected whenever γ is in the interval $[\gamma_{\mathrm{T}_n}, \gamma_{\mathrm{T}_{n+1}})$, where we have defined $\gamma_{\mathrm{T}_{N+1}} = \infty$ for convenience. When $\gamma \in [0, \gamma_{\mathrm{T}_1})$ no transmission occurs and the data are buffered.

Then, by defining P_n as the probability that constellation n is employed at any time, where $f_\gamma(\gamma)$ is the probability density function (pdf) of the SNR, the average spectral efficiency η of the adaptive modulation system is given as

$$\eta = \sum_{n=1}^{N} R_n P_n. \tag{1}$$

The average spectral efficiency (1) is a measure of the amount of information that can be transmitted over a given bandwidth for a specific system [32]. Given the fundamental issue of limited available frequency spectrum in wireless communications, and the ever-increasing demand for

[2]Note that γ is in linear scale.

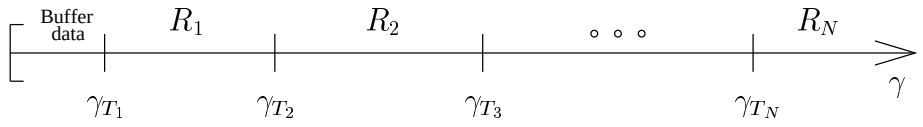

Figure 1: The range of γ is partitioned into SNR regions where the γ_{T_n}'s are the switching thresholds.

higher data rates, the ASE is an intuitively good performance criterion, as it measures how efficiently the spectrum is utilized.

Before we proceed, note that other partitions of the SNR range are also possible [33; 34], and in Paper B we compare two such partitions and the corresponding link adaptation strategies.

2 Diversity Combining

Uncertainty is a main characteristic of wireless communications, manifesting itself through randomness: the channel state is random, the number of users and their location are random, the interference from co-existing users and systems is random, and so on. Diversity is a vigorous technique that can, at relatively low cost, provide wireless link improvements by exploiting this random nature of the wireless communication system, by creating and utilizing independent or strongly uncorrelated signal paths for communication [28].

The promised gains of diversity can be explained as follows [35]: without diversity the system performance depends on the strength of a *single* signal path, and whenever this path exhibits a deep fade the system will suffer from poor performance. By facilitating information transmission over *multiple* independent signal paths, reliable communication can be established provided that *at least one* signal path is strong. Indeed, diversity can be defined as "the method of conveying information through multiple independent instantiations of the random signal attenuations" [36], and can significantly improve the performance in fading environments, by inherently stabilizing the quality of the wireless channel.

Diversity can be achieved in several ways, examples being

- *Time diversity*, obtained by averaging the fading state of the channel over time.
- *Frequency diversity*, in which carrier frequencies with a separation of one or more coherence bandwidths are used.
- *Space diversity*, by equipping the receiver with two or more antennas

sufficiently separated in space to experience independent fading, as depicted in Fig. 2

In this thesis we will be concerned with space diversity, and it is worth pointing out that this form of diversity can be realized without using extra bandwidth or transmit power [37]. Specifically, consider a generic receive diversity system with L available diversity branches, and denote by γ_l ($l = 1, 2, \cdots, L$) the SNR of the lth iid diversity branch. Then, the idea is to combine the different branches containing replicas of the same information-bearing signal to obtain a resultant signal for the demodulator. Combining the different branches can be done in many ways, three of which are briefly described below. As will be seen, the choice of a combining algorithm represents a complexity versus performance trade-off.

A well-known technique for reception diversity combining is *maximum ratio combining* (MRC), in which the combined signal is an optimally weighted sum of *all* the available branches, yielding a received SNR γ_{MRC} as the sum of the individual branch SNRs [38], i.e.,

$$\gamma_{\text{MRC}} = \sum_{l=1}^{L} \gamma_l. \tag{2}$$

MRC is the optimal combining technique in terms of maximum combined SNR, but also comes with the highest complexity, both in terms of the required channel state knowledge and in terms the number of active branches. Specifically, a separate receiver chain is needed for each available branch, adding to the overall receiver complexity.

As a complexity and performance counterpart to MRC, *selection combining* (SC) is a popular alternative due to its simplicity [39]. In SC, only one of the diversity branches needs to be processed, specifically the SC combiner chooses the branch with the highest SNR, i.e.,

$$\gamma_{\text{SC}} = \max_{1 \le l \le L} \gamma_l. \tag{3}$$

Selection combining avoids the need for multiple active receiver chains and the corresponding coherent summation of individual branches. In terms of SNR, it increases with L, but not linearly, as would be the case for MRC, assuming iid branches.

The complexity of MRC may be too high, whereas for the case of SC, the potential *diversity gain* G_{d} offered by the channel is not exploited fully, where G_{d} is defined as the slope of the error probability P_{e} versus SNR curve [38; 40]:

$$\lim_{\gamma \to \infty} \frac{\log P_{\text{e}}(\gamma)}{\log \gamma} = -G_{\text{d}}. \tag{4}$$

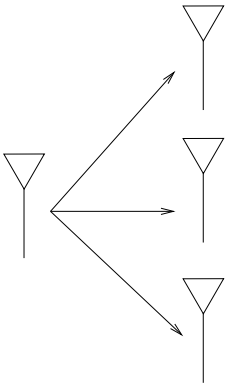

Figure 2: Receive diversity with $L = 3$ available branches.

As a tradeoff to bridge the gap between the two extremes, consider that due to hardware complexity and other relevant constraints, only L_c branches can be combined ($L_c \leq L$). With *generalized selection combining* (GSC), the receiver then applies MRC to the L_c strongest diversity paths of the total available ones, where L_c is usually much smaller than L [41; 42]. Denoting the L instantaneous branch SNRs in descending order as $\gamma_{1:L} > \gamma_{2:L} > \cdots > \gamma_{L:L}$, then GSC will combine the L_c best branches only, using MRC weights, yielding a combined SNR of

$$\gamma_{\text{GSC}} = \sum_{l=1}^{L_c} \gamma_{l:L}. \tag{5}$$

Since only L_c paths need to be processed in the fashion of MRC, GSC has a lower hardware complexity than traditional MRC. Associated with combining multiple branches is a *diminishing return* characteristic [43; 44], i.e., the largest improvement in combined SNR is obtained by going from one to two branches, while the gain decreases as the number of combined branches increases. From this perspective, the GSC approach of combining only the L_c best branches is intuitively satisfying. Additional benefits are increased robustness to channel estimation errors due to the fact that the weakest (and hence most exposed to estimation errors) SNR branches are omitted from the combining process [38].

3 Power Control

In wireless communication systems, power control is applied to dynamically adjust the transmitted power according to some chosen criterion. It

represents a flexible tool for exploiting the degrees of freedom offered by the wireless channel. There are a variety of motivations behind the use of power control, including maintaining communication quality in the presence of fading and user mobility [45; 7]. In CDMA systems it is typically used for the purpose of suppressing multiuser interference, e.g., to mitigate the "near-far problem" [46; 28]. Another reason for implementing power control is that of maximizing the spectral efficiency over a transmission link by allocating the power according to a waterfilling strategy [47; 48] (or similar), i.e., by using more power when the channel is good and less when the channel is bad.

Associated with power control are always one or more power constraints, the two most common being *average* and *peak* power constraints. Under an average power constraint $\overline{S}$, the average transmitted power is required to be below $\overline{S}$, i.e., typically the system adjusts its power level according to the channel state, with no constraint on instantaneous signal power, as long as the system, averaged over all time, does not transmit with a higher power than $\overline{S}$. Obviously, in many cases, it is however also important that the instantaneous transmit power be limited by a peak power constraint. Peak constraints could be imposed for several reasons:

- to control the power radiation to limit the interference to other users and systems.
- to control the emitted power to avoid harm to humans and animals.
- from a practical perspective, since many components in a communication system are peak power limited, e.g., the power amplifier [49].

Independent of whether an average or a peak power constraint is enforced, it also important to discuss constraints on the power adaptation flexibility. That is, how capable is the power control unit? Can it adjust the power on a continuous scale, over a set of discrete levels, or simply to a single non-zero transmit power level? In Fig. 3, we have illustrated these three different schemes. Using *continuous power* control (Fig. 3a) the system is able to fully track the channel state and thus has the largest potential for achieving the desired performance measure, be it maximizing the spectral efficiency or providing an identical signal quality to all the users in the system. However, continuous power control is not realistic as it would require an infinite capacity feedback channel. In addition, it is not likely that the transmitter is able to transmit at a very large (infinite) number of power levels. For practical scenarios the resolution of power control will be limited: as an example, for the Universal Mobile Telecommunications System (UMTS), power control step sizes on the order of 1 dB are proposed [50; 51].

Discrete-power schemes (Fig. 3b) solve these problems by using only a

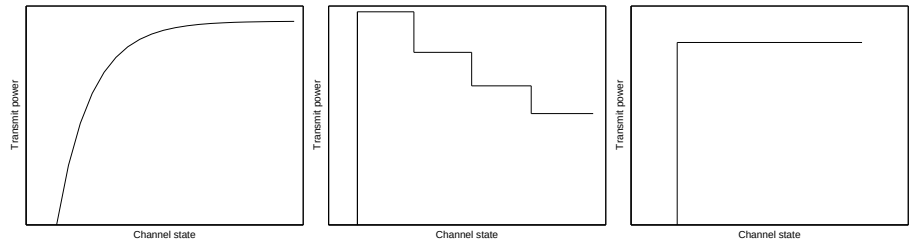

(a) Continuous (b) Discrete (c) Constant

Figure 3: Power control schemes

finite set of power levels, requiring less feedback. Finally, simplifying the power control even more, when only a single non-zero transmission power is used in addition to the zero level (Fig. 3c), we adopt the term *constant-power* transmission scheme[3] [52]. In this thesis, we shall consider both average and peak power constraints, and all the three power adaptation schemes.

4 Single Link Communications

Now, consider jointly applying the concepts of adaptive modulation and power control to single link communications. Common for both techniques is that they enable the transmitter to adapt to the channel state. Thus, in the design and analysis of such systems, a channel model is obviously needed. Therefore, before we proceed further, we take a small detour explaining some basic concepts of radio wave propagation.

In wireless communications, information is transmitted using modulation of electromagnetic waves. These waves propagate from the transmitter to the receiver following Maxwell's laws [28; 53]. In theory, the electromagnetic field equations, taking into account the physical parameters of the propagation space, could be solved to find the exact channel model. However, since these equations in general are very complicated and require a large number of parameters expressing the physical signal path obstructions, a common practice is to resort to statistical modelling of the channel.

The variation in signal power at the receiver can be attributed to three main factors: *path loss* caused by signal attenuation due to transmitter-receiver separation, *shadowing* caused by signal energy absorption in obstacles such as buildings, and finally, multipath *fading* which results in rapid

[3] Also termed *on-off* power transmission, see e.g., [19].

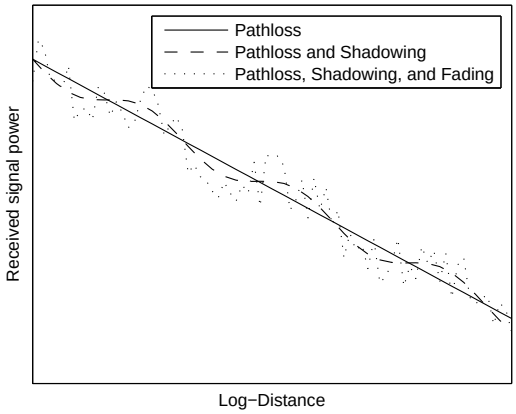

Figure 4: Variation of received signal power as a function of distance due to path loss, shadowing, and fading effects.

signal fluctuations, and is caused by constructive and destructive summation of multiple signal components, in turn causing random phase variations in the received signal. In Fig. 4, we have illustrated the combined impact of path loss, shadowing and multipath fading on the received signal power as a function of distance. As seen from the figure, path-loss and shadowing occur over large distances, and are referred to as large-scale propagation effects, while fading takes place over short distances and is termed small-scale propagation effects [37]. The channel state depends on all these signal attenuation factors. For most problems treated in this thesis however, the main effect considered is multipath fading, which we consider next.

There are various stochastic models used to describe the envelope of multipath fading depending on the scenario considered. A common model for scenarios without a direct line-of-sight component is the Rayleigh distribution, which is the distribution of the envelope of the complex sum of two quadrature Gaussian processes [28]. The distribution of the channel fading amplitude α is then described by the pdf

$$f(\alpha) = \frac{2\alpha}{\Omega} \exp\left(-\frac{\alpha^2}{\Omega}\right), \tag{6}$$

where $\Omega = E\{\alpha^2\}$ is the expected value of α^2.

In our performance analysis, we will find it convenient to work with the signal-to-noise ratio γ rather than the fading amplitude α. Thus we

follow [38], and define

$$\gamma = \alpha^2 \frac{E_s}{N_0}, \tag{7}$$

where E_s is the energy per symbol and N_0 is the one-sided power spectral density of the additive white Gaussian noise. Then, using the Rayleigh fading model, the SNR is exponentially distributed and given as

$$f(\gamma) = \frac{1}{\overline{\gamma}} \exp\left(-\frac{\gamma}{\overline{\gamma}}\right), \tag{8}$$

where $\overline{\gamma}$ is the average SNR. Throughout this thesis we will make extensive use of this distribution, both because it models well the multipath effect in urban areas, and because it in many cases allows for relatively easy mathematical manipulations.

Equipped with a statistical model of the channel, we can now return to adaptive modulation and power adaptation for single link communications. The average spectral efficiency from (1) can now be written as

$$\eta = \sum_{n=1}^{N} R_n P_n = \sum_{n=1}^{N} R_n \int_{\gamma_{T_n}}^{\gamma_{T_{n+1}}} f(\gamma)\, \mathrm{d}\gamma, \tag{9}$$

where given a power control function $S(\gamma)$, we can state the average power constraint as

$$E\{S(\gamma)\} = \int_0^\infty S(\gamma) f_\gamma(\gamma)\, \mathrm{d}\gamma \leq \overline{S}. \tag{10}$$

Though seemingly simple, (9) and (10) open up for a large number of interesting research questions, with a close link to practical applications. For example, i) what is the maximum achievable average spectral efficiency that can be obtained, under an average transmit power constraint, if we assume that capacity-achieving codes are available for any SNR, and ii) what is the corresponding optimal power control? These are among the questions we address in this thesis.

5 Multiple Link Communications

In a shared wireless environment concurrent transmissions may incur undesired interference to the transmitted signal, adding another dimension compared to the single-link problem, further increasing the challenge of creating a reliable high-performance communication system. Also, in the multi-link context the previously discussed techniques of adaptive modulation and power control can be applied, opening a door to multi-link

resource allocation. In this setting power control becomes particularly interesting, as it can be used both to aid battery savings and for interference management.

As already mentioned, traditional power control for wireless networks is primarily designed for voice traffic, and aims at providing a target signal-to-noise-and-interference level for all users [5; 6; 8]. In modern networks data traffic is however more dominating, and throughput maximization becomes a more relevant metric. The conventional approach for dealing with resource allocation over multiple links has been a divide and conquer one, as outlined in the following, where we, for the purpose of exposition, adopt a cellular network terminology:

Divide: First, network frequency (or, more generally, resource) planning is used to allow the fragmentation of the network area into smaller zones, isolated from each other from a radio point of view. Within a cluster of neighboring links, the spectral resource is not reused at all (such as e.g. in GSM [54]), or reused only partially (e.g. CDMA networks, where each cell limits the number of assigned codes to only a fraction of the theoretical limit defined by the spreading factor) [28]. In ad-hoc networks, isolation of transmit-receive pairs from each other is also sought, via an interference-avoidance medium access control (MAC), typically by means of carrier-sense based protocols [55; 56]. The need for high efficiency figures however leads the system designer towards a planning featuring even more aggressive spectral reuse, for instance in the cellular case from a cluster size of 5 to 7 in early GSM deployments, down to close to 1 in today's available networks such as WiMAX [2]. Power control techniques and per-cell dynamic resource allocation (e.g., frequency hopping) methods help alleviate the problem of out-of-cell interference, but in practice aggressive resource reuse will still inevitably lead to an increased level of interference in the network, which undermines the link-level performance.

Conquer: In turn this loss (due to interference) of link efficiency for a given cell or for a local transmit-receive pair may be compensated, via a careful design of the radio air interface. The latter may exploit advanced processing such as efficient forward error correction (FEC) coding [57], fast link adaptation protocols, multiple-antenna transceivers [37], and more recently channel aware scheduling techniques [58]. In the multiuser diversity approach, the scheduling protocol is designed towards a better utilization of the spectrum inside each cell, by encouraging channel access for data-access users temporarily experiencing better propagation conditions, giving rise to the socalled *multi-user diversity* gain [59]. It is worth noting that this gain can be realized only if link adaptation techniques are available to take advantage of the improvement in channel conditions. Clearly,

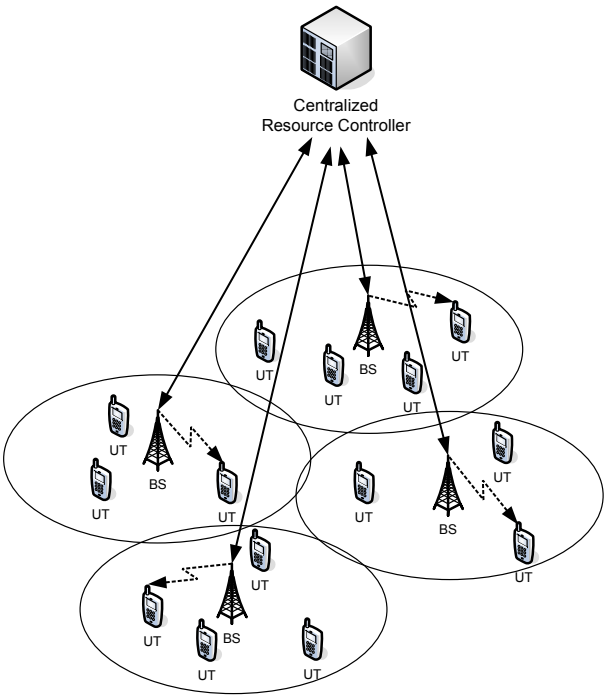

Figure 5: A multicell system, consisting of base stations (BS) and user terminals (UT), managed by a centralized resource controller. This controller processes all network information jointly.

multi-user diversity is also gained at the expense of (at least short term) throughput fairness, which may however be at least partially restored by modifying or constraining the scheduling criteria in one of several possible manners [60].

Instead of the traditional approach based on decoupling the multicell resource allocation from the optimization of the single cell capacity, one may naturally think that a joint optimization of resources in *all* cells simultaneously will give better system performance, as illustrated in Fig. 5 using a centralized controller. When doing so, the type of optimization proposed previously on a per-cell basis, involving e.g., code assignment, power control, multiple antenna beam design, is now expanded to take into account the dimension offered by the multiple links of the network.

Evidently, such a joint multicell resource allocation offers an enormous number of degrees of freedom (governed by the number of cells, times the number of users, times the number of possible scheduling slots, codes, power levels etc.) that can be exploited to optimize the network perfor-

mance at all times. As a key instance of such an optimization problem, we will in this thesis be considering the problem of joint power allocation over multiple cells, for the purpose of maximizing the sum network capacity under an ideal link adaptation protocol.

The potential in coordinated resource allocation across cells also comes with several practical challenges. This includes among other things, the need for slot level synchronization over large network areas. However, this problem may be partly alleviated by clustering the optimization. Other challenges are the increasing complexity of centralized resource allocation, i.e., the centralized controller in Fig. 5 has to search over a large feasible set spanned by the large number of degrees of freedom, and the overhead signalling incurred by traffic and channel quality parameters by all network nodes to a central unit. In this thesis, we contribute to this problem by demonstrating some promising methods for how multi-link coordination gains may be realized with limited complexity.

6 Practical Schemes

In 1965 Intel co-founder Gordon E. Moore forecasted that the number transistors on an integrated circuit for minimum component cost doubles every 24 months [61]. This has led the computer component industry to focus an immense energy towards the aim of achieving this specified increase in processing power, presuming it be possible. Since 1965, history has indeed shown the law to be largely true, as evidenced for example by the dramatic increase in CPU perfomance. However, for the mobile units we consider, there is a significant challenge in the fact that more transistors for the same price is great for computers, but terrible for batteries. Indeed, up to the present day, Moore's law has not at all been applicable to battery capacity. Hence, for battery powered mobile units it is of paramount importance to also focus on what is possible when the signal processing capabilities of the unit is limited. Thus, in the final parts of the thesis we try to combine the adaptive schemes of the earlier parts taking into account the specific challenges faced by limited battery and complexity constraints.

Facing implementation issues and restricted battery capacity, we turn our attention to the design of practical schemes and apply M-ary quadrature amplitude modulation (M-QAM) constellations, power control, and adaptive diversity techniques. In [27], adaptive modulation schemes using M-QAM constellations and power control are proposed. The schemes are designed with a bit error rate (BER) constraint in mind, and hence the constellations and power control are selected such that the system oper-

ates at a BER less than or equal to the constraint BER_0. In terms of power control, the main focus is on continuous power control; however for practical implementation this is not feasible due to hardware complexity and feedback load. Extending [27], in [45] a fully discrete-rate discrete-power adaptive M-QAM scheme is introduced, jointly optimizing the constellation switching thresholds and the discrete power levels, showing that a practical scheme can a achieve a good trade-off between spectral efficiency and feedback load.

Turning to diversity combining, we look for an adaptive approach that minimizes the processing power at the receiver, while still providing considerable performance improvements. In particular, an approach in which the receiver adaptively combines as many diversity paths *as necessary*, and no more, would be ideal. What is considered "necessary" will vary from application to application, as discussed below.

A power saving implementation of the generalized selection combining scheme termed *minimum selection* GSC (MS-GSC) was recently proposed by Kim et al. [62]. With MS-GSC, the receiver combines the least number of best diversity paths such that the *combined* SNR is above a certain threshold. Thus, while requiring the same hardware complexity as a conventional GSC scheme, MS-GSC can save considerable amount of processing power by keeping less MRC branches active on average [63]. Mathematically speaking, given a threshold γ_{T}, and MS-GSC receiver combines the minimum number of branches $L' \in \{1, 2, \ldots, L_{\text{c}}\}$, such that the condition

$$\gamma_{\text{MS-GSC}} = \sum_{l=1}^{L'} \gamma_{l:L} \geq \gamma_{\text{T}}, \tag{11}$$

is satisfied [63], where, as before, $L_{\text{c}} \leq L$ is the maximum number of combined branches, and $\gamma_{l:L}$ is an ordered SNR.

Then, in a very recent contribution, Yang et al. pointed out that both the adaptive modulation and adaptive diversity combining concepts are based on using predetermined thresholds in their operations. Following this observation, the two techniques can be jointly designed and analyzed [64]. Specifically, employing constant power transmission with M-QAM constellations and MS-GSC diversity combining, [64] introduces joint adaptive modulation and diversity combining schemes. The underlying idea is to adapt both the combiner structure and constellation based on the channel state and the bit error rate constraint.

By using the adaptive modulation switching thresholds as inputs to the MS-GSC combiner, the system can be designed according to different objectives. For example, by using the lowest constellation threshold γ_{T_1} as

γ_T in (11) we obtain a system that tries to combine the minimum number of branches needed to achieve the smallest signal constellation. I.e., the main purpose of design is the receiver processing power measured by the number of combined branches. The combining of branches yields discrete steps in SNR when the number of branches increases. Hence, the combiner might, at a given instance, provide a non-zero SNR margin such that the system are able to support a higher constellation than the smallest. Thus, this scheme will still benefit from the availability of higher rates should the channel be in a good enough state.

Another obvious candidate for the MS-GSC threshold is the minimum SNR required for the highest constellation, that is letting $\gamma_T = \gamma_{T_N}$ in (11). Then, an average spectral efficiency maximizing scheme is obtained, while still achieving a lower average number of combined branches compared to GSC or MRC.

Now, some questions naturally arise. For example, what is the effect of power control in the framework of joint adaptive modulation and diversity combining? And perhaps more interesting, how can this framework be extended to the case of multiple interfering links? In this dissertation we address these questions, and more.

7 Overview of the Included Papers

This thesis consists of six papers, which are numbered by the capital letters A to F. Below, a short summary of the included papers is given.

Paper A

Anders Gjendemsjø, Geir E. Øien, Henrik Holm, Mohamed-Slim Alouini, David Gesbert, Kjell J. Hole, and Pål Orten, "Capacity-Optimal Rate and Power Allocation for Discrete-Rate Link Adaptation," revised for possible publication in the *EURASIP Journal on Wireless Communications and Networking*, October 2007.

The results are also partially published in *Proc. IEEE Global Communications Conference (GLOBECOM'05)*, St. Louis, MO, USA, Nov.-Dec. 2005, and in *Proc. IEEE International Conference on Communications (ICC'06)*, Istanbul, Turkey, June 2006.

In Paper A, link adaptation schemes with a finite number of transmission rates are studied. Using the zero information outage approach of buffering data at poor channel state levels, and assuming that the wireless channel can be approximated by an AWGN channel within the length of a codeword, constant, discrete and, continuous-power adaptation schemes are proposed. Employing the average spectral efficiency as a measure of system performance, as described in Section 1, and enforcing an average transmit power constraint, the rate switching thresholds and power adaptation policies are optimized for a given fading distribution. The constrained optimization problems are simplified using classical results on waterfilling [9].

The main contribution of this paper consists of deriving optimal power allocation policies for adaptive transmission systems equipped with only a finite number of transmission rates. Through numerical results it is shown that the proposed schemes can achieve a throughput performance approaching the theoretical upper bound of continuous-rate and continuous-power bound, denoted C_{OPRA}, on spectral efficiency [15] using only a small number of codes. Specifically, using a fully discrete scheme with just four codes, each associated with four power levels, a spectral efficiency within 1 dB of C_{OPRA} can be achieved.

Paper B

Anders Gjendemsjø, Sébastien de la Kethulle de Ryhove, and Geir E. Øien, "A Cross-Layer Comparison of Two Design Philosophies for Discrete-Rate

Adaptive Transmission," submitted for possible publication in *Proc. IEEE Wireless Communications and Networking Conference (WCNC'08)*, Las Vegas, NV, USA, March-April 2008.

As mentioned in Section 1, in the literature at least two different approaches to the design of throughput maximizing adaptive transmission systems can be identified [15; 27; 23; 24; 26; 33; 25; 34].

In the framework of slowly-varying flat-fading wireless channels, we analyze two such approaches using a finite number of transmission rates and power levels, under an average power constraint. The contrasted methods are the maximum average spectral efficiency for adaptive coded modulation (MASA) scheme, and the average reliable throughput (ART) maximizing scheme. Both schemes utilize capacity-achieving codes for AWGN channels, and one power level per code. However, the schemes differ in their design objectives, and how they deal with information outage. The MASA scheme maximizes the ASE, given a fixed and finite number (N) of *available rates*, and by design has zero outage. On the other hand, the ART scheme starts from a fixed and finite number (L) of *available SNR quantization regions*, and then maximizes the ASE. As opposed to MASA, the ART approach thus allows for a non-zero information outage. To facilitate reliable communications, we extend the traditional ART scheme in a cross layer fashion, to include a retransmission option.

A main contribution of Paper B is to provide a rigorous comparison of two widely used design approaches, and through this comparison challenge some previous conclusions on the relative performance of these schemes. The claim that the "artificial constraint of zero outage leads to a big performance penalty" [33] is shown to be debatable. In particular, the results of Paper B discover scenarios where the MASA scheme offers *both* the highest spectral efficiency and the lowest feedback load (in terms of feedback source entropy).

Paper C

Anders Gjendemsjø, Hong-Chuan Yang, Mohamed-Slim Alouini, and Geir E. Øien, "Joint Adaptive Transmission and Combining with Optimized Rate and Power Allocation", in *Proc. IEEE International Workshop on Signal Processing Advances for Wireless Communications (SPAWC'06)*, Cannes, France, July 2006.

In this paper we combine the framework developed in Paper A with the framework of diversity combining. Specifically, we consider a system operating over a flat-fading slowly-varying wireless channel, using a fi-

nite number of capacity-achieving channel codes and discrete-level power control. Further, the receiver is assumed to be equipped with a diversity combining capability.

Capitalizing on previous results on both generalized selection combining (GSC) and minimum selection GSC, as discussed in Sections 2 and 6, we tackle the problem of maximizing the average spectral efficiency by finding optimal transmission rates and power control schemes for adaptive diversity combining over Rayleigh fading channels. The results obtained show that contrary to previous work on power control for discrete rate link adaptation, when jointly optimized with adaptive combining, power control does not significantly increase the average spectral efficiency. However, it does significantly decrease the probability of no transmission (due to increased diversity order), which is important for applications with real-time or low-latency requirements.

Paper D

Anders Gjendemsjø, David Gesbert, Geir E. Øien and Saad G. Kiani, "Binary Power Control for Sum Rate Maximization over Multiple Interfering Links," to appear in the *IEEE Transactions on Wireless Communications*.

The results are also partially published in *Proc. International Symposium on Modeling and Optimization in Mobile, Ad Hoc and Wireless Networks (WiOpt'06)*, Boston, MA, USA, April 2006, and in *Proc. IEEE International Workshop on Signal Processing Advances for Wireless Communications (SPAWC'07)*, Helsinki, Finland, June 2007.

In Paper D we leave point-to-point communications and turn to the analysis of multi-link systems, as introduced in Section 5. The application we have in mind is a wireless data network with best-effort type of quality of service, and the total aggregate throughput (sum rate) across the network is the figure of merit. The system is assumed to be enabled with a perfect link adaptation protocol, so the user rate is adapted instantaneously as a function of the user's signal to noise and interference ratio. We consider a wireless network featuring a number of transmitters and receivers, of which there are N active pairs selected for transmission by a scheduling (MAC) protocol. Allowing for centralized control, our aim is to investigate transmit power allocation under full frequency reuse.

The main contribution of this paper lies in deriving simple power allocation schemes. In particular, under short term minimum and maximum power constraints, we show that in the two-link case, the optimal power allocation then has a remarkably simple nature termed *binary* power control: Depending on the noise and channel gains, assign full power to one link

and minimum to the other, or full power on both. Further, when the sum network throughput can be approximated either by a geometric-arithmetic means inequality or by a low signal-to-noise-and-interference ratio (SNIR) assumption, the optimality of binary power control is established. In the general case when $N > 2$, it is demonstrated by extensive computer simulations that a restriction to binary power levels yields only a negligible capacity loss. Discretizing the optimization space to binary values is highly beneficial: the feedback rate needed to communicate between network nodes is reduced and the transmitter design is simplified.

To reduce the complexity of exhaustively searching for the optimal binary power allocation for large networks, simple algorithms based on clustering and greedy approaches are derived, and shown to achieve up to 99% of the capacity promised by an exhaustive search. Finally, limiting the potential solutions to search over better facilitates distributed resource allocation, and the results in this paper have been used to approach this problem in [65; 66].

Paper E

Anders Gjendemsjø, Hong-Chuan Yang, Geir E. Øien, and Mohamed-Slim Alouini, "Joint Adaptive Modulation and Diversity Combining with Downlink Power Control," to appear in the *IEEE Transactions on Vehicular Technology*.

The results are also partially published in *Proc. IEEE Wireless Communications and Networking Conference (WCNC'07)*, Hong Kong, China, March 2007.

We consider the problem of finding practical low-complexity, bandwidth-efficient, and processing-power efficient transmission schemes for a downlink scenario under the framework of diversity combining.

Specifically, following the discussion of Section 6, we consider joint adaptive modulation, using practical M-QAM constellations, and MS-GSC diversity combining for downlink transmission, where it is of interest to have low processing costs at the battery powered mobile unit (hence, to combine the fewest number of branches). Additionally, reducing the transmitted power from the base stations is beneficial, as this will introduce less interference to other users and systems. Depending on the key purpose of the design, we arrive at either a processing-power efficient or a bandwidth-efficient scheme.

Based on a rigorous mathematical analysis the statistics of the combined SNR after power control are derived, and both schemes are evaluated in terms of spectral efficiency, combiner complexity and bit error rate. For

both the processing-power and bandwidth efficient schemes, a reduction of transmitted power on the order of $30-50\%$ is feasible over a large SNR range, thus significantly decreasing the level of interference to co-existing systems/users, making them ideal in a multi-link scenario, while upholding high spectral efficiency, maintaining low diversity combining complexity, and satisfying the BER constraints.

Paper F

Anders Gjendemsjø, Hong-Chuan Yang, Mohamed-Slim Alouini, and Geir E. Øien, "Joint Adaptive Modulation, Diversity Combining, and Power Control in Two-cell Wireless Networks," under revision for possible publication in the *IEEE Transactions on Wireless Communications*.

The paper will be presented in part at the IEEE International Symposium on Wireless Communication Systems (ISWCS'07), Trondheim, Norway, October 2007, and at the Asilomar Conference on Signals, Systems, and Computers (Asilomar '07), Pacific Grove, CA, USA, November 2007.

In Paper F, we extend the framework of Paper E to perform the joint application of a centralized power control, adaptive modulation, and diversity combining in a two-cell wireless network, by explicitly taking interference into account. The goal is to derive practical low-complexity, bandwidth-efficient, and battery-power-efficient transmission schemes addressing the challenges of uplink and downlink transmission in a multi-link scenario.

To address the particular challenges faced in up- and downlink transmission, this paper contributes by proposing and analyzing two different practical adaptive modulation and diversity combining schemes targeted at two-cell networks. In this scenario, coordinated transmit power levels are used to i) reduce the transmitted power to extend the battery lifetime of the mobile user (uplink), ii) increase the spectral efficiency (downlink), and iii) minimize the interference to co-existing systems and cells.

It is observed in this paper that there is a tradeoff between the combiner complexity, transmit power, and spectral efficiency. Comparing to selected reference schemes, we demonstrate that the novel uplink scheme yields a significant reduction in average transmit power, thus extending the battery lifetime, and decreasing the level of interference to co-existing systems and cells, while upholding spectral efficiency. Taking into account the power consumption from diversity combining, the proposed downlink transmission scheme uses power control to provide a significant increase of spectral efficiency compared to a reference scheme, while achieving a low combiner complexity. For systems of more than two cells, we can apply the results

presented in this paper by clustering groups of two cells, over which optimization would be effected.

8 Suggestions for Further Research

In the following list, we briefly discuss some ideas for further research that might be of interest.

- Consider the application of a finite number of capacity-achieving codes in an uplink transmission scenario, where transmit power is limited. Further, assume diversity combining at the receiver, then an interesting problem would be to investigate policies minimizing the average transmit power, subject to an average rate constraint. Perhaps it is possible to exploit some results from Papers A and C in terms of duality?
- Paper D identifies several scenarios for which the optimal power control for sum throughput maximization in a multi-link system is *binary*. I.e., in these scenarios, under minimum and peak short term power constraints, each transmitter can without loss of optimality restrict the transmit power level to be either the minimum or maximum allowed. It is interesting to note that the optimality of binary adaptation also surfaces in other scenarios, e.g., in power allocation for relay channels [67], in the uplink of single-cell systems [68], and for QoS-constrained CDMA systems [69]. It would be very interesting to understand better *why* binary power control performs so well, and ideally identify a general framework for which the optimality of binary power allocation can be shown. The work of Prof. Holger Boche on general interference functions seems interesting in this respect [70–72].
- In Papers D and F a *centralized* power control is used for interference management in multi-link systems. An interesting direction of research would be to search for distributed algorithms realizing some or all of the coordination gains without the need for centralized control. A potential application of distributed versions of the schemes presented in Papers D and F (with suitable additional constraints) would be in cognitive radio [73; 74].
- In the system model used for both Papers D and F it is assumed that the receivers are *not* equipped with an interference cancellation mechanism [75], and hence the interference is treated as noise. Investigating the effect of (partial) interference cancellation for the problems considered in Papers D and F could be a topic for future work.

Introducing a cancellation ability is expected to increase the overall system capacity at the cost of increased complexity, and the corresponding trade-off between performance improvements and complexity could also by analyzed.

- The adaptive power algorithms presented in this thesis assume that the radio frequency (RF) power amplifier is operated in the linear region, implying a higher power consumption. For devices with limited battery capacity it is apparent that there will be a tradeoff between efficiency and linearity. This can be a topic for further research.

9 Papers Not Included in the Thesis

In addition to the Papers A-F, the author has participated in the writing of the following papers, listed here for completeness, during the period of his PhD studies.

Paper 1

David Gesbert, Saad G. Kiani, Anders Gjendemsjø, and Geir E. Øien, "Adaptation, coordination and distributed resource allocation in interference-limited wireless networks," to appear in the *Proc. of the IEEE, Special Issue on Adaptive Transmission*, (Invited paper), December 2007.

A sensible design of wireless networks involves striking a good balance between an aggressive reuse of the spectral resource throughout the network and managing the resulting co-channel interference. Traditionally this problem has been tackled using a "divide and conquer" approach. The latter consists in deploying the network with a static or semi-dynamic pattern of resource reutilization. The chosen reuse factor, while sacrificing a substantial amount of efficiency, brings the interference to a tolerable level. The resource can then be managed in each cell so as to optimize the per cell capacity using an advanced air interface design.

In this paper, using the overall network capacity as a measure of system performance, the problem of resource allocation and adaptive transmission in multicell scenarios is considered. As a key instance, the problem of joint scheduling and power control simultaneously in multiple transmit-receive links, which employ capacity-achieving adaptive codes, is studied. In principle, the solution of such an optimization hinges on tough issues such as the computational complexity and the requirement for heavy receiver-to-transmitter feedback and, for cellular networks, cell-to-cell channel state information signaling. Asymptotic properties pertaining to rate-maximizing

power control and scheduling in multicell networks are presented. Finally, some promising leads for substantial complexity and signaling reduction via the use of newly developed distributed and game theoretic techniques are discussed.

Paper 2

Greg H. Håkonsen, Tor A. Ramstad, and Anders Gjendemsjø, "Image Transmission with Adaptive Power and Rate Allocation over Flat Fading Channels using Joint Source Channel Coding," in *Proc. International Conference on Wireless Information Networks and Systems (WINSYS '06)*, Setubal, Portugal, August 2006.

A revised version of the paper will be published by Springer in an ICETE-SIGMAP 2006 best papers book, 2007.

A joint source channel coder for image transmission over flat fading channels is presented. By letting the transmitter have information about the channel, and by letting the code-rate vary slightly around a target code-rate, it is shown how a robust image coder is obtained by using time-discrete amplitude-continuous symbols generated through the use of non-linear dimension changing mappings. Due to their robustness these mappings are well suited for the changing conditions on a fading channel.

Paper 3

Saad G. Kiani, David Gesbert, Jan E. Kirkebø, Anders Gjendemsjø, and Geir E. Øien, "A Simple Greedy Scheme for Multicell Capacity Maximization," in *Proc. IEEE International Telecommunications Symposium (ITS '06)*, Fortaleza, Brazil, September 2006.

This paper studies the joint optimization of transmit power and scheduling in a multicell wireless network. Despite promising significant gains, this problem is known to be NP-hard and thus difficult to tackle in practice. However, it is shown that this problem lends itself to analysis for large wireless networks which allows simpler modeling of inter-cell interference, and a low complexity greedy algorithm that is efficient for large networks is introduced. As the number of users per cell increases, the solution converges to all cells being active and employing maximum SNIR scheduling, which can be implemented in a distributed manner. By using simulation parameters equivalent to those used in realistic wireless networks, the scheme, though simple, is shown to exhibit substantial gains over existing resource allocation schemes.

References

[1] D. Gesbert, S. G. Kiani, A. Gjendemsjø, and G. E. Øien, "Adaptation, coordination and distributed resource allocation in interference-limited wireless networks," *Proc. of the IEEE, Special Issue on Adaptive Transmission*, (Invited Paper), to appear Dec. 2007. [Online]. Available: http://www.iet.ntnu.no/~gjendems/publications/

[2] *Physical and Medium Access Control Layers for Combined Fixed and Mobile Operation in Licensed Bands*, IEEE Std. Std 802.16e-2005, 2005.

[3] K. Lu, Y. Qian, and H.-H. Chen, "Wireless broadband access: WiMAX and beyond - A secure and service-oriented network control framework for WiMAX networks," *IEEE Communications Magazine*, vol. 45, no. 5, pp. 124–130, May 2007.

[4] 3rd generation - Long Term Evolution. 3rd Generation Partnership Project. [Online]. Available: http://www.3ggp.org

[5] J. Zander, "Performance of optimum transmitter power control in cellular radio systems," *IEEE Transactions on Vehicular Technology*, vol. 41, no. 1, pp. 57–62, Feb. 1992.

[6] G. J. Foschini and Z. Miljanic, "A simple distributed autonomous power control algorithm and its convergence," *IEEE Transactions on Vehicular Technology*, vol. 42, no. 4, pp. 641–646, Nov. 1993.

[7] R. D. Yates, "A framework for uplink power control in cellular radio systems," *IEEE Journal on Selected Areas in Communications*, vol. 13, no. 7, pp. 1341–1347, Sept. 1995.

[8] Y.-H. Lin and R. L. Cruz, "Power control and scheduling for interfering links," in *Proc. IEEE Information Theory Workshop*, San Antonio, TX, Oct. 2004, pp. 288–291.

[9] T. M. Cover and J. A. Thomas, *Elements of Information Theory*. New York: John Wiley & Sons, 1991.

[10] E. Biglieri, J. Proakis, and S. Shamai (Shitz), "Fading channels: Information-theoretic and communications aspects," *IEEE Transactions on Information Theory*, vol. 44, no. 6, pp. 2619–2692, Oct. 1998.

[11] C. E. Shannon, "Communication in the presence of noise," *Proceedings of the IRE*, vol. 37, no. 1, pp. 10–21, Jan. 1949.

[12] X. Qiu and K. Chawla, "On the performance of adaptive modulation in cellular systems," *IEEE Transactions on Communications*, vol. 47, no. 6, pp. 884–895, June 1999.

[13] M. Chiang, C. W. Tan, D. P. Palomar, D. O'Neill, and D. Julian, "Power control by geometric programming," *IEEE Transactions on Wireless Communications*, vol. 6, no. 7, pp. 2640–2651, July 2007.

[14] P. Viswanath, D. N. C. Tse, and R. Laroia, "Opportunistic beamforming using dumb antennas," *IEEE Transactions on Information Theory*, vol. 48, no. 6, pp. 1277–1294, June 2002.

[15] A. J. Goldsmith and P. P. Varaiya, "Capacity of fading channels with channel side information," *IEEE Transactions on Information Theory*, vol. 43, no. 6, pp. 1986–1992, Nov. 1997.

[16] S. Falahati, A. Svensson, T. Ekman, and M. Sternad, "Adaptive modulation systems for predicted wireless channels," *IEEE Transactions on Communications*, vol. 52, no. 2, pp. 307–316, Feb. 2004.

[17] M. Sternad and S. Falahati, "Maximizing throughput with adaptive m-qam based on imperfect channel predictions," in *Proc. IEEE International Symposium on Personal, Indoor and Mobile Radio Communications*, Barcelona, Spain, Sept. 2004, pp. 2289–2293.

[18] G. E. Øien, H. Holm, and K. J. Hole, "Impact of Channel Prediction on Adaptive Coded Modulation Performance in Rayleigh Fading," *IEEE Transactions on Vehicular Technology*, vol. 53, no. 3, pp. 758–769, May 2004.

[19] S. T. Chung and A. J. Goldsmith, "Degrees of freedom in adaptive modulation: A unified view," *IEEE Transactions on Communications*, vol. 49, no. 9, pp. 1561–1571, Sep. 2001.

[20] V. Lau and T. Wu, "On the encoding rate and discrete modulation adaptation design for MIMO links," *IEEE Transactions on Wireless Communications*, vol. 6, no. 1, pp. 50–54, Jan. 2007.

[21] ETSI. Digital Video Broadcasting - Satellite Version 2. [Online]. Available: http://www.dvb.org.

[22] G. Albertazzi, S. Cioni, G. Corazza, M. Neri, R. Pedone, P. Salmi, A. Vanelli-Coralli, and M. Villanti, "On the adaptive DVB-S2 physical layer: design and performance," *IEEE Wireless Communications*, vol. 12, no. 6, pp. 62–68, Dec. 2005.

[23] K. J. Hole, H. Holm, and G. E. Øien, "Adaptive multidimensional coded modulation over flat fading channels," *IEEE Journal on Selected Areas in Communications*, vol. 18, no. 7, pp. 1153–1158, July 2000.

[24] H. Holm, "Adaptive coded modulation performance and channel estimation tools for flat fading channels," Ph.D. dissertation, Norwegian University of Science and Technology, 2002. [Online]. Available: http://www.iet.ntnu.no/projects/beats/

[25] B. Holter, "Adaptive coded modulation in spatial and multiuser diversity systems," Ph.D. dissertation, Norwegian University of Science and Technology, 2005. [Online]. Available: http://www.iet.ntnu.no/projects/beats/

[26] L. Hanzo, C. H. Wong, and M.-S. Yee, *Adaptive Wireless Transceivers: Turbo-Coded, Turbo-Equalized and Space-Time Coded TDMA, CDMA and OFDM Systems*. John Wiley & Sons, Inc., 2002.

[27] A. J. Goldsmith and S.-G. Chua, "Variable-rate variable-power M-QAM for fading channels," *IEEE Transactions on Communications*, vol. 45, no. 10, pp. 1218–1230, Oct. 1997.

[28] T. S. Rappaport, *Wireless Communications Principles & Practice*, 2nd ed. New Jersey: Prentice Hall, 2002.

[29] A. G. i Fàbregas and G. Caire, "Coded modulation in the block-fading channel: Coding theorems and code construction," *IEEE Transactions on Information Theory*, vol. 52, no. 1, pp. 91–114, Jan. 2006.

[30] R. J. McEliece and W. E. Stark, "Channels with block interference," *IEEE Transactions on Information Theory*, vol. IT-30, no. 1, pp. 44–53, Jan. 1984.

[31] L. H. Ozarow, S. Shamai (Shitz), and A. D. Wyner, "Information theoretic considerations for cellular mobile radio," *IEEE Transactions on Vehicular Technology*, vol. 43, no. 2, pp. 359–378, May 1994.

[32] Wikipedia: The Free Encyclopedia, Spectral efficiency. [Online]. Available: http://en.wikipedia.org/wiki/Spectral_efficiency

[33] L. Lin, R. D. Yates, and P. Spasojević, "Adaptive transmission with discrete code rates and power levels," *IEEE Transactions on Communications*, vol. 51, no. 12, pp. 2115–2125, Dec. 2003.

[34] T. T. Kim and M. Skoglund, "On the expected rate of slowly fading channels with quantized side information," *IEEE Transactions on Communications*, vol. 8, no. 4, pp. 820–829, April 2007.

[35] D. Tse and P. Viswanath, *Fundamentals of Wireless Communication*. Cambridge: Cambridge University Press, 2005.

[36] S. N. Diggavi, N. Al-Dhahir, A. Stamoulis, and A. R. Calderbank, "Great expectations: The value of spatial diversity in wireless networks," *Proceedings of the IEEE*, vol. 92, no. 2, Feb. 2004.

[37] A. Goldsmith, *Wireless Communications*. New York: Cambridge University Press, 2005.

[38] M. K. Simon and M.-S. Alouini, *Digital Communication over Fading Channels*, 2nd ed. Wiley-IEEE Press, 2005.

[39] T. Eng, N. Kong, and L. B. Milstein, "Comparison of diversity combining techniques for Rayleigh fading channels," *IEEE Transactions on Communications*, vol. 44, pp. 1117–1129, Sept. 1996.

[40] L. Zheng and D. N. C. Tse, "Diversity and multiplexing: A fundamental tradeoff in multiple-antenna channels," *IEEE Transactions on Information Theory*, vol. 49, no. 5, pp. 1073–1096, May 2003.

[41] N. Kong and L. B. Milstein, "Average SNR of a generalized diversity selection combining scheme," *IEEE Communications Letters*, vol. 3, no. 3, pp. 57–59, Mar. 1999.

[42] M.-S. Alouini and M. K. Simon, "An MGF-based performance analysis of generalized selection combining over Rayleigh fading channels," *IEEE Transactions on Communications*, vol. 48, no. 3, pp. 401–415, March 2000.

[43] W. C. Jakes, *Microwave Mobile Communications*, 2nd ed. Piscataway, NJ: Wiley-IEEE Press, 1994.

[44] M.-S. Alouini and A. J. Goldsmith, "Capacity of Rayleigh fading channels under different adaptive transmission and diversity-combining techniques," *IEEE Transactions on Vehicular Technology*, vol. 48, no. 4, pp. 1165–1181, July 1999.

[45] J. F. Paris, M. del Carmen Aguayo-Torres, and J. T. Entrambasaguas, "Optimum discrete-power adaptive QAM scheme for Rayleigh fading channels," *IEEE Communication Letters*, vol. 5, no. 1, pp. 281–283, July 2001.

[46] W. C. Y. Lee, "Overview of cellular CDMA," *IEEE Transactions on Vehicular Technology*, vol. 40, no. 2, pp. 291–302, May 1991.

[47] D. P. Palomar and J. R. Fonollosa, "Practical algorithms for a family of waterfilling solutions," *Signal Processing, IEEE Transactions on*, vol. 53, no. 2, pp. 686–695, Feb. 2005.

[48] A. Lozano, A. M. Tulino, and S. Verdú, "Optimum power allocation for parallel gaussian channels with arbitrary input distributions," *IEEE Transactions on Information Theory*, vol. 52, no. 7, pp. 3033–3051, July 2006.

[49] S. A. Maas, *Nonlinear Microwave Circuits*. Piscataway, NJ: IEEE Press, 1997.

[50] A. Samukic, "UMTS universal mobile telecommunications system: development of standards for the third generation," *IEEE Transactions on Vehicular Technology*, vol. 47, no. 4, pp. 1099–1104, Nov. 1998.

[51] *Physical Layer Procedures (TDD)*, Third Generation Partnership Project, Technical Specification Group Radio Access Network Std., Rev. TS25.224 (Release 7), March 2006.

[52] C. Köse and D. L. Goeckel, "On power adaptation in adaptive signalling systems," *IEEE Transactions on Communications*, vol. 48, no. 11, pp. 1769–1773, Nov. 2000.

[53] D. L. Sengupta and T. K. Sarkar, "Maxwell, hertz, the maxwellians, and the early history of electromagnetic waves," *IEEE Antennas and Propagation Magazine*, vol. 45, no. 2, pp. 13–19, Apr. 2003.

[54] GSM World. The GSM Association. [Online]. Available: http://www.gsmworld.com

[55] L. Kleinrock and F. Tobagi, "Packet switching in radio channels: Part I - Carrier Sense Multiple-Access modes and their throughput-delay characteristics," *IEEE Transactions on Communications*, vol. 23, no. 12, pp. 1400–1416, Dec. 1975.

[56] A. S. Tanenbaum, *Computer Networks*, 3rd ed. Englewood Cliffs, NJ: Prentice Hall, 1996.

[57] S. Lin and D. J. Costello, *Error Control Coding*, 2nd ed. Upper Saddle River, NJ: Prentice Hall, 2004.

[58] G. Song and Y. Li, "Utility-based resource allocation and scheduling in OFDM-based wireless broadband networks," *IEEE Communications Magazine*, vol. 43, no. 12, Dec. 2005.

[59] R. Knopp and P. Humblet, "Information capacity and power control in single-cell multiuser communications," in *Proc. IEEE International Conference on Communications*, Seattle, WA, June 1995, pp. 331–335.

[60] M. Andrews, K. Kumaran, K. Ramanan, A. Stoylar, P. Whiting, and R. Vijayakumar, "Providing quality of service over a shared wireless link," *IEEE Communications Magazine*, vol. 39, no. 2, pp. 150–154, Feb. 2001.

[61] G. E. Moore, "Cramming more components onto integrated circuits electronics," *Electronics*, pp. 114–117, April 1965.

[62] S. W. Kim, D. S. Ha, and J. Reed, "Minimum selection GSC and adaptive low-power RAKE combining scheme," in *Proc. IEEE International Symposium on Circuits and Systems*, Bangkok, Thailand, May 2003, pp. 357–360.

[63] H.-C. Yang, "New results on ordered statistics and analysis of minimum-selection generalized selection combining (GSC)," *IEEE Transactions on Wireless Communications*, vol. 5, no. 7, pp. 1876–1885, July 2006.

[64] H.-C. Yang, N. Belhaj, and M.-S. Alouini, "Performance analysis of joint adaptive modulation and diversity combining over fading channels," *IEEE Transactions on Communications*, vol. 55, no. 3, pp. 520–528, March 2007.

[65] S. G. Kiani, D. Gesbert, J. E. Kirkebø, A. Gjendemsjø, and G. E. Øien, "A simple greedy scheme for multicell capacity maximization," in *Proc. IEEE International Telecommunications Symposium*, Fortaleza, Brazil, Sept. 2006.

[66] S. G. Kiani, G. E. Øien, and D. Gesbert, "Maximizing multi-cell capacity using distributed power allocation and scheduling," in *Proc. IEEE Wireless Communications and Networking Conference*, Hong Kong, China, March 2007, pp. 1690 – 1694.

[67] K. Tourki, D. Gesbert, and L. Deneire, "Cooperative diversity using per-user power control in the MAC channel," submitted to the IEEE Transactions on Information Theory. [Online]. Available: http://www.eurecom.fr/~gesbert/publications.html

[68] W. Wang, T. Peng, and W. Wang, "Optimal power control under interference temperature constraints in cognitive radio network," in *Proc. IEEE Wireless Communications and Networking Conference*, March 2007, pp. 116–120.

[69] S.-J. Oh and A. C. K. Soong, "QoS-constrained information-theoretic sum capacity of reverse link CDMA systems," *IEEE Transactions on Wireless Communications*, vol. 5, no. 1, pp. 3–7, Jan. 2006.

[70] M. Schubert and H. Boche, "QoS-based resource allocation and transceiver optimization," *Foundations and Trends in Communications and Information Theory*, vol. 2, no. 6, pp. 383–529, July 2006.

[71] H. Boche, "Advanced network calculus for interference functions," Plenary talk at the IEEE Workshop on Signal Processing Advances in Wireless Communications, Helsinki, Finland, June 2007.

[72] S. Stanczak and H. Boche, "On the convexity of feasible QoS regions," *IEEE Transactions on Information Theory*, vol. 53, no. 2, pp. 779–783, Feb. 2007.

[73] Z. Ji and K. J. R. Liu, "Cognitive radios for dynamic spectrum access - Dynamic spectrum sharing: A game theoretical overview," *IEEE Communications Magazine*, vol. 45, no. 5, pp. 88–94, May 2007.

[74] Q. Zhao and B. M. Sadler, "A survey of dynamic spectrum access," *IEEE Signal Processing Magazine*, vol. 24, no. 3, pp. 79–89, May 2007.

[75] A. Zanella, M. Chiani, and M. Z. Win, "MMSE reception and successive interference cancellation for MIMO systems with high spectral efficiency," *IEEE Transactions on Wireless Communications*, vol. 4, no. 3, pp. 1244–1253, May 2005.

Part II

Included papers

Paper A

Rate and Power Allocation for Discrete-Rate Link Adaptation

Anders Gjendemsjø, Geir E. Øien, Henrik Holm, Mohamed-Slim Alouini, David Gesbert, Kjell J. Hole, and Pål Orten

Revised for possible puclication in the *EURASIP Journal on Wireless Communications and Networking*, October 2007.

Abstract

Link adaptation, in particular adaptive coded modulation (ACM), is a promising tool for bandwidth-efficient transmission in a fading environment. The main motivation behind employing ACM schemes is to improve the spectral efficiency of wireless communication systems. In this paper, using a finite number of capacity achieving component codes, we propose new transmission schemes employing constant power transmission, as well as discrete and continuous power adaptation, for slowly varying flat-fading channels.

We show that the proposed transmission schemes can achieve throughputs close to the Shannon limits of flat-fading channels using only a small number of codes. Specifically, using a fully discrete scheme with just four codes, each associated with four power levels, we achieve a spectral efficiency within 1 dB of the continuous-rate continuous-power Shannon capacity. Furthermore, when restricted to a fixed number of codes, the introduction of power adaptation has significant gains with respect to average spectral efficiency and probability of no transmission compared to a constant power scheme.

Parts of this paper were presented at the IEEE Global Telecommunications Conference, St. Louis, MO, USA, November 2005, and at the IEEE International Conference on Communications, Istanbul, Turkey, June 2006.

A. Gjendemsjø (contact author, e-mail: gjendems@iet.ntnu.no) and G. E. Øien are with the Dept. of Electronics and Telecommunications, Norwegian University of Science and Technology (NTNU), Trondheim, Norway.

H. Holm (e-mail: henrik@henrikholm.com) was with the Dept. of Electronics and Telecommunications, NTNU, Trondheim, Norway. He is now with Honeywell Laboratories, Minneapolis, MN, USA.

M.-S. Alouini (e-mail: alouini@qatar.tamu.edu) is with the Dept. of Electrical and Computer Eng., TAMU-Q, Education City, Doha, Qatar.

D. Gesbert (e-mail: gesbert@eurecom.fr) is with the Institut Eurécom, Sophia-Antipolis, France.

K. J. Hole (e-mail: kjell.hole@ii.uib.no) is with the Department of Informatics, University of Bergen, Bergen, Norway.

P. Orten (e-mail: po@thrane.com) is with Thrane & Thrane Norge AS, Billingstad, Norway and with the University Graduate Center, Oslo, Norway.

1 Introduction

In wireless communications bandwidth is a scarce resource. By employing link adaptation, in particular adaptive coded modulation (ACM), we can achieve bandwidth-efficient transmission schemes. Today, adaptive schemes are already being implemented in wireless systems such as Digital Video Broadcasting - Satellite Version 2 (DVB-S2) [1], WiMAX [2], and 3GPP [3]. A generic ACM system [4–12] is illustrated in Fig. A.1. Such a system adapts to the channel variations by utilizing a set of component channel codes and modulation constellations with different spectral efficiencies (SEs).

We consider a wireless channel with additive white Gaussian noise (AWGN) and fading. Under the assumption of slow, frequency-flat fading, a block-fading model can be used to approximate the wireless fading channel by an AWGN channel within the length of a codeword [13; 14]. Hence, the system may use codes which typically guarantee a certain spectral efficiency within a range of signal-to-noise ratios (SNRs) on an AWGN channel. At specific time instants, a prediction of the instantaneous SNR is utilized to decide the highest-SE code that can be used. The system thus compensates for periods with low SNR by transmitting at a low SE, while transmitting at a high SE when the SNR is favorable. In this way, a significant overall gain in *average spectral efficiency* (ASE)—measured in information bits/s/Hz—can be achieved compared to fixed rate transmission systems. This translates directly into a throughput gain, since the average throughput in bits/s is simply the ASE multiplied by the bandwidth.

In the current literature we can identify two main approaches to the design of adaptive systems with a finite number of transmission rates [4; 15–20]. One key point is the starting point for the design. In [18–20] the problem can be stated as follows: Given that the system quantizes any channel state to one of L levels, what is the maximum spectral efficiency that can be obtained using discrete rate signalling? On the other hand, in [4; 15–17] the question is: Given that the system can utilize N transmission rates, what is the maximum spectral efficiency? Another key difference is that in [4; 15–17] the system is designed to maximize the average spectral efficiency according to a *zero information outage* principle, such that at poor channel conditions transmission is disabled, and data buffered. However, in [18–20], data are allowed to be transmitted at all time instants, and an *information* outage occurs when the mutual information offered by the channel is lower than the transmitted rate. While seemingly similar, these approaches actually lead to different designs as will be demonstrated. Though allowing for a non-zero outage can offer more flexibility in the design, it also comes with

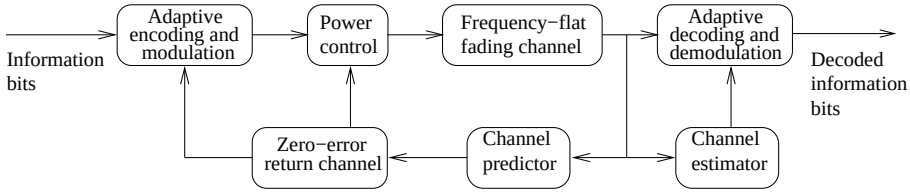

Figure A.1: Adaptive coded modulation system.

the drawbacks of losing data and wasting system resources (e.g., power). Furthermore, in [18–20] the important issues of how often data are lost due to an information outage, and how to deal with it are not discussed, e.g., many applications would then require the communication system to be equipped with a retransmission capability. These differences render a fair comparison between the approaches difficult; however we provide a numerical example later to illustrate the key points above.

In [18–20] adaptive transmission with a finite number of capacity-achieving codes, and a single power level per code are considered. However, from previous work by Chung and Goldsmith [8] we know that the spectral efficiency of such a restricted adaptive system increases if more degrees of freedom are allowed. In particular, for a finite number of transmission rates, power control is expected to have a significant positive impact on the system performance, and hence in this paper we propose and analyze more flexible power control schemes, for which the single power level per code scheme of [18–20] can be seen as a special case.

In this paper we focus on data communications which, as emphasized in [21], cannot "tolerate any loss". For such applications it thus seems more reasonable to follow the zero information outage design philosophy of [4; 15–17]. This choice is also supported by the work done in the design of adaptive coding and modulation for real-life systems, e.g., in DVB-S2 [1]. Based on this philosophy we derive transmission schemes that are optimal with regard to maximal ASE for a given fading distribution. By the assuming codes to be operating at AWGN channel capacity, we formulate constrained ASE maximization problems and proceed to find the optimal switching thresholds and power control schemes as their solutions. Considering both constant power transmission as well as discrete and continuous power adaptation, we show that the introduction of power adaptation provides a substantial average spectral efficiency increase and a significant reduction in the probability of no transmission, when the number of rates is finite. Specifically, spectral efficiencies within 1 dB of the continuous-rate continuous-power Shannon capacity are obtained using a completely dis-

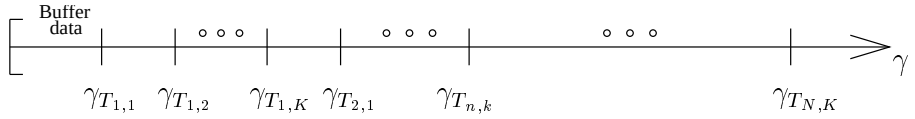

Figure A.2: The pre-adaptation SNR range is partitioned into regions where $\gamma_{\mathrm{T}_{n,k}}$ are the switching thresholds.

crete transmission scheme with only four codes and four power levels per code.

The remainder of the present paper is organized as follows. We introduce the wireless model under investigation and describe the problem under study in Section 2. Optimal transmission schemes for link adaptation are derived and analyzed in Section 3. Numerical examples and plots are presented in Section 4. Finally, conclusions and discussions are given in Section 5.

2 System Model and Problem Formulation

2.1 System Model

We consider the single-link wireless system depicted in Fig. C.1. The discrete-time channel is a stationary fading channel with time-varying gain. The fading is assumed to be slowly varying and frequency-flat. Assuming, as in [4; 22], that the transmitter receives perfect channel predictions we can adapt the transmit power instantaneously at time i according to a power adaptation scheme $S(\cdot)$. Then, denote the instantaneous *pre-adaptation* received signal-to-noise ratio (SNR) by $\gamma[i]$, and the average pre-adaptation received SNR by $\overline{\gamma}$. These are the SNRs that would be experienced using signal constellations of average power $\overline{S}$ without power control [6]. Adapting the transmit power based on the channel state $\gamma[i]$, the received SNR after power control, termed *post-adaptation* SNR, at time i is then given by $\gamma[i]S(\gamma[i])/\overline{S}$. By virtue of the stationarity assumption, the distribution of $\gamma[i]$ is independent of i, and is denoted by $f_\gamma(\gamma)$. To simplify the notation we omit the time reference i from now on.

Following [23; 4], we partition the range of γ into $NK+1$ pre-adaptation SNR regions, which are defined by the switching thresholds $\{\gamma_{\mathrm{T}_{n,k}}\}_{n,k=1,1}^{N,K}$, as illustrated in Fig. A.2. Code n, with spectral efficiency R_n, is selected whenever γ is in the interval $[\gamma_{\mathrm{T}_{n,1}}, \gamma_{\mathrm{T}_{n+1,1}})$, $n = 1, \cdots, N$. Within this interval the transmission rate is constant, however the system can adapt the transmitted power to one of K levels (per code) according to

the channel conditions, in order to maximize the ASE, subject to an average power constraint of $\overline{S}$. I.e., for a given code n, a transmit power level indexed by $k = 1, \cdots, K$ is selected for $\gamma \in [\gamma_{\mathrm{T}_{n,k}}, \gamma_{\mathrm{T}_{n,k+1}})$, where $\gamma_{\mathrm{T}_{n,K+1}} \triangleq \gamma_{\mathrm{T}_{n+1,1}}$. If the pre-adaptation SNR is below $\gamma_{\mathrm{T}_{1,1}}$, data are buffered. For convenience, we let $\gamma_{\mathrm{T}_{0,1}} = 0$ and $\gamma_{\mathrm{T}_{N+1,1}} = \infty$.

2.2 Problem Formulation

The capacity of an AWGN channel is well known to be $C(\gamma) = \log_2\big(1 + \frac{S(\gamma)}{\overline{S}}\gamma\big)$ information bits/s/Hz, where $\frac{S(\gamma)}{\overline{S}}\gamma$ is the received SNR. This means that there exist codes that can transmit with arbitrarily small error rate at all spectral efficiencies up to $C(\gamma)$ bits/s/Hz, provided that the received SNR is (at least) $\frac{S(\gamma)}{\overline{S}}\gamma$[1]. Our goal is now to find an optimal set of capacity-achieving transmission rates, switching levels, and power adaptation schemes in order to maximize the average spectral efficiency for a given fading distribution.

Using the results of [18], an information outage can only occur for a set of channel states within the first interval, which in our setup corresponds to that data should only be buffered for channel states in the first interval. Whereas in the other SNR regions, the assigned rate supports the worst channel state of that region. The average spectral efficiency of the system (in information bit per channel use) can then be written as

$$\overline{R} = \sum_{n=1}^{N} R_n P_n, \tag{A.1}$$

where P_n which is the probability that code n is used:

$$P_n = \int_{\gamma_{\mathrm{T}_{n,1}}}^{\gamma_{\mathrm{T}_{n+1,1}}} f_\gamma(\gamma)\,\mathrm{d}\gamma. \tag{A.2}$$

3 Optimal Design for Maximum Average Spectral Efficiency

Based on the above setup, we now proceed to design spectral efficiency maximizing schemes. Recall that the pre-adaptation SNR range is divided into regions lower bounded by $\gamma_{\mathrm{T}_{n,1}}$, for $n = 0, 1, \cdots, N$. Thus, we let

[1] The existence of such codes is guaranteed by Shannon's channel coding theorem [24]. However, we do not address the important problem of constructing such codes, which is a research problem in itself.

$R_n = C_n$, where $C_n = \log_2\left(1 + \frac{S(\gamma_{T_{n,1}})}{\overline{S}}\gamma_{T_{n,1}}\right)$ is shown below to be the highest spectral efficiency that can be supported within the range $[\gamma_{T_{n,1}}, \gamma_{T_{n+1,1}})$ for $1 \leq n \leq N$, after transmit power adaptation. Note that the fading is nonergodic within each codeword, so that the results of [25, Section IV] do not apply.

An upper bound on the ASE of the ACM scheme—for a given set of codes/switching levels—is therefore the *maximum ASE for ACM* (MASA), defined as

$$\text{MASA} = \sum_{n=1}^{N} C_n P_n = \sum_{n=1}^{N} \log_2\left(1 + \frac{S(\gamma_{T_{n,1}})}{\overline{S}}\gamma_{T_{n,1}}\right) \int_{\gamma_{T_{n,1}}}^{\gamma_{T_{n+1,1}}} f_\gamma(\gamma)\,\mathrm{d}\gamma, \quad \text{(A.3)}$$

subject to the average power constraint,

$$\sum_{n=0}^{N} \int_{\gamma_{T_{n,1}}}^{\gamma_{T_{n+1,1}}} S(\gamma) f_\gamma(\gamma)\,\mathrm{d}\gamma \leq \overline{S}, \quad \text{(A.4)}$$

where $\overline{S}$ denotes the average transmit power. (A.3) is basically a discrete-sum approximation of the integral expressing the Shannon capacity in [22, Eq. (4)]. If arbitrarily long codewords can be used, the bound can be approached from below with arbitrary precision for an arbitrarily low error rate. Using N distinct codes we analyze the MASA for constant, discrete, and continuous transmit power adaptation schemes, deriving the optimal rate and power adaptation for maximizing the average spectral efficiency. We shall assume that the fading is so slow that capacity-achieving codes for AWGN channels can be employed, giving tight bounds on the MASA [26; 27]. In the remainder of this document, we shall use the term MASA both for the ASE-maximizing transmission scheme and for the ASEs obtained after optimizing the switching thresholds and power levels, respectively.

3.1 Continuous-Power Transmission Scheme

In an ideal adaptive power control scheme, the transmitted power can be varied to entirely track the channel variations. Then, for the N regions where we transmit, we show that the optimal continuous power adaptation scheme is *piecewise channel inversion*[2] to keep the received SNR constant within each region, much like the bit error rate is kept constant in optimal

[2]The results of this section were in part presented in [28]. Similar results on continuous power adaptation, when allowing for information outage (loss of data), were also later independently reported in [29].

adaptation for constellation restrictions in [4]. For each rate region we use a capacity-achieving code which ensures an arbitrarily low probability of error for any AWGN channel with a received SNR greater than or equal to $\frac{S(\gamma_{\mathrm{T}_{n,1}})}{\overline{S}}\gamma_{\mathrm{T}_{n,1}} \triangleq \kappa_n$. The optimality of this strategy is formally proven below.

Lemma A.1
For the $N+1$ SNR regions the optimal continuous power control scheme is of the form

$$\frac{S(\gamma)}{\overline{S}} = \begin{cases} \frac{\kappa_n}{\gamma}, & \text{if } \gamma_{T_{n,1}} \leq \gamma < \gamma_{T_{n+1,1}},\ 1 \leq n \leq N, \\ 0, & \text{if } \gamma < \gamma_{T_{1,1}}, \end{cases} \tag{A.5}$$

where $\{\kappa_n, \gamma_{T_{n,1}}\}_{n=1}^{N}$ are parameters to be optimized.

Proof: Assume for the purpose of contradiction that the power scheme given in (A.5) is not optimal, i.e., it uses too much power for a given rate. Then, by assumption, there exists at least one point in the set

$$\bigcup_{n=1}^{N} \{\gamma : \gamma_{\mathrm{T}_{n,1}} \leq \gamma < \gamma_{\mathrm{T}_{n+1,1}}\} \tag{A.6}$$

where it is possible to use less power; denote this point by γ'. Fix any $\epsilon > 0$ and let $\frac{S(\gamma')}{\overline{S}} = \frac{\kappa_n}{\gamma'} - \epsilon$. This yields a received SNR of $\kappa_n - \epsilon\gamma' < \kappa_n$, but is less than the minimum required SNR for a rate of $\log_2(1+\kappa_n)$. Hence, it does not exist any point where the proposed power scheme can be improved, and the assumption is contradicted. □

Using (A.5), the received SNR, after power adaptation, is then for $n = 1, 2, \cdots, N$ given as:

$$\frac{S(\gamma)}{\overline{S}}\gamma = \begin{cases} \kappa_n, & \text{if } \gamma_{\mathrm{T}_{n,1}} \leq \gamma < \gamma_{\mathrm{T}_{n+1,1}}, \\ 0, & \text{if } \gamma < \gamma_{\mathrm{T}_{1,1}}, \end{cases} \tag{A.7}$$

i.e., we have a constant received SNR of κ_n within each region, supporting a maximum spectral efficiency of $\log_2(1 + \frac{S(\gamma_{\mathrm{T}_{n,1}})}{\overline{S}}\gamma_{\mathrm{T}_{n,1}}) = \log_2(1+\kappa_n)$.

Introducing the continuous power adaptation scheme (A.5) in (A.3), (A.4), and changing the average power inequality to an equality for maximization, we arrive at a scheme we denote MASA$_{N\times\infty}$[3], posing the following optimization problem with variables $\{\kappa_n, \gamma_{\mathrm{T}_{n,1}}\}_{n=1}^{N}$:[4]

[3]The notation $N \times \infty$ reflects the fact that the scheme can employ N codes combined with continuous power control, i.e., infinitely many power levels are allowed per code.

[4]Strictly speaking, we should add the constraints $0 \leq \gamma_{\mathrm{T}_{1,1}} \leq \cdots \leq \gamma_{\mathrm{T}_{N,1}}$, and $\kappa_n \geq 0, \forall n$. However, we instead verify that the solutions we find satisfy these constraints.

$$\text{maximize} \quad \text{MASA}_{N\times\infty} = \sum_{n=1}^{N} \log_2(1+\kappa_n) P_n \tag{A.8a}$$

$$\text{s.t} \qquad \sum_{n=1}^{N} \kappa_n d_n = 1, \tag{A.8b}$$

where we have introduced the notation $d_n = \int_{\gamma_{\mathrm{T}_{n,1}}}^{\gamma_{\mathrm{T}_{n+1,1}}} \frac{1}{\gamma} f_\gamma(\gamma)\, \mathrm{d}\gamma$, and P_n is given in (A.2). Note that for $N = 1$, (A.8) reduces to the truncated channel inversion Shannon capacity scheme given in [22, Eq. 12]. Inspecting (A.8), we see that for any *given* set of $\{\gamma_{\mathrm{T}_{n,1}}\}$, the problem is a standard convex optimization problem in $\{\kappa_n\}$, with a waterfilling solution given as [30]

$$\kappa_n = \frac{P_n}{\lambda d_n} - 1, \; n = 1, \cdots, N, \tag{A.9}$$

where λ is a Lagrange multiplier to satisfy the average power constraint, which from (A.8b) can be expressed as a function of the switching thresholds:

$$\lambda = \frac{1 - F_\gamma(\gamma_{\mathrm{T}_{1,1}})}{1 + \sum_{n=1}^{N} d_n}, \tag{A.10}$$

where $F_\gamma(\cdot)$ denotes the cumulative distribution function (cdf) of γ. Thus, using (A.9) and (A.10), (A.8) simplifies to an optimization problem in $\{\gamma_{\mathrm{T}_{n,1}}\}$, reducing the problem size from $2N$ to N variables:

$$\text{maximize} \quad \text{MASA}_{N\times\infty} = \sum_{n=1}^{N} \log_2\left(\frac{P_n}{\lambda d_n}\right) P_n. \tag{A.11}$$

Finally, the optimal values of $\{\gamma_{\mathrm{T}_{n,1}}\}$, can be found by: i) equating the gradient of $\text{MASA}_{N\times\infty}$ to zero, i.e., $\nabla \text{MASA}_{N\times\infty} = \mathbf{0}$, and solving the resulting set of equations by means of a numerical routine such as "fzero" in Matlab, or ii) directly feeding (A.11) to a numerical optimization routine such as "fmincon" in the Matlab Optimization Toolbox. Numerical results for the resulting adaptive power policy and the corresponding spectral efficiencies are presented in Section 4.

3.2 Discrete-Power Transmission Scheme

For practical scenarios the resolution of power control will be limited, e.g., for the Universal Mobile Telecommunications System (UMTS) power control step sizes on the order of 1 dB are proposed [31]. We thus extend the

MASA analysis by considering discrete power adaptation. Specifically, we introduce the MASA$_{N\times K}$ scheme where we allow for $K \geq 1$ power regions *within* each of the N rate regions. For each rate region we again use a capacity-achieving code for any AWGN channel with a received SNR greater than or equal to $\frac{S(\gamma_{\mathrm{T}_{n,1}})}{\overline{S}}\gamma_{\mathrm{T}_{n,1}} = \kappa_n$. The optimal discrete power adaptation is discretized piecewise channel inversion, closely related to the discrete power scheme in [16].

Lemma A.2
The optimal discrete-power adaptation scheme is of the form

$$\frac{S(\gamma)}{\overline{S}} = \begin{cases} \frac{\kappa_n}{\gamma_{T_{n,k}}}, & \text{if } \gamma_{T_{n,k}} \leq \gamma < \gamma_{T_{n,k+1}}, 1 \leq n \leq N,\ 1 \leq k \leq K \\ 0, & \text{if } \gamma < \gamma_{T_{1,1}}, \end{cases} \tag{A.12}$$

$\{\kappa_n\}_{n=1}^{N}$ *and* $\{\gamma_{T_{n,k}}\}_{n,k=1,1}^{N,K}$ *are the parameters to be optimized.*

Proof: To ensure reliable transmission in each rate region $1 \leq n \leq N$, we require $\frac{S(\gamma)}{\overline{S}}\gamma \geq \kappa_n$, assuming $\gamma \in [\gamma_{\mathrm{T}_{n,1}}, \gamma_{\mathrm{T}_{n+1,1}})$. Thus, following the proof of Lemma A.1, since the rate is restricted to be constant in each region, it is obviously optimal from a capacity maximization perspective to reduce the transmitted power, when the channel conditions are more favorable. (A.12) is then obtained by reducing the power in a stepwise manner ($K-1$ steps), and at each step obtaining a received SNR of κ_n, i.e., $\frac{S(\gamma_{\mathrm{T}_{n,k}})}{\overline{S}}\gamma_{\mathrm{T}_{n,k}} = \kappa_n$, thus using the least possible power, while still ensuring transmission with an arbitrarily low error rate. □

Compared to the continuous-power transmission scheme (A.5), discrete-level power control (A.12) will be suboptimal. As seen from the proof of Lemma A.2, this is due to fact that (A.12) is only optimal at K points $(\gamma_{\mathrm{T}_{n,1}}, \cdots, \gamma_{\mathrm{T}_{n,K}})$ within each pre-adaptation SNR region n, at all other points the transmitted power is greater than what is required for reliable transmission at $\log_2(1+\kappa_n)$ bits/s/Hz. Clearly, increasing the number of power levels per code K gives a better approximation to the continuous power control (A.5), resulting in a higher average spectral efficiency. However, as we will see from the numerical results in Section 4, using only a few power levels per code will yield spectral efficiencies close to the upper bound of continuous power adaptation.

Using (A.12) in (A.3), (A.4), we arrive at the following optimization problem:

$$\text{maximize} \quad \sum_{n=1}^{N} \log_2(1+\kappa_n) P_n \tag{A.13a}$$

$$\text{s.t.} \quad \sum_{n=1}^{N} \kappa_n e_n = 1, \tag{A.13b}$$

where we have introduced $e_n = \sum_{k=1}^{K} \frac{1}{\gamma_{\mathrm{T}_{n,k}}} \int_{\gamma_{\mathrm{T}_{n,k}}}^{\gamma_{\mathrm{T}_{n,k+1}}} f_\gamma(\gamma)\,\mathrm{d}\gamma$. As in the case of continuous-power transmission, for fixed $\{\gamma_{\mathrm{T}_{n,k}}\}$, (A.13) is a standard convex optimization problem in $\{\kappa_n\}$, yielding optimal values according to waterfilling as

$$\kappa_n = \frac{P_n}{\lambda e_n} - 1,\ n = 1, \cdots, N, \tag{A.14}$$

where again λ is a Lagrange multiplier for the power constraint, and from (A.13b) expressed as

$$\lambda = \frac{1 - F_\gamma(\gamma_{\mathrm{T}_{1,1}})}{1 + \sum_{n=1}^{N} e_n} \tag{A.15}$$

Then, using (A.14) and (A.15) the optimal switching thresholds $\{\gamma_{\mathrm{T}_{n,k}}\}_{n=1,k=1}^{N,K}$ are found as the solution to the following simplified optimization problem:

$$\text{maximize} \quad \mathrm{MASA}_{N\times K} = \sum_{n=1}^{N} \log_2\left(\frac{P_n}{\lambda e_n}\right) P_n, \tag{A.16}$$

which, analogously to the previously discussed case of continuous power adaptation, can be approached by either solving the set of equations $\nabla \mathrm{MASA}_{N\times K} = \mathbf{0}$, or feeding (A.16) to a numerical optimization routine.

3.3 Constant-Power Transmission Scheme

When a single transmission power is used for all codes, we adopt the term *constant-power transmission scheme*[5] [15]. The optimal constant power policy is then to save power when $\gamma < \gamma_{\mathrm{T}_{1,1}}$, i.e., when there is no transmission, while transmitting at a constant power level S for $\gamma \geq \gamma_{\mathrm{T}_{1,1}}$, such that the average power constraint (A.4) is satisfied with an equality. Mathematically, from (A.4),

$$\begin{aligned} \sum_{n=0}^{N} \int_{\gamma_{\mathrm{T}_{n,1}}}^{\gamma_{\mathrm{T}_{n+1,1}}} S(\gamma) f_\gamma(\gamma)\,\mathrm{d}\gamma &= 0 \int_{0}^{\gamma_{\mathrm{T}_{1,1}}} f_\gamma(\gamma)\,\mathrm{d}\gamma + S \int_{\gamma_{\mathrm{T}_{1,1}}}^{\infty} f_\gamma(\gamma)\,\mathrm{d}\gamma \\ &= S\left(1 - F_\gamma(\gamma_{\mathrm{T}_{1,1}})\right) = \overline{S}. \end{aligned} \tag{A.17}$$

[5] Also termed *on-off* power transmission, see e.g., [8].

Then, we arrive at the following transmit power adaptation scheme:

$$\frac{S(\gamma)}{\overline{S}} = \begin{cases} \frac{1}{1-F_\gamma(\gamma_{\mathrm{T}_{1,1}})}, & \text{if } \gamma_{\mathrm{T}_{n,1}} \le \gamma < \gamma_{\mathrm{T}_{n+1,1}},\ 1 \le n \le N, \\ 0, & \text{if } \gamma < \gamma_{\mathrm{T}_{1,1}}. \end{cases} \tag{A.18}$$

From (A.18) we see that the post-adaptation SNR monotonically increases within $[\gamma_{\mathrm{T}_{n,1}}, \gamma_{\mathrm{T}_{n+1,1}})$, for $1 \le n \le N$. Hence, $\log_2\big(1 + \frac{S(\gamma_{\mathrm{T}_{n,1}})}{\overline{S}}\gamma_{\mathrm{T}_{n,1}}\big)$ is the highest possible spectral efficiency that can be supported over the whole of region n. Introducing (A.18) in (A.3) we obtain a new expression for the MASA, denoted by MASA_N:

$$\mathrm{MASA}_N = \sum_{n=1}^{N} \log_2\Big(1 + \frac{\gamma_{\mathrm{T}_{n,1}}}{1 - F_\gamma(\gamma_{\mathrm{T}_{1,1}})}\Big) \int_{\gamma_{\mathrm{T}_{n,1}}}^{\gamma_{\mathrm{T}_{n+1,1}}} f_\gamma(\gamma)\,\mathrm{d}\gamma. \tag{A.19}$$

In order to find the optimal set of switching levels $\{\gamma_{\mathrm{T}_{n,1}}\}_{n=1}^{N}$, we first calculate the gradient of the MASA_N—as defined by (A.19)—with respect to the switching levels. The gradient is then set to zero, and we attempt to solve the resulting set of equations with respect to $\{\gamma_{\mathrm{T}_{n,1}}\}_{n=1}^{N}$:

$$\nabla\mathrm{MASA}_N = \begin{bmatrix} \frac{\partial \mathrm{MASA}_N}{\partial \gamma_{\mathrm{T}_{1,1}}} \\ \vdots \\ \frac{\partial \mathrm{MASA}_N}{\partial \gamma_{\mathrm{T}_{N,1}}} \end{bmatrix} = \mathbf{0}. \tag{A.20}$$

For $n = 2, \cdots, N$ the partial derivatives in (A.20) can be expressed as follows:

$$\frac{\partial \mathrm{MASA}_N}{\partial \gamma_{\mathrm{T}_{n,1}}} = \log_2(e)\Big(\frac{\int_{\gamma_{\mathrm{T}_{n,1}}}^{\gamma_{\mathrm{T}_{n+1,1}}} f_\gamma(\gamma)\,\mathrm{d}\gamma}{1 - F_\gamma(\gamma_{\mathrm{T}_{1,1}}) + \gamma_{\mathrm{T}_{n,1}}} - \ln\left(\frac{1 - F_\gamma(\gamma_{\mathrm{T}_{1,1}}) + \gamma_{\mathrm{T}_{n,1}}}{1 - F_\gamma(\gamma_{\mathrm{T}_{1,1}}) + \gamma_{\mathrm{T}_{n-1,1}}}\right) f_\gamma(\gamma_{\mathrm{T}_{n,1}})\Big), \tag{A.21}$$

where $\ln(\cdot)$ is the natural logarithm. The integral in (A.21) is recognized as the difference between the cdf of γ, $F_\gamma(\cdot)$, evaluated at the two points $\gamma_{\mathrm{T}_{n+1,1}}$ and $\gamma_{\mathrm{T}_{n,1}}$. Setting $\frac{\partial \mathrm{MASA}_N}{\partial \gamma_{\mathrm{T}_{n,1}}}$ for $2 \le n \le N$ equal to zero then yields a set of $N-1$ equations, each with a similar form to the one shown here:

$$F_\gamma(\gamma_{\mathrm{T}_{n+1,1}}) - F_\gamma(\gamma_{\mathrm{T}_{n,1}}) - (1 - F_\gamma(\gamma_{\mathrm{T}_{1,1}}) + \gamma_{\mathrm{T}_{n,1}})\times \ln\left(\frac{1 - F_\gamma(\gamma_{\mathrm{T}_{1,1}}) + \gamma_{\mathrm{T}_{n,1}}}{1 - F_\gamma(\gamma_{\mathrm{T}_{1,1}}) + \gamma_{\mathrm{T}_{n-1,1}}}\right) f_\gamma(\gamma_{\mathrm{T}_{n,1}}) = 0, \qquad \text{for } n = 2, \cdots, N. \tag{A.22}$$

Noting that $\gamma_{\mathrm{T}_{n+1,1}}$ appears only in one place in this equation, it is trivial to rearrange the $N-2$ first equations into a recursive set of equations where $\gamma_{\mathrm{T}_{n+1,1}}$ is written as a function of $\gamma_{\mathrm{T}_{n,1}}$, $\gamma_{\mathrm{T}_{n-1,1}}$, and $\gamma_{\mathrm{T}_{1,1}}$ for $n = 2, \ldots, N-1$:

$$\gamma_{\mathrm{T}_{n+1,1}} = F_{\gamma}^{-1}\left[F_{\gamma}(\gamma_{\mathrm{T}_{n,1}}) + (1 - F_{\gamma}(\gamma_{\mathrm{T}_{1,1}}) + \gamma_{\mathrm{T}_{n,1}}) \ln\left(\frac{1 - F_{\gamma}(\gamma_{\mathrm{T}_{1,1}}) + \gamma_{\mathrm{T}_{n,1}}}{1 - F_{\gamma}(\gamma_{\mathrm{T}_{1,1}}) + \gamma_{\mathrm{T}_{n-1,1}}}\right) f_{\gamma}(\gamma_{\mathrm{T}_{n,1}})\right] \tag{A.23}$$

where $F_{\gamma}^{-1}[\cdot]$ is the inverse cdf, whose existence can be guaranteed under the assumption that $f_{\gamma}(\gamma)$ is non-zero except at isolated points [32].

For $N \geq 3$, (A.23) can be expanded in order to yield a set $\gamma_{\mathrm{T}_{3,1}}, \cdots, \gamma_{\mathrm{T}_{N,1}}$ which is optimal for given $\gamma_{\mathrm{T}_{1,1}}$ and $\gamma_{\mathrm{T}_{2,1}}$. The MASA can then be expressed as a function of $\gamma_{\mathrm{T}_{1,1}}$ and $\gamma_{\mathrm{T}_{2,1}}$ only. We have now used $N-2$ equations from the set in (A.20), and the two remaining equations could be used in order to reduce the problem to one equation of one unknown. However, both because of the recursion and the complicated expression for $\frac{\partial \mathrm{MASA}_N}{\partial \gamma_{\mathrm{T}_{1,1}}}$, the resulting equation would become prohibitively involved. The final optimization is done by numerical maximization of $\mathrm{MASA}_N(\gamma_{\mathrm{T}_{1,1}}, \gamma_{\mathrm{T}_{2,1}})$, thus reducing the N-dimensional optimization problem to 2 dimensions. After solving the reduced problem $\gamma_{\mathrm{T}_{3,1}}, \cdots, \gamma_{\mathrm{T}_{N,1}}$ are found via (A.23).

Before we proceed, note that in a practical system, given a $\overline{\gamma}$-range of interest, the switching thresholds and corresponding power levels could be computed offline for each relevant $\overline{\gamma}$ and stored as lookup tables in the system. The correct thresholds, power levels, and associated coding schemes could then be selected by table look-up based on an estimate of $\overline{\gamma}$.

4 Numerical Results

One important outcome of the research presented here is the opportunity the results provide for assessing the relative significance of the number of codes and power levels used. It is in many ways desirable to use as few codes and power levels as possible in link adaptation schemes, as this may help overcome several problems, e.g., relating to implementation complexity, and adaptation with faulty channel state information (CSI). Thus, if we can come close to the maximum MASA (i.e., the channel capacity) with small values of N and K by choosing our link adaptation schemes optimally, this is potentially of great practical interest.

The constant and discrete schemes offer several advantages considering implementation [33]. In these schemes the transmitter adapts its power and

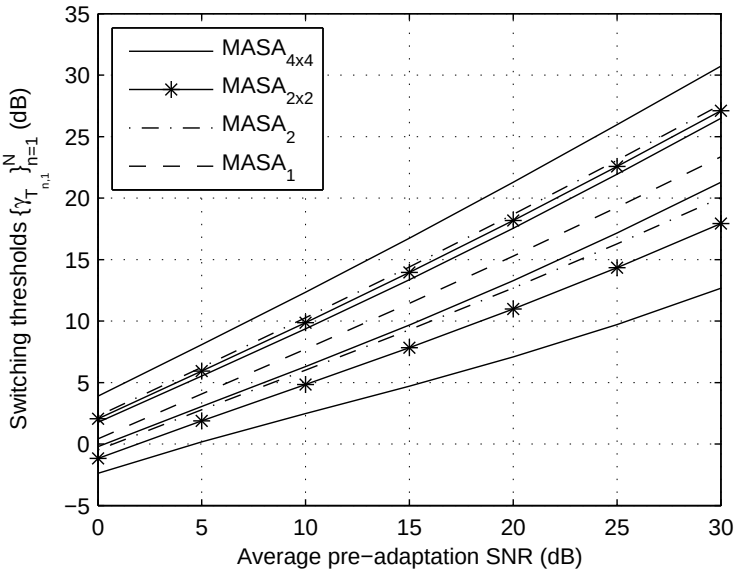

Figure A.3: Switching thresholds $\{\gamma_{\mathrm{T}_{n,1}}\}_{n=1}^{N}$ as a function of average pre-adaptation SNR. For each data series, the lowermost curve shows $\gamma_{\mathrm{T}_{1,1}}$, while the uppermost shows $\gamma_{\mathrm{T}_{N,1}}$.

rate from a limited set of values, thus the receiver only needs to feed back an indexed rate and power pair for each fading block. Obviously, compared to the feedback of continuous channel state information, this results in reduced requirements of the feedback channel bandwidth and transmitter design. Further, completely discrete schemes are more resilient towards errors in channel estimation and prediction.

Two performance merits will be taken into account: The MASA, representing an approachable upper bound on the throughput when the scheme is under the restriction of a certain number of codes and power adaptation flexibility, and the probability of no transmission, $P_{\text{no tr.}}$, representing the probability that data must be buffered. For the system designer, this probability is an important quantity as it influences e.g. the system's ability to operate under delay requirements. For the following numerical results, a Rayleigh fading channel model has been assumed.

4.1 Switching Levels and Power Adaptation Schemes

Fig. A.3 shows the set of optimal switching levels $\{\gamma_{\mathrm{T}_{n,1}}\}_{n=1}^{N}$ for selected MASA schemes and for $0\,\mathrm{dB} < \overline{\gamma} < 30\,\mathrm{dB}$. (For the $\mathrm{MASA}_{2\times 2}$ and

Table A.1: Rate and Power Adaptation for Four Regions, $\overline{\gamma} = 10$ dB

	MASA_4	$\text{MASA}_{4\times4}$	$\text{MASA}_{4\times\infty}$
$\gamma_{\text{T}_{1,1}}, \cdots, \gamma_{\text{T}_{4,1}}$ (dB)	4.4, 7.3, 9.8, 12.4	2.5, 6.3, 9.4, 12.3	1.4, 5.5, 8.9, 12.3
$\kappa_1, \cdots, \kappa_4$	-	2.4, 6.6, 13.9, 29.0	2.0, 6.0, 13.8, 31.3
$\text{SE}_1, \cdots, \text{SE}_4$	1.9, 2.7, 3.4, 4.2	1.8, 2.9, 3.9, 4.9	1.6, 2.8, 3.9, 5.0

$\text{MASA}_{4\times4}$ schemes the internal switching thresholds $\{\gamma_{\text{T}_{n,k}}\}_{n=1,k=2}^{N,K}$ are not shown in Fig. A.3 due to clarity reasons). Table A.1 shows numerical values, correct to the first decimal place, for designing optimal systems with $N = 4$ at $\overline{\gamma} = 10\,\text{dB}$. Fig. A.3 and Table A.1 should be interpreted as follows: With the mean pre-adaptation SNR $\overline{\gamma}$, the number of codes N and a power adaptation scheme in mind, find the set of switching levels and the corresponding maximal spectral efficiencies, given by

$$\text{SE}_n = \begin{cases} \log_2(1 + \frac{\gamma_{\text{T}_{n,1}}}{1-F(\gamma_{\text{T}_{1,1}})}) & \text{for } \text{MASA}_N, \\ \log_2(1+\kappa_n) & \text{for } \text{MASA}_{N\times K} \quad \text{and} \quad \text{MASA}_{N\times\infty}. \end{cases} \tag{A.24}$$

Then design optimal codes for these spectral efficiencies, for each $\overline{\gamma}$ of interest.

Examples of optimized power adaptation schemes are shown in Fig. A.4, illustrating the piecewise channel inversion power adaptation schemes of the $\text{MASA}_{N\times K}$ and $\text{MASA}_{N\times\infty}$ schemes. For $\gamma \leq 15\,\text{dB}$ the discrete-power scheme of $\text{MASA}_{4\times4}$ closely follows the continuous power adaptation scheme of $\text{MASA}_{4\times\infty}$. Fig. A.4 also depicts the optimal power allocation (denoted C_{OPRA}) for continuous-rate adaptation [22, Eq. 5]. At $\overline{\gamma} = 10\,\text{dB}$, two discrete-rate MASA schemes allocate more power to codes with higher spectral efficiency, following the water-filling nature of C_{OPRA}. In the analysis of Section 3 no stringent peak power constraint has been imposed, and it is interesting to note the limited range of $S(\gamma)$ that still occurs for both $\text{MASA}_{4\times4}$ and $\text{MASA}_{4\times\infty}$.

4.2 Comparison of MASA Schemes

Under the average power constraint of (A.4) the average spectral efficiencies corresponding to MASA_N, $\text{MASA}_{N\times K}$, and $\text{MASA}_{N\times\infty}$ are plotted in Figs. A.5 and A.6. From Fig. A.5a we see that the average spectral efficiency increases with the number of codes, while Fig. A.6 shows that the ASE also increases with flexibility of power adaptation.

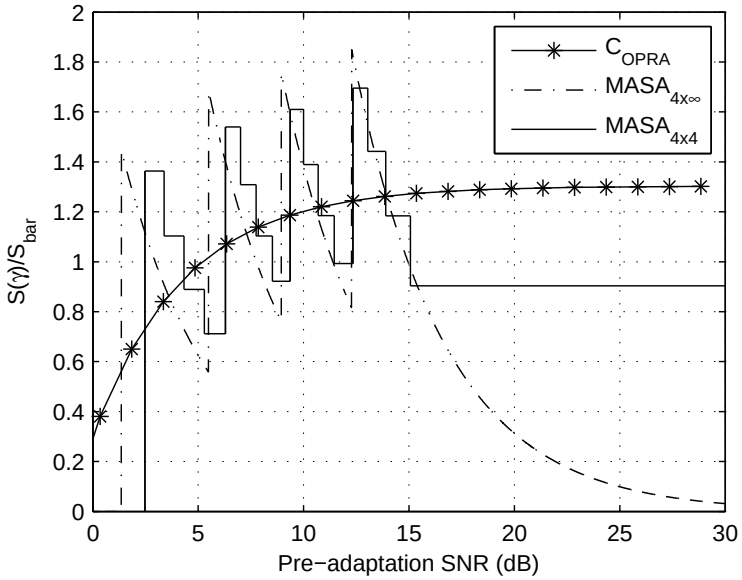

Figure A.4: Power adaptation schemes for $\text{MASA}_{4\times\infty}$ and $\text{MASA}_{4\times4}$ as a function of pre-adaptation SNR, plotted for an average pre-adaptation SNR $\overline{\gamma} = 10$ dB. Optimal power adaptation for continuous-rate adaptation C_{OPRA} as reference.

Fig. A.5b compares four MASA schemes with the product $N \times K = 8$, showing that number of codes has a slightly larger impact on the spectral efficiency than the number of power levels. However, we see that the three schemes with $N \geq 2$ have almost similar performance, indicating that the number of rates and power levels can be traded against each other, while still achieving approximately the same ASE. From an implementation point of view this is valuable as it gives more freedom to design the system.

Finally, as mentioned in the introduction, there are at least two distinct design philosophies for link adaptation systems, depending on whether the number of *regions* in the partition of the pre-adaptation range γ or the number of *rates* is the starting point of the design, and correspondingly on whether information *outage* can be tolerated. Now, a direct comparison is not possible, but to highlight the differences between the two philosophies we provide a numerical example.

Example 1 *Consider designing a simple rate-adaptive system with two regions, where the goal is to maximize the expected rate using a single power level per region. Assuming the average pre-adaptation SNR on the channel to be* 5 *dB and*

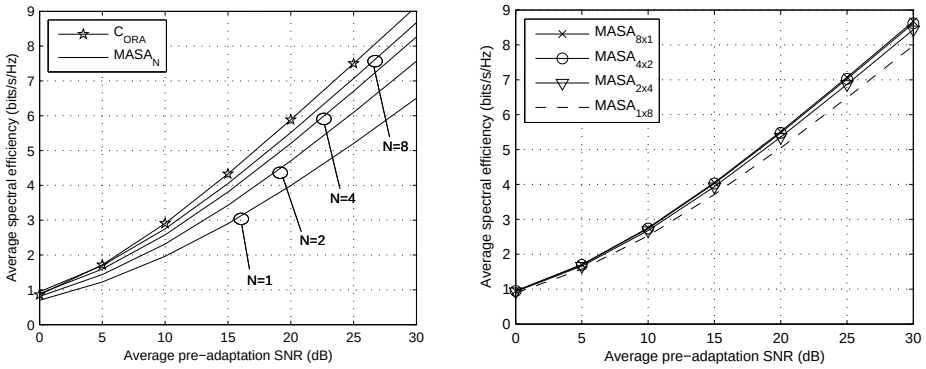

(a) Average spectral efficiency of MASA_N for $N = 1, 2, 4, 8$ and C_{ORA} for reference.

(b) Average spectral efficiency of $\text{MASA}_{N\times K}$ as a function of $\overline{\gamma}$, for four MASA schemes with $N \times K = 8$.

Figure A.5: Average spectral efficiency of different MASA schemes.

following the setup of [18–20], we find the maximum average reliable throughput (ART), defined as the "average data rate assuming zero rate when the channel is in outage"[18] that can be achieved to be 1.2444 *bits/s/Hz, and that the probability of information outage, or equivalent the probability that an arbitrary transmission will be corrupted, is* 0.3098*. Thus, without retransmissions, the system is likely to be useless for many applications.*

Now, turning to the MASA schemes discussed in this paper, using two regions, but only one constellation and power level, i.e., $MASA_1$, we see from Fig. A.5a that this scheme achieves a spectral efficiency of 1.2263 *bits/s/Hz at $\overline{\gamma} = 5\,dB$ without outage. This is only marginally less than the scheme from [18–20] when using two constellations and allowing for a non-zero outage.*

4.3 Comparison of MASA schemes with Shannon Capacities

Assume that the channel state information γ is known to the transmitter and the receiver. Then, given an average transmit power constraint the channel capacity of a Rayleigh fading channel with optimal *continuous* rate adaptation and constant transmit power, C_{ORA}, is given in [22; 34] as

$$C_{\text{ORA}} = \log_2(e) e^{\frac{1}{\overline{\gamma}}} E_1\left(\frac{1}{\overline{\gamma}}\right), \tag{A.25}$$

where $E_1(\cdot)$ is the exponential integral of first order [35, p. xxxv]. Furthermore, if we include *continuous* power adaptation, the channel capacity,

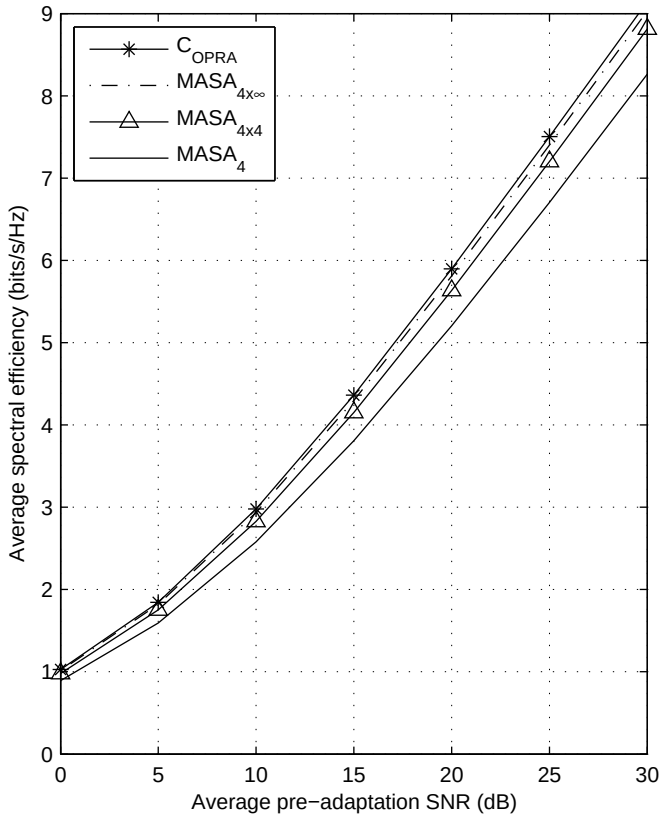

Figure A.6: Average spectral efficiency for various MASA schemes with $N = 4$ codes as a function of $\overline{\gamma}$. C_{OPRA} as reference.

C_{OPRA}, becomes [22; 34]

$$C_{\text{OPRA}} = \log_2(e)\Big(\frac{e^{\frac{-\gamma_{\text{cut}}}{\overline{\gamma}}}}{\frac{\gamma_{\text{cut}}}{\overline{\gamma}}} - \overline{\gamma}\Big), \tag{A.26}$$

where the "cutoff" value γ_{cut} can be found by solving

$$\int_{\gamma_{\text{cut}}}^{\infty}\Big(\frac{1}{\gamma_{\text{cut}}} - \frac{1}{\gamma}\Big) f_\gamma(\gamma)\,\mathrm{d}\gamma = 1. \tag{A.27}$$

Thus, MASA_N is compared to C_{ORA}, while $\text{MASA}_{N\times K}$ and $\text{MASA}_{N\times\infty}$ are measured against C_{OPRA}.

The capacity in (A.26) can be achieved in the case that a continuum of capacity-achieving codes for AWGN channels, and corresponding opti-

mal power levels, are available. That is, for each SNR there exists an optimal code and power level. Alternatively, if the fading is ergodic within each codeword, as opposed to the assumptions in this paper, C_{OPRA} can be obtained by a fixed rate transmission system using a single Gaussian code [25; 36].

As the number of codes (switching thresholds) goes to infinity, MASA_N will reach the C_{ORA} capacity, while $\text{MASA}_{N\times K}$ will reach the C_{OPRA} capacity when $N, K \to \infty$. Of course this is not a practically feasible approach; however, as illustrated in Figs. A.5a and A.6, a small number of optimally designed codes, and possibly power adaptation levels, will indeed yield a performance that is close to the theoretical upper bounds, C_{ORA} and C_{OPRA}, for any given $\overline{\gamma}$.

From Fig. A.6 we see that the power adapted MASA schemes perform close to the theoretical upper bound (C_{OPRA}) using only four codes. Specifically, restricting our adaptive policy to just four rates and four power levels per rate results in a spectral efficiency that is within 1 dB of the efficiency obtained with continuous-rate and continuous-power (A.26), demonstrating the remarkable impact of power adaptation. This is in contrast to the case of continuous rate adaptation, where introducing power adaptation gives negligible gain [22].

4.4 Probability of no transmission

When the pre-adaptation SNR falls below $\gamma_{\text{T}_{1,1}}$ no data are sent. The probability of no transmission $P_{\text{no tr.}}$ for the Rayleigh fading case can then be calculated as follows,

$$P_{\text{no tr.}} = \int_0^{\gamma_{\text{T}_{1,1}}} f_\gamma(\gamma)\,\mathrm{d}\gamma = 1 - e^{-\frac{\gamma_{\text{T}_{1,1}}}{\overline{\gamma}}}. \tag{A.28}$$

When the number of codes is increased, the SNR range will be partitioned into a larger number of regions. As shown in Fig. A.3, the lowest switching level $\gamma_{\text{T}_{1,1}}$ will then become smaller. $P_{\text{no tr.}}$ will therefore decrease, as illustrated in Fig. A.7. Similarly, as seen from Fig. A.3, $\gamma_{\text{T}_{1,1}}$ also decreases with an increasing number of power levels, when N is constant. Thus, both rate and power adaptation flexibility reduce the probability of no transmission.

For applications with low delay requirements, it could be beneficial to enforce a constraint that $P_{\text{no tr.}}$ should not exceed a prescribed maximal value. Then, we may simply—using (A.28)—compute $\gamma_{\text{T}_{1,1}}$ to be the highest SNR value which ensures that this constraint is fulfilled. The MASA schemes are then optimized to obtain the highest possible ASE under the given constraint on no transmission, i.e., optimization with $\gamma_{\text{T}_{1,1}}$ as a pre-

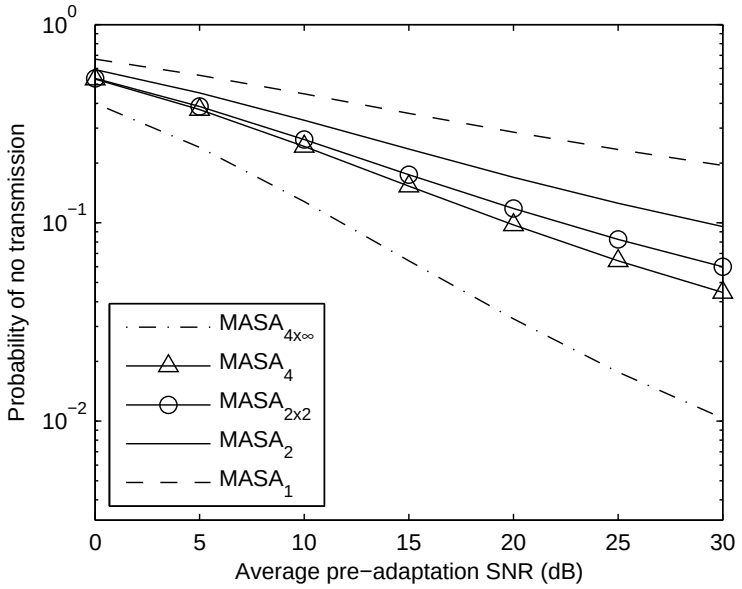

Figure A.7: The probability of no transmission $P_{\text{no tr.}}$ as a function of average pre-adaptation SNR.

determined parameter. As an example, in Fig. A.8, the obtainable average spectral efficiency for the MASA$_N$ scheme with the additional constraint that $P_{\text{no tr.}} \leq 10^{-3}$ (dashed lines) is compared to the case without a constraint on no transmission probability (solid lines). We see that for $N = 2$ the constraint has a severe influence on the ASE, while for $N = 8$ the constraint can be fulfilled without significant losses in spectral efficiency.

5 Conclusions and Discussions

Using a zero information outage approach, and assuming that capacity-achieving component codes are available, we have devised spectral efficiency maximizing link adaptation schemes for flat block-fading wireless communication channels. Constant, discrete, and continuous-power adaptation schemes are proposed and analyzed. Switching levels and power adaptation policies are optimized in order to maximize the average spectral efficiency for a given fading distribution.

We have shown that a performance close to the Shannon limits can be achieved with all schemes using only a small number of codes. However, utilizing power adaptation is shown to give significant average spectral

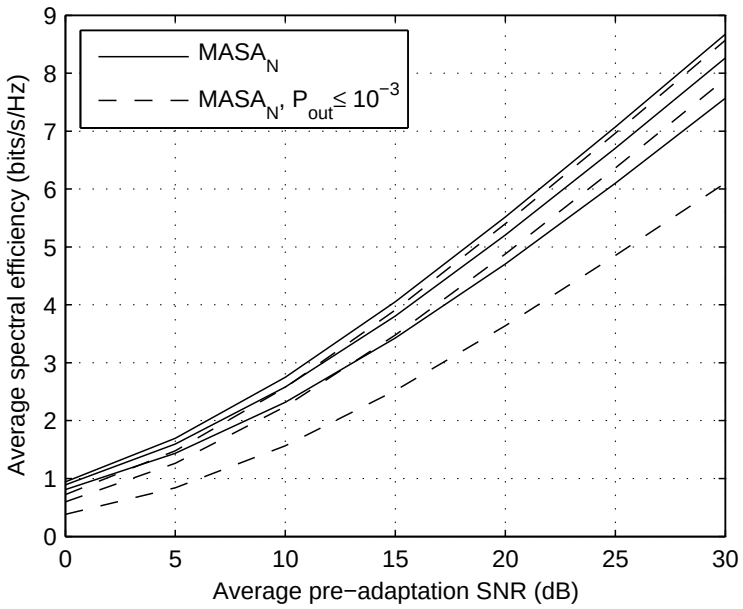

Figure A.8: MASA$_N$ as a function of $\overline{\gamma}$, with a constraint on the probability of no transmission (solid lines) and without (dashed lines). Plotted for $N = 2$ (lowermost curve for both series), 4, and 8 (uppermost curve for both series).

efficiency and probability of no transmission gains over the constant transmission power scheme. In particular, using a fully discrete scheme with just four codes, each associated with four power levels, we achieve a spectral efficiency within 1 dB of the Shannon capacity for continuous rate and power adaptation. Additionally, constant and discrete-power adaptation schemes render the system more robust against imperfect channel estimation and prediction, reduce the feedback load and resolve implementation issues, compared to continuous power adaptation.

We have also seen that the number of rates N can be traded against the number of power levels K. This flexibility is of practical importance since it may be easier to implement the proposed power adaptation schemes than to design capacity-achieving codes for a large number of rates. The analysis can be augmented to encompass more practical scenarios, e.g., by taking imperfect CSI [37] and SNR margins due to various implementation losses, into account. Finally, we note that the adaptive power algorithms presented in this paper require that the radio frequency (RF) power amplifier is operated in the linear region, implying a higher power consumption.

For devices with limited battery capacity it is apparent that there will be a tradeoff between efficiency and linearity. This can be a topic for further research.

Acknowledgement

The authors wish to express their gratitude to Professor Tom Luo, University of Minnesota, for suggesting the modified optimization when the first switching level is constrained due to requirements on the probability of no transmission. A similar idea has independently been proposed by Dr. Ola Jetlund, NTNU [37].

References

[1] ETSI. Digital Video Broadcasting - Satellite Version 2. [Online]. Available: http://www.dvb.org.

[2] *Physical and Medium Access Control Layers for Combined Fixed and Mobile Operation in Licensed Bands*, IEEE Std. Std 802.16e-2005, 2005.

[3] *Physical Layer Procedures (FDD)*, Third Generation Partnership Project, Technical Specification Group Radio Access Network Std., Rev. TS25.214 (Release 6), Sept. 2005.

[4] A. J. Goldsmith and S.-G. Chua, "Variable-rate variable-power M-QAM for fading channels," *IEEE Transactions on Communications*, vol. 45, no. 10, pp. 1218–1230, Oct. 1997.

[5] ——, "Adaptive coded modulation for fading channels," *IEEE Transactions on Communications*, vol. 46, no. 5, pp. 595–602, May 1998.

[6] K. J. Hole, H. Holm, and G. E. Øien, "Adaptive multidimensional coded modulation over flat fading channels," *IEEE Journal on Selected Areas in Communications*, vol. 18, no. 7, pp. 1153–1158, July 2000.

[7] K. J. Hole and G. E. Øien, "Spectral efficiency of adaptive coded modulation in urban microcellular networks," *IEEE Transactions on Vehicular Technology*, vol. 50, no. 1, pp. 205–222, Jan. 2001.

[8] S. T. Chung and A. J. Goldsmith, "Degrees of freedom in adaptive modulation: A unified view," *IEEE Transactions on Communications*, vol. 49, no. 9, pp. 1561–1571, Sep. 2001.

[9] L. Hanzo, C. H. Wong, and M.-S. Yee, *Adaptive Wireless Transceivers: Turbo-Coded, Turbo-Equalized and Space-Time Coded TDMA, CDMA and OFDM Systems*. John Wiley & Sons, Inc., 2002.

[10] H. Holm, "Adaptive coded modulation performance and channel estimation tools for flat fading channels," Ph.D. dissertation, Norwegian University of Science and Technology, 2002. [Online]. Available: http://www.iet.ntnu.no/projects/beats/

[11] S. Catreux, V. Erceg, D. Gesbert, and R. W. Heath, Jr., "Adaptive modulation and MIMO coding for broadband wireless data networks," *IEEE Transactions on Communications*, vol. 40, no. 6, pp. 108–115, June 2002.

[12] J. Torrance and L. Hanzo, "Optimisation of switching levels for adaptive modulation in a slow Rayleigh fading channel," *Electronics Letters*, vol. 32, pp. 1167–1169, June 1996.

[13] R. J. McEliece and W. E. Stark, "Channels with block interference," *IEEE Transactions on Information Theory*, vol. IT-30, no. 1, pp. 44–53, Jan. 1984.

[14] L. H. Ozarow, S. Shamai (Shitz), and A. D. Wyner, "Information theoretic considerations for cellular mobile radio," *IEEE Transactions on Vehicular Technology*, vol. 43, no. 2, pp. 359–378, May 1994.

[15] C. Köse and D. L. Goeckel, "On power adaptation in adaptive signalling systems," *IEEE Transactions on Communications*, vol. 48, no. 11, pp. 1769–1773, Nov. 2000.

[16] J. F. Paris, M. del Carmen Aguayo-Torres, and J. T. Entrambasaguas, "Optimum discrete-power adaptive QAM scheme for Rayleigh fading channels," *IEEE Communication Letters*, vol. 5, no. 1, pp. 281–283, July 2001.

[17] C. Byoungjo and L. Hanzo, "Optimum mode-switching-assisted constant power single- and multicarrier adaptive modulation," *IEEE Transactions on Vehicular Technology*, vol. 52, no. 3, pp. 536–560, May 2003.

[18] L. Lin, R. D. Yates, and P. Spasojević, "Adaptive transmission with discrete code rates and power levels," *IEEE Transactions on Communications*, vol. 51, no. 12, pp. 2115–2125, Dec. 2003.

[19] T. T. Kim and M. Skoglund, "On the expected rate of slowly fading channels with quantized side information," in *Proc. Asilomar Conference on Signals, Systems and Computers*, Pacific Grove, CA, 2005, pp. 633–637.

[20] ——, "On the expected rate of slowly fading channels with quantized side information," *IEEE Transactions on Communications*, vol. 8, no. 4, pp. 820–829, April 2007.

[21] A. Goldsmith, *Wireless Communications*. New York: Cambridge University Press, 2005.

[22] A. J. Goldsmith and P. P. Varaiya, "Capacity of fading channels with channel side information," *IEEE Transactions on Information Theory*, vol. 43, no. 6, pp. 1986–1992, Nov. 1997.

[23] A. Gjendemsjø, G. E. Øien, and P. Orten, "Optimal discrete-level power control for adaptive coded modulation schemes with capacity-approaching component codes," in *Proc. IEEE International Conference on Communications*, Istanbul, Turkey, June 2006, pp. 5047–5052.

[24] C. E. Shannon, "A mathematical theory of communication," *Bell System Technical Journal*, vol. 27, pp. 379–423 and 623–656, July and Oct. 1948.

[25] G. Caire and S. Shamai (Shitz), "On the capacity of some channels with channel state information," *IEEE Transactions on Information Theory*, vol. 45, no. 6, pp. 2007–2019, Sept. 1999.

[26] S. Dolinar, D. Divsalar, and F. Pollara, "Code performance as a function of code block size," in *JPL TDA Progress Report 42-133*, 1998. [Online]. Available: http://tmo.jpl.nasa.gov/tmo/progress_report/42-133/133K.pdf

[27] ——, "Turbo code performance as a function of code block size," in *Proc. IEEE International Symposium on Information Theory*, Cambridge, MA, Aug. 1998, p. 32.

[28] A. Gjendemsjø, G. E. Øien, and H. Holm, "Optimal power control for discrete-rate link adaptation schemes with capacity-approaching coding," in *Proc. IEEE Global Telecommunications Conference*, St. Louis, MO, Nov.-Dec. 2005, pp. 3498–3502.

[29] L. Lin, R. D. Yates, and P. Spasojević, "Adpative transmission with discrete code rates and power levels," *IEEE Transactions on Information Theory*, vol. 52, no. 5, pp. 1847–1860, May 2006.

[30] T. M. Cover and J. A. Thomas, *Elements of Information Theory*. New York: John Wiley & Sons, 1991.

[31] *Physical Layer Procedures (TDD)*, Third Generation Partnership Project, Technical Specification Group Radio Access Network Std., Rev. TS25.224 (Release 7), March 2006.

[32] G. Casella and R. Berger, *Statistical inference*, 2nd ed. Duxbury Press, 2002.

[33] F. F. Digham and M.-S. Alouini, "Diversity combining with discrete power loading over fading channels," in *Proc. IEEE Wireless Communications and Networking Conference*, Atlanta, GA, March 2004, pp. 328–332.

[34] M.-S. Alouini and A. J. Goldsmith, "Capacity of Rayleigh fading channels under different adaptive transmission and diversity-combining techniques," *IEEE Transactions on Vehicular Technology*, vol. 48, no. 4, pp. 1165–1181, July 1999.

[35] I. Gradshteyn and I. Ryzhik, *Table of Integrals, Series and Products*, 6th ed. San Diego: Academic Press, 2000.

[36] E. Biglieri, J. Proakis, and S. Shamai (Shitz), "Fading channels: Information-theoretic and communications aspects," *IEEE Transactions on Information Theory*, vol. 44, no. 6, pp. 2619–2692, Oct. 1998.

[37] O. Jetlund, G. E. Øien, H. Holm, and K. J. Hole, "Spectral efficiency bounds for adaptive coded modulation with outage probability constraints and imperfect channel prediction," in *Nordic Radio Symposium*, Oulu, Finland, Aug. 2004.

Paper B

A Cross-Layer Comparison of Two Design Philosophies for Discrete-Rate Adaptive Transmission

Anders Gjendemsjø, Sébastien de la Kethulle de Ryhove, and Geir E. Øien

Submitted for possible publication in *Proc. IEEE Wireless Communications and Networking Conference (WCNC'08)*, Las Vegas, NV, USA, March-April 2008.

Abstract

We analyze two different approaches found in the literature for throughput maximization of an adaptive transmission system operating over a slowly-varying flat-fading wireless channel with limited channel state information at the transmitter. While both approaches employ a finite number of transmission power levels and capacity-achieving codes, they differ in the number of quantization levels for the channel state, and whether or not information outage is allowed. Focusing on reliable data communications, we extend earlier works in a cross-layered fashion by adding an ARQ protocol, such that data received during such an outage can be retransmitted.

We accurately analyze and compare the performance of the two approaches in terms of average spectral efficiency, probability of outage, and average feedback load, here defined in terms of the entropy of the feedback source. Numerical results show that, in general, there is a trade-off between the two approaches in terms of spectral efficiency and feedback load. However, scenarios in which one of the schemes can achieve a higher throughput at a lower feedback load are also identified.

A. Gjendemsjø (contact author, e-mail: gjendems@iet.ntnu.no) and G. E. Øien are with the Dept. of Electronics and Telecommunications, Norwegian University of Science and Technology (NTNU), Trondheim, Norway.

S. de la Kethulle de Ryhove (e-mail: sryhove@emgs.com) was with the Dept. of Electronics and Telecommunications, NTNU, Trondheim, Norway. He is now with Electromagnetic Geoservices, Trondheim, Norway.

1 Introduction

Link adaptation, in particular adaptive coded modulation (ACM), is a promising technique to increase throughput in wireless communication systems affected by fading. Today, adaptive schemes are already being implemented in wireless systems such as Digital Video Broadcasting - Satellite Version 2 (DVB-S2) [1]. ACM has the ability to adapt to a time-varying channel through variation of channel codes, modulation constellations, and transmitted power [2–10].

In the current literature, we can identify at least two different approaches to the design of such adaptive systems using a finite number of transmission rates and power levels, under an average transmit power constraint [3; 11–14; 7; 9]. One key point is the manner in which the design problem is posed. In [7; 9] the problem can be stated as follows: Given that the system quantizes any channel signal-to-noise ratio (SNR) to L levels, what is the maximum spectral efficiency that can be obtained using discrete rate signalling? On the other hand, in [3; 11–13] the question that is asked is: Given that the system can utilize N transmission rates, what is the maximum spectral efficiency that can be attained? While seemingly similar, these two starting points give differing designs, as will be discussed in more detail.

Another key difference is that in [3; 11–14] the system is designed to maximize the average spectral efficiency (ASE) under the constraint of *zero information outage*. In the event of an information outage, the transmitted data will be corrupted, and thus when the code with the lowest spectral efficiency can not be supported by the channel, transmission is disabled, and data buffered. Following the terminology of [14], we will refer to such schemes as *maximum ASE for ACM* (MASA) schemes. In the family of schemes from [7; 9], data are transmitted at all time instants, and an *information outage* occurs when the mutual information offered by the channel is lower than the transmitted rate. The data transmitted during outage are then ignored, and the performance is characterized by the concept of *average reliable throughput* (ART), assuming zero rate when the channel is in outage [7]. Henceforth, we shall refer to such schemes as ART schemes.

Although allowing for a non-zero outage can offer more flexibility in the design, and has been suggested in the literature to be the better choice [7; 9], it also comes with the drawbacks of data loss and the spilling of system resources (e.g., power). In [7; 9] the important issues of how often data are lost due to an information outage, and how to deal with it, are not discussed. Moreover it is clear that the if the information outage is large, many applications would require the communication system to be equipped with

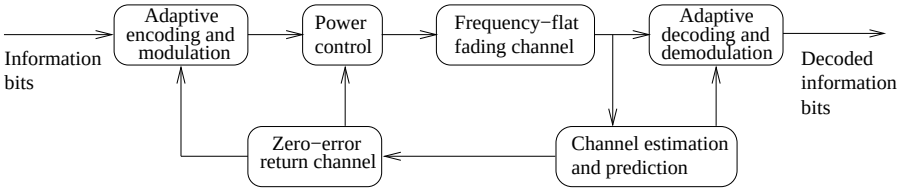

Figure B.1: Adaptive coded modulation system.

a retransmission capability. This is not discussed in [7; 9].

In this paper we compare the MASA and ART approaches in a scenario where the integrity of the information bits to be transmitted must be preserved. We therefore extend the ART scheme with an ARQ protocol for retransmitting bits that are received during an information outage. This strategy fits well applications in data communications which "cannot tolerate any loss, so packets that are corrupted or lost in the end-to-end transmission must be retransmitted" [15, p. 553]. By performing a mathematical analysis of the two approaches and looking at numerical examples, we show that there in general is a compromise between spectral efficiency and feedback load. Changing from one scheme to another in general allows to trade spectral efficiency for feedback load. However, in some scenarios, the MASA scheme can offer a higher throughput at a lower feedback cost. This is in contrast to conclusions found in the literature [7; 9].

The remainder of the present paper is organized as follows. In Section 2 the system model is presented, outlining the MASA and ART schemes. The two schemes are then analyzed in terms of average spectral efficiency, outage probability, and feedback load in Section 3. Numerical results are shown in Section 4, and finally we conclude in Section 5.

2 System Model

Consider the single-link wireless system depicted in Fig. B.1. The discrete-time channel is a stationary fading channel with time-varying gain. Under the assumption of frequency-flat fading, we will use an independent, identically distributed (iid) block-fading model, i.e., we approximate the wireless fading channel by an AWGN channel within the length of one coherence time (data burst) [16]. Following the setup of [7; 9; 14], the receiver is assumed to have perfect channel state information (CSIR), whereas the transmitter exploits partial CSIT, in the form of quantized SNR, to select a transmit rate and power pair.

We denote the instantaneous *pre-adaptation* received signal-to-noise ratio (SNR) at time i by $\gamma[i]$, and the average pre-adaptation received SNR by $\overline{\gamma}$. These are the SNRs that would be experienced using signal constellations of average power $\overline{S}$ without power control [4]. Given a channel fading state $\gamma[i]$, and a transmit power of $\kappa(\gamma[i])$, the received SNR after power control, termed *post-adaptation* SNR, at time i is then given by $\gamma[i]\kappa(\gamma[i])/\overline{S}$. Associated with the transmit power control is an average power constraint[1]:

$$E\{\kappa(\gamma)\} \leq \overline{S}. \tag{B.1}$$

By virtue of the iid block-fading assumption, the distribution of $\gamma[i]$ is independent of i, and is denoted by $f_\gamma(\gamma)$. To simplify the notation we omit the time reference i from now on.

We will compare the adaptive transmission design philosophies of MASA and ART in this setup, and, based on this comparison challenge some previous conclusions on the relative performance of these schemes. Following the zero information outage approach, denote by $\text{MASA}_{N\times 1}$ the MASA scheme that utilizes N power and rate pairs, and also has the option of buffering data at poor channel conditions. Thus, as illustrated in Fig. B.2a the pre-adaptation SNR range is partitioned into $N+1$ regions, which are defined by the code switching thresholds $\{\gamma_{\text{T}_n}\}_{n=1}^{N}$. Specifically, whenever γ is in the interval $[\gamma_{\text{T}_n}, \gamma_{\text{T}_{n+1}})$, $n = 1, \cdots, N$, code n, with spectral efficiency R_n, and transmit power κ_n is used. If the pre-adaptation SNR is below $\gamma_{\text{T}_{1,1}}$, data are buffered. For convenience, we let $\gamma_{\text{T}_0} = 0$ and $\gamma_{\text{T}_{N+1}} = \infty$.

Turning to the design philosophy allowing for information outage, we define ART_L to be the ART scheme where channel state feedback is quantized to L levels. With ART_L, data are potentially transmitted at every point in time. The rationale behind this is to attempt to increase the spectral efficiency by supporting transmission also when $\gamma < \gamma_{\text{T}_1}$ [7; 9]. Specifically, the pair of code l and transmit power κ_l is selected whenever γ is in the interval $[\gamma_{\text{T}_l}, \gamma_{\text{T}_{l+1}})$, $l = 0, \cdots, L-1$, as depicted in Fig. B.2b.

We re-emphasize that the key difference between the two schemes is that in the ART scheme, for $\gamma \in [0, \gamma_{\text{T}_1})$, data are always transmitted at a rate R_0, requiring a pre-adaptation SNR of γ_0^* for the transmission to be reliable. I.e., for all $\gamma < \gamma_0^*$, the instantaneous mutual information is less than the operating rate. An outage hence occurs, and the transmitted data are corrupted and must be ignored by the receiver. Due to the assumption of perfect CSIR, the receiver knows whether the received data are transmitted in outage, and can thus disregard unreliable data. Focusing on reliable data

[1] Termed *long-term* power constraint in [9].

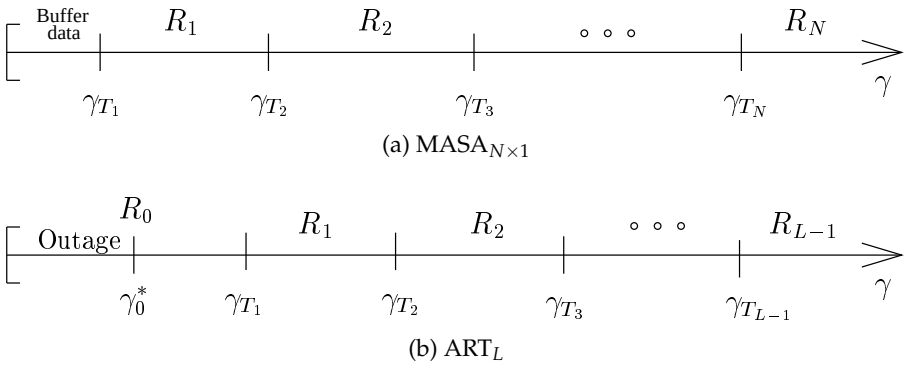

(a) MASA$_{N\times 1}$

(b) ART$_L$

Figure B.2: Pre-adaptation SNR range partitioning for the MASA$_{N\times 1}$ and ART$_L$ schemes.

communications, we extend the ideas of [7; 9] in a cross-layered fashion by adding to the ART$_L$ scheme an ARQ protocol, allowing to retransmit data that are corrupted during information outages.

3 Performance Analysis

Based on the above setup, we now proceed to analyze and compare the MASA$_{N\times 1}$ and ART$_L$ schemes in terms of average spectral efficiency, outage probability, and feedback load.

3.1 Average Spectral Efficiency

First, following [14], we consider the MASA$_{N\times 1}$ scheme, using N distinct rate and power pairs (R_n, κ_n), where for $\gamma \in [\gamma_{\mathrm{T}_n}, \gamma_{\mathrm{T}_{n+1}})$, R_n is the highest spectral efficiency rate that can be supported using a transmit power level of $\frac{\kappa(\gamma)}{\overline{S}} = \kappa_n$, i.e., $R_n = \log_2(1 + \kappa_n \gamma_{\mathrm{T}_n})$. The average spectral efficiency maximization problem can then be formulated as follows, where $\{\kappa_n, \gamma_{\mathrm{T}_n}\}_{n=1}^N$ are the optimization variables:

$$\mathrm{MASA}_{N\times 1} = \max. \quad \sum_{n=1}^{N} \log_2(1 + \kappa_n \gamma_{\mathrm{T}_n}) \int_{\gamma_{\mathrm{T}_n}}^{\gamma_{\mathrm{T}_{n+1}}} f_\gamma(\gamma)\, \mathrm{d}\gamma, \tag{B.2a}$$

$$\text{s.t.} \quad \sum_{n=1}^{N} \kappa_n \int_{\gamma_{\mathrm{T}_n}}^{\gamma_{\mathrm{T}_{n+1}}} f_\gamma(\gamma)\, \mathrm{d}\gamma = 1, \tag{B.2b}$$

$$\kappa_n \geq 0,\ \gamma_{\mathrm{T}_{n+1}} - \gamma_{\mathrm{T}_n} \geq 0. \tag{B.2c}$$

where we have changed the inequality in (B.1) to an equality for maximization purposes [7, Lemma 2]. Problem (B.2) can be solved using the procedure outlined in [14].

Proceeding to the ART_L scheme, L distinct rate and power pairs are used, and the spectral efficiency performance is characterized by the average reliable throughput, (i.e., the spectral efficiency is taken to be zero when the channel is in outage). As for the MASA scheme above, in the $L-1$ upper intervals, a power κ_l is used and a rate of $R_l = \log_2(1+\kappa_l\gamma_{\text{T}_l})$ can be supported. As depicted in B.2b, for the lowermost pre-adaptation SNR region, transmission occurs at a power κ_0 and a rate of $R_0 = \log_2(1+\kappa_0\gamma_0^*)$, however this rate can only be supported for $\gamma \in [\gamma_0^*, \gamma_{\text{T}_1})$. Thus, for $\gamma \in [0, \gamma_0^*)$ the system is in outage. Then, the spectral efficiency maximization problem with variables $\gamma_0^*, \kappa_0, \{\kappa_l, \gamma_{\text{T}_l}\}_{l=1}^{L-1}$ is given as:

$$\begin{aligned}\text{ART}_L = \max. \quad & \log_2(1+\kappa_0\gamma_0^*)\int_{\gamma_0^*}^{\gamma_{\text{T}_1}} f_\gamma(\gamma)\,\text{d}\gamma + \\ & \sum_{l=1}^{L-1}\log_2(1+\kappa_l\gamma_{\text{T}_l})\int_{\gamma_{\text{T}_l}}^{\gamma_{\text{T}_{l+1}}} f_\gamma(\gamma)\,\text{d}\gamma, \end{aligned} \tag{B.3a}$$

$$\text{s.t.} \quad \sum_{l=0}^{L-1}\kappa_l\int_{\gamma_{\text{T}_l}}^{\gamma_{\text{T}_{l+1}}} f_\gamma(\gamma)\,\text{d}\gamma = 1, \tag{B.3b}$$

$$\kappa_l \geq 0,\ \gamma_0^* \geq 0,\ \gamma_{\text{T}_{l+1}} - \gamma_{\text{T}_l} \geq 0. \tag{B.3c}$$

where the contribution from $R_0 = \log_2(1+\kappa_0\gamma_0^*)$ is taken to be zero when the channel is in outage, as reflected by the integration limits. The solution to (B.3) can be found using the procedure described in [7; 9].

In the remainder of this document, we shall use the terms $\text{MASA}_{N\times 1}$ and ART_L both for the transmission schemes and for the ASEs obtained by solving (B.2) and (B.3), respectively. When comparing the two different design philosophies, an obvious question is the relative spectral efficiency performance. To this end, we give the following general result:

Proposition 1 *The average spectral efficiencies of the $MASA_{N\times 1}$ and ART_L schemes satisfy:*

a) $MASA_{N\times 1} > ART_L$, $\forall N = L \geq 1$.
b) $MASA_{N\times 1} > ART_L \geq MASA_{(N-1)\times 1}$, $\forall N = L \geq 2$.

Proof: In the solution to the ART_L optimization problem (B.3), κ_0 can be either positive or zero [7], and we consider the two cases separately. First,

recall that $N = L$, and rewrite the ART_L power constraint (B.3c) as

$$\begin{aligned}&\sum_{n=0}^{N-1} \kappa_n \int_{\gamma_{\text{T}_n}}^{\gamma_{\text{T}_{n+1}}} f_\gamma(\gamma)\,\mathrm{d}\gamma \\ &= \underbrace{\kappa_0 \int_0^{\gamma_0^*} f_\gamma(\gamma)\,\mathrm{d}\gamma}_{\text{Power waste}} + \kappa_0 \int_{\gamma_0^*}^{\gamma_{\text{T}_1}} f_\gamma(\gamma)\,\mathrm{d}\gamma + \sum_{n=1}^{N-1} \kappa_n \int_{\gamma_{\text{T}_n}}^{\gamma_{\text{T}_{n+1}}} f_\gamma(\gamma)\,\mathrm{d}\gamma.\end{aligned} \tag{B.4}$$

For $\kappa_0 > 0$, this shows that power is wasted for $\gamma \in [0, \gamma_0^*)$, $\forall N \geq 1$. Comparing (B.2) to (B.3), we thus see that the ART_L optimization problem is equivalent to the $\text{MASA}_{N\times 1}$ optimization problem, but with a more restrictive average power constraint, and hence

$$\text{MASA}_{N\times 1} > \text{ART}_L, \quad \kappa_0 > 0. \tag{B.5}$$

Note that for $N = 1$, we always have $\kappa_0 > 0$. For $N \geq 2$, it is also possible that $\kappa_0 = 0$, and in this case we see from (B.4), (B.2) that

$$\text{ART}_L = \text{MASA}_{(N-1)\times 1}. \tag{B.6}$$

Now, trivially, $\text{MASA}_{N\times 1} > \text{MASA}_{(N-1)\times 1}$, and combining (B.5) and (B.6) we obtain a). Finally, κ_0 is only positive if there is a gain in spectral efficiency by supporting the rate $\log_2(1 + \kappa_0\gamma_0^*)$ over not doing so, hence $\text{ART}_L > \text{MASA}_{(N-1)\times 1}$ for $\kappa_0 > 0$, $N \geq 2$. This combined with (B.6) establishes b). □

3.2 Probability of Outage

As previously mentioned, the ART_L scheme allows for information outage, and when the system is in outage, the data that are transmitted will be lost. A central measure to evaluate the performance of the scheme in a practical scenario is then the probability of information outage, P_{out}. This was not explicitly quantified (numerically) in [7; 9]. P_{out} quantifies the average fraction of transmissions that will be corrupted, and can be calculated as

$$P_{\text{out}} = \int_0^{\gamma_0^*} f_\gamma(\gamma)\,\mathrm{d}\gamma. \tag{B.7}$$

3.3 Feedback Load

Now, consider the minimum average feedback load (AFL) of the two schemes in question. The AFL — measured in average number of information bits per feedback symbol — will be calculated using the entropy

of the feedback source. This is a natural measure, since it represents the lower limit of achievable compression of the feedback source, assuming the source is memoryless. Note that this notion of feedback load differs from [7; 9], where the feedback load was simply taken to be the number of regions.

Let us first consider the $\text{MASA}_{N\times 1}$ scheme. For each fading block, an index pointing to one of $N+1$ (rate, power) pairs (including the zero-rate zero-power pair) is fed back. Due to the iid block fading assumption, the feedback indices can be considered as the outcomes of a discrete memoryless $\mathcal{X}_{\text{MASA}_{N\times 1}}$ source with an alphabet of cardinality $N+1$, and associated symbol probabilities

$$P_n = \int_{\gamma_{\text{T}_n}}^{\gamma_{\text{T}_{n+1}}} f_\gamma(\gamma)\,\mathrm{d}\gamma, \quad n = 0, 1, \ldots, N. \tag{B.8}$$

Thus, according the Shannon's source coding theorem [17], the minimum average feedback load $\text{AFL}_{\text{MASA}_{N\times 1}}$ can be found by calculating the entropy as follows:

$$\text{AFL}_{\text{MASA}_{N\times 1}} = \mathcal{H}\{\mathcal{X}_{\text{MASA}_{N\times 1}}\} = -\sum_{n=0}^{N} P_n \log_2(P_n), \tag{B.9}$$

where $\mathcal{H}\{\mathcal{X}\}$ denotes the entropy of the source $\mathcal{X}$.

When employing the ART_L scheme for data communications, it is required that all data be reliably conveyed from the transmitter to the receiver. This implies that data that are lost during outage must be retransmitted, making the feedback load calculation slightly more involved. That is, for the current block, we need to consider two cases: i) transmission in the previous block occurred with rate $R > R_0$ and outage is not possible or ii) the previous transmission used a rate $R = R_0$ and outage can occur.

In the first case, the transmitter knows that the previous transmission was successful, and then it suffices to feed back the SNR region index only. Following the steps used above, the feedback is then given by a source $\mathcal{X}_{\text{ART}_L,\text{No out.}}$, with symbol probabilities $P_l = \int_{\gamma_{\text{T}_l}}^{\gamma_{\text{T}_{l+1}}} f_\gamma(\gamma)\,\mathrm{d}\gamma, \quad l = 0, 1, \ldots, L-1$, yielding an entropy of

$$\mathcal{H}\{\mathcal{X}_{\text{ART}_L,\text{No out.}}\} = -\sum_{l=0}^{L-1} P_l \log_2 P_l. \tag{B.10}$$

In the event that an outage might have occurred in the previous transmission, the transmitter needs to be informed whether or not a retransmission is required. We introduce a simple ACK/NACK scheme to this

end. Specifically, an ACK or NACK has to be given in addition to the pre-adaptation SNR region for the next transmission. The alphabet for the feedback source $\mathcal{X}_{\mathrm{ART}_{L+\mathrm{ACK/NACK}}}$, given that transmission occurred with R_0 in the previous block, is that obtained by pairing the rates $R_0, \cdots, R_{L-1}$ with ACK and NACK symbols, yielding $2L$ entries. By virtue of the iid block fading assumption, the probability of the entries in the alphabet are found to be:

$$\Pr\left(R_l, \mathrm{ACK}\right) = P_l \frac{(P_0 - P_{\mathrm{out}})}{P_0},\ l = 0, \ldots L-1 \tag{B.11a}$$

$$\Pr\left(R_l, \mathrm{NACK}\right) = P_l \frac{P_{\mathrm{out}}}{P_0},\ l = 0, \ldots L-1. \tag{B.11b}$$

In the case that the optimization problem (B.3) yields a $\kappa_0 > 0$, we can calculate the average feedback load of the ART_L scheme using (B.10) and (B.11) as

$$\begin{aligned}
\mathrm{AFL}_{\mathrm{ART}_L} &= \mathcal{H}\{\mathcal{X}_{\mathrm{ART}_{L+\mathrm{ACK/NACK}}}\} P_0 + \mathcal{H}\{\mathcal{X}_{\mathrm{ART}_L,\mathrm{No\ out.}}\}(1-P_0) \\
&= \Bigg[-\sum_{l=0}^{L-1} P_l \frac{P_0 - P_{\mathrm{out}}}{P_0} \log_2\left(P_l \frac{P_0 - P_{\mathrm{out}}}{P_0}\right) \\
&\quad - \sum_{l=0}^{L-1} P_l \frac{P_{\mathrm{out}}}{P_0} \log_2\left(P_l \frac{P_{\mathrm{out}}}{P_0}\right) \Bigg] P_0 \\
&\quad - \left(\sum_{l=0}^{L-1} P_l \log_2 P_l\right)(1-P_0) \\
&\overset{\text{i)}}{=} \Big[-\frac{P_0 - P_{\mathrm{out}}}{P_0} \log_2\left(\frac{P_0 - P_{\mathrm{out}}}{P_0}\right) - \frac{P_{\mathrm{out}}}{P_0} \log_2\left(\frac{P_{\mathrm{out}}}{P_0}\right) \Big] P_0 \\
&\quad - \sum_{l=0}^{L-1} P_l \log_2 P_l,
\end{aligned} \tag{B.12}$$

where i) follows from routine rearrangements and the fact that $\sum_{l=0}^{L-1} P_l = 1$. Inspecting (B.12), we see that it can be rewritten as

$$\mathrm{AFL}_{\mathrm{ART}_L} = \mathcal{H}\{\mathcal{X}_{\mathrm{ART}_L,\mathrm{No\ out.}}\} + P_0 \mathcal{H}\{\mathcal{X}_{\mathrm{ACK/NACK}}\}, \tag{B.13}$$

where we have defined $\mathcal{X}_{\mathrm{ACK/NACK}}$ as a source with binary alphabet and symbol probabilities

$$P_{\mathrm{ACK}} = \frac{P_0 - P_{\mathrm{out}}}{P_0},\ P_{\mathrm{NACK}} = \frac{P_{\mathrm{out}}}{P_0}. \tag{B.14}$$

That is, the total feedback load is given as the sum of the entropy of an ART_L scheme performing without outage and the entropy of a binary (ACK/NACK) source weighted by P_0, i.e., the probability of having to give ACK/NACK.

In the case of $\kappa_0 = 0$, outage is not possible, and the feedback load of the ART_L scheme is simply given by (B.10). To summarize, we have that

$$\text{AFL}_{\text{ART}_L} = \begin{cases} \mathcal{H}\{\mathcal{X}_{\text{ART}_L,\text{No out.}}\} + P_0\mathcal{H}\{\mathcal{X}_{\text{ACK/NACK}}\}, & \kappa_0 > 0, \\ \mathcal{H}\{\mathcal{X}_{\text{ART}_L,\text{No out.}}\}, & \kappa_0 = 0. \end{cases} \tag{B.15}$$

Following the ASE discussion in Section 3.1, from (B.15) and (B.9) it is clear that in the case of $\kappa_0 = 0$, $\text{AFL}_{\text{ART}_L} = \text{AFL}_{\text{MASA}_{(N-1)\times 1}}$, due to equivalent optimization problems (B.2) and (B.3).

4 Numerical Results

For the following numerical results, a Rayleigh fading channel model is assumed.

4.1 Probability of Outage and Average Spectral Efficiency

Fig. B.3 shows the probability of outage for the ART_L scheme as a function of the average pre-adaptation SNR γ (dB). We see that ART_1 scheme has, as expected, a non-zero probability of outage for all values of γ. At low pre-adaptation SNRs, for $L \geq 2$, the probability of outage is zero, or equivalently $\kappa_0 = 0$. For larger γ, a non-zero outage probability can not be avoided. As an example, for ART_2, $P_{\text{out}} = 0.3098$ at $\gamma = 5\,\text{dB}$, implying that more than 30% of the transmissions will be corrupted, thus for many applications there is a need for a retransmission capability. Somewhat surprisingly this is not discussed in [7; 9].

In Fig. B.4, we have plotted the average spectral efficiency of the two schemes versus the average pre-adaptation SNR γ. The plots confirm the results from Proposition 1, namely that for $N = L$, $\text{MASA}_{N\times 1}$ achieves a higher ASE than ART_L. Also, for low values of γ, when $\kappa_0 = 0$, we see that $\text{ART}_L = \text{MASA}_{(N-1)\times 1}$ for $N = L \geq 2$.

4.2 Feedback Load

In Fig. B.5, we have plotted the minimum average feedback load of each of the two schemes (given in (B.9) and (B.15)). Comparing Fig. B.4 and Fig. B.5 the general picture is, as expected, that there is a trade-off between average spectral efficiency and feedback load. Also, when $\kappa_0 = 0$,

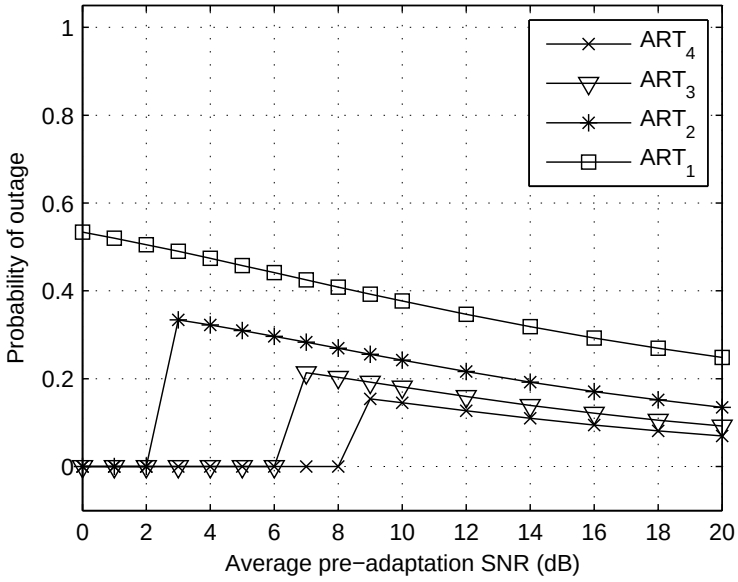

Figure B.3: Probability of outage for the ART schemes.

$\text{AFL}_{\text{ART}_L} = \text{AFL}_{\text{MASA}_{(N-1)\times 1}}$, see for example the feedback load of MASA_3 and ART_4 for $\gamma = 0$-8 dB in Fig. B.5b. However, it is very interesting to note that at some points the $\text{MASA}_{N\times 1}$ scheme offers a *higher* spectral efficiency at a *lower* feedback load. This contrasts previous claims that the "artificial constraint of zero outage leads to a big performance penalty" [7]. For example, consider ART_2 from Fig. B.5a in the range of γ between $3 - 7$ dB, then the feedback load is higher than that of $\text{MASA}_{2\times 1}$, while from Proposition 1, and as seen in Fig. B.4a, $\text{MASA}_{2\times 1}$ has a higher spectral efficiency.

5 Conclusions

We have studied two different design philosophies for adaptive transmission over slowly-varying flat-fading wireless channels with limited channel state information at the transmitter. The contrasted methods are the maximum average spectral efficiency for adaptive coded modulation (MASA) scheme, and the average reliable throughput (ART) maximizing scheme. Both schemes utilize capacity-achieving codes for AWGN channels, and one power level per code. However, the schemes differ in their design objectives, and how they deal with information outage. The $\text{MASA}_{N\times 1}$

scheme maximizes the ASE, given a fixed and finite number (N) of *available rates*, and by design has zero outage. On the other hand, the ART_L scheme starts from a fixed and finite number (L) of *available SNR quantization regions*, and then maximizes the ASE. As opposed to MASA, the ART approach thus allows for a non-zero information outage. To facilitate reliable communications, we extended the traditional ART scheme in a cross layer fashion, to include a retransmission option.

Through a mathematical analysis both schemes are evaluated in terms of average spectral efficiency and average feedback load. In addition, for the ART_L scheme, the probability of outage is also quantified numerically. Comparing the two approaches, our results show that for $N = L$, $\text{MASA}_{N\times 1}$ achieves the highest spectral efficiency, whereas in general the ART_L scheme has the lowest feedback load, and hence there is a trade-off. However, we also identify some settings for which the $\text{MASA}_{N\times 1}$ scheme offers *both* the highest spectral efficiency and the lowest feedback load for a given average SNR. This is a consequence of our cross-layered approach and our feedback load metric, and is in contrast to conclusions previously found in the literature.

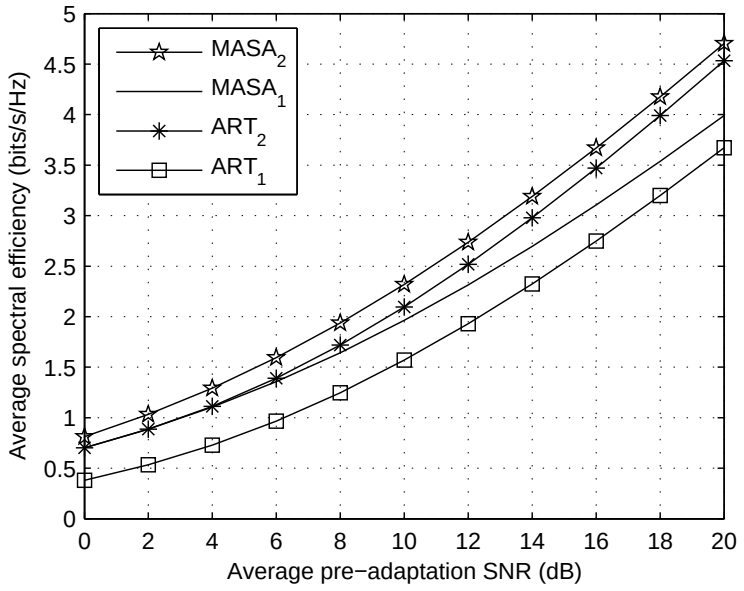

(a) $N, L \in \{1, 2\}$

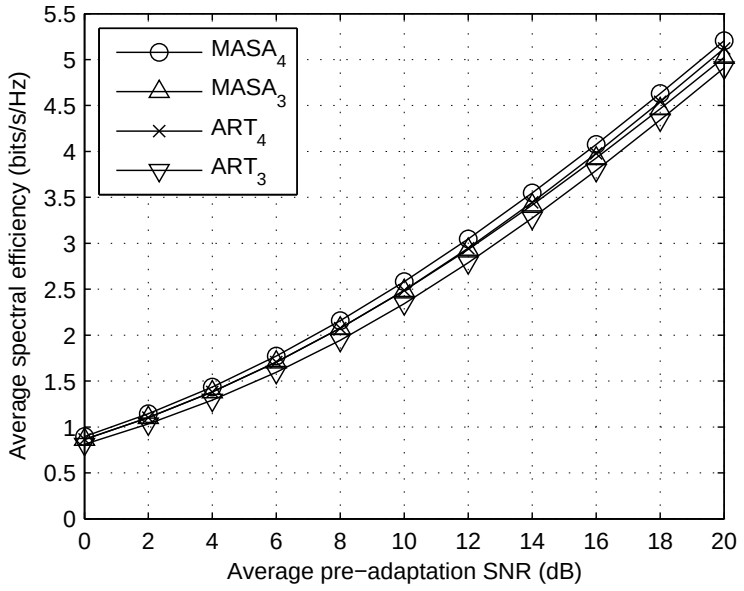

(b) $N, L \in \{3, 4\}$

Figure B.4: Average spectral efficiency versus average pre-adaptation SNR.

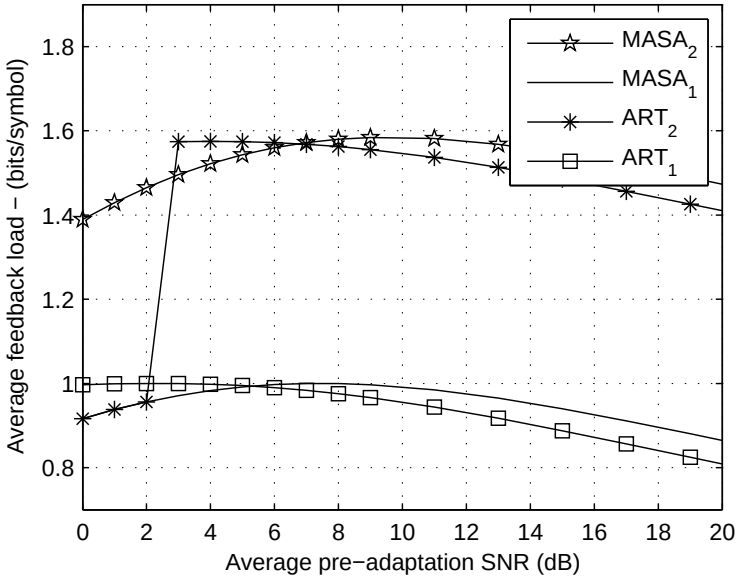

(a) $N, L \in \{1, 2\}$

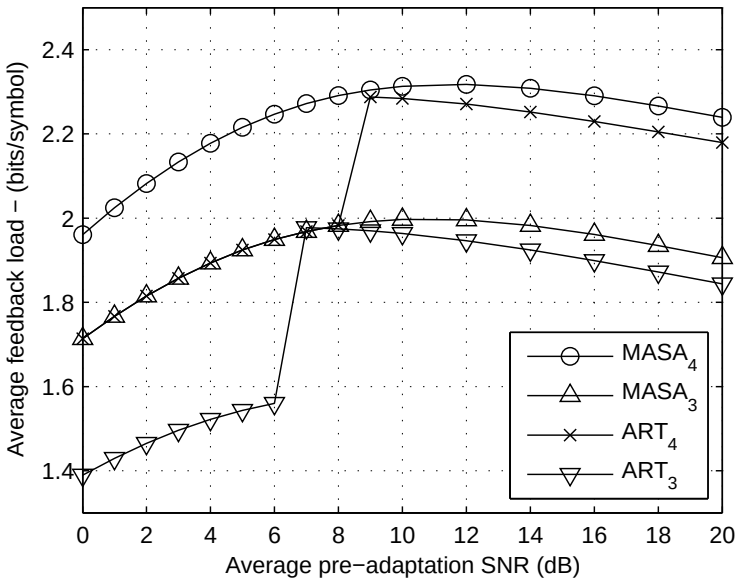

(b) $N, L \in \{3, 4\}$

Figure B.5: Feedback load versus average pre-adaptation SNR.

References

[1] ETSI. Digital Video Broadcasting - Satellite Version 2. [Online]. Available: http://www.dvb.org.

[2] A. J. Goldsmith and P. P. Varaiya, "Capacity of fading channels with channel side information," *IEEE Transactions on Information Theory*, vol. 43, no. 6, pp. 1986–1992, Nov. 1997.

[3] A. J. Goldsmith and S.-G. Chua, "Variable-rate variable-power M-QAM for fading channels," *IEEE Transactions on Communications*, vol. 45, no. 10, pp. 1218–1230, Oct. 1997.

[4] K. J. Hole, H. Holm, and G. E. Øien, "Adaptive multidimensional coded modulation over flat fading channels," *IEEE Journal on Selected Areas in Communications*, vol. 18, no. 7, pp. 1153–1158, July 2000.

[5] H. Holm, "Adaptive coded modulation performance and channel estimation tools for flat fading channels," Ph.D. dissertation, Norwegian University of Science and Technology, 2002. [Online]. Available: http://www.iet.ntnu.no/projects/beats/

[6] L. Hanzo, C. H. Wong, and M.-S. Yee, *Adaptive Wireless Transceivers: Turbo-Coded, Turbo-Equalized and Space-Time Coded TDMA, CDMA and OFDM Systems*. John Wiley & Sons, Inc., 2002.

[7] L. Lin, R. D. Yates, and P. Spasojević, "Adaptive transmission with discrete code rates and power levels," *IEEE Transactions on Communications*, vol. 51, no. 12, pp. 2115–2125, Dec. 2003.

[8] B. Holter, "Adaptive coded modulation in spatial and multiuser diversity systems," Ph.D. dissertation, Norwegian University of Science and Technology, 2005. [Online]. Available: http://www.iet.ntnu.no/projects/beats/

[9] T. T. Kim and M. Skoglund, "On the expected rate of slowly fading channels with quantized side information," *IEEE Transactions on Communications*, vol. 8, no. 4, pp. 820–829, April 2007.

[10] *Proceedings of the IEEE, Special Issue on Adaptive Transmission*, Oct. 2007.

[11] C. Köse and D. L. Goeckel, "On power adaptation in adaptive signalling systems," *IEEE Transactions on Communications*, vol. 48, no. 11, pp. 1769–1773, Nov. 2000.

[12] J. F. Paris, M. del Carmen Aguayo-Torres, and J. T. Entrambasaguas, "Optimum discrete-power adaptive QAM scheme for Rayleigh fading channels," *IEEE Communication Letters*, vol. 5, no. 1, pp. 281–283, July 2001.

[13] C. Byoungjo and L. Hanzo, "Optimum mode-switching-assisted constant power single- and multicarrier adaptive modulation," *IEEE Transactions on Vehicular Technology*, vol. 52, no. 3, pp. 536–560, May 2003.

[14] A. Gjendemsjø, G. E. Øien, H. Holm, M. S. Alouini, D. Gesbert, K. J. Hole, and P. Orten, "Rate and power allocation for discrete-rate link adaptation," revised for the EURASIP Journal on Wireless Communications and Networking, Oct. 2007. [Online]. Available: http://www.iet.ntnu.no/~gjendems/publications

[15] A. Goldsmith, *Wireless Communications*. New York: Cambridge University Press, 2005.

[16] R. J. McEliece and W. E. Stark, "Channels with block interference," *IEEE Transactions on Information Theory*, vol. IT-30, no. 1, pp. 44–53, Jan. 1984.

[17] C. E. Shannon, "A mathematical theory of communication," *Bell System Technical Journal*, vol. 27, pp. 379–423 and 623–656, July and Oct. 1948.

Paper C

Joint Adaptive Transmission and Combining with Optimized Rate and Power Allocation

Anders Gjendemsjø, Hong-Chuan Yang, Mohamed-Slim Alouini, and Geir E. Øien

In *Proc. IEEE Workshop on Signal Processing Advances in Wireless communications (SPAWC'06)*, Cannes, France, July 2006, pp. 1-5.

Abstract

We consider the problem of finding optimal transmission rates and power allocation under the framework of diversity combining. Capitalizing on recent results for both link adaptation schemes and adaptive combining, we design and analyze two joint link adaptation and diversity combining schemes. Based on the channel fading, the proposed schemes adaptively select both the signal constellation and diversity combiner structure. We show that the novel schemes provide significant throughput gains compared to existing joint adaptive QAM and diversity schemes. Further, contrary to previous results on power control for discrete rate link adaptation, power control does not give significant average spectral efficiency gains in this jointly adaptive setting. However, power control yields significant probability of no transmission gains over the constant power schemes.

Compared to the published version, we have made minor modifications to this paper in order to be consistent, over the papers included in this thesis, with respect to use of the terms outage, information outage and probability of no transmission.

A. Gjendemsjø, and G. E. Øien (e-mails: {gjendems,oien}@iet.ntnu.no) are with the Department of Electronics and Telecommunications, Norwegian University of Science and Technology, Trondheim, Norway.

H.-C. Yang (e-mail: hyang@ece.uvic.ca) is with the Dept. of ECE, University of Victoria, Victoria, Canada.

M.-S. Alouini (e-mail: alouini@qatar.tamu.edu) is with the Dept. of ECE, Texas A&M University-Qatar, Education City, Doha, Qatar.

1 Introduction

The need for ever higher spectrum efficiency motivates the search for optimization of the wireless resources. Resource management in wireless communications is a difficult task due to user mobility and highly time-variant propagation environments, thus implying adaptive solutions. Key adaptive techniques are those of adaptive modulation [1; 2], power control [3; 4], and adaptive combining [5–8].

In [6; 5] new jointly adaptive modulation and combining schemes based on a multiple threshold idea are introduced. [6; 5] evaluate the proposed schemes by adopting a constant-power variable-rate uncoded M-QAM scheme. Given a target bit error rate (BER), the adaptive modulator thresholds are then *predetermined*. Since the thresholds are predetermined, the scheme will not be able to fully take advantage of the time-varying nature of the fading channel, in terms of spectral and power efficiency. It is then natural to seek optimal thresholds based on the fading statistics. Further, by utilizing the framework of [4] power control can be introduced.

In this paper we tackle the problem of maximizing the average spectral efficiency (ASE) by finding optimal transmission rates and power control schemes for adaptive diversity combining over Rayleigh fading channels. We show that the proposed schemes offer large ASE gains over the previous QAM schemes discussed in [6; 5], by better taking advantage of the time-varying nature of the wireless channel. Introducing power control gives a significant reduction in probability of no transmission. However, as opposed to previous results on power control for discrete rate link adaptation, power control does not give significant ASE gains in this jointly adaptive setting [4].

The remainder of the present paper is organized as follows. In Section 2, we introduce the diversity model and review results on QAM-based adaptation. Optimal transmission schemes are derived and analyzed in Section 3. Numerical examples and plots are presented in Section 4. Finally, conclusions are given in Section 5.

2 Diversity System and QAM Adaptation

2.1 GSC Diversity

We assume a generic diversity system with L available diversity branches, as shown in Fig. C.1. The received signal on each diversity branch is assumed to experience independent identically distributed (iid) Rayleigh fading. Due to hardware complexity and power considerations, a maxi-

mum of L_c branches can be combined at the receiver side ($L_c \leq L$).

By estimating and ranking the L instantaneous branch SNRs in descending order, i.e., $\gamma_{1:L} > \gamma_{2:L} > \cdots > \gamma_{L:L}$, then GSC will combine the L_c best branches only, using MRC weights, yielding a combined SNR of $\gamma_{\text{GSC}} = \sum_{l=1}^{L_c} \gamma_{l:L}$.

Let $\overline{\gamma}$ denote the common average SNR on each branch. Then, the probability density function of the received SNR at the output of a GSC combiner is given by [9, Eq. (16)]:

$$\begin{aligned} f_{\gamma\text{GSC}}^{(L/L_c)}(\gamma_c) = \binom{L}{L_c} \Bigg[& \frac{{\gamma_c}^{L_c-1} e^{-\gamma_c/\overline{\gamma}}}{{\gamma_c}^{L_c}(L_c-1)!} + \frac{1}{\overline{\gamma}} \\ & \times \sum_{l=1}^{L-L_c} (-1)^{L_c+l-1} \binom{L-L_c}{l} \left(\frac{L_c}{l}\right)^{L_c-1} e^{-\gamma_c/\overline{\gamma}} \\ & \times \left(e^{-l\gamma_c/L_c\overline{\gamma}} - \sum_{m=0}^{L_c-2} \frac{1}{m!} \left(\frac{-l\gamma_c}{L_c\overline{\gamma}} \right)^m \right) \Bigg]. \end{aligned} \tag{C.1}$$

Now, by integrating (C.1) we find the cumulative density function of the received SNR as [9, Eq. (24)]

$$\begin{aligned} F_{\gamma\text{GSC}}^{(L/L_c)}(\gamma_c) = \binom{L}{L_c} \Bigg[& 1 - e^{-\gamma_c/\overline{\gamma}} \sum_{l=0}^{L_c-1} \frac{\left(\frac{\gamma_c}{\overline{\gamma}}\right)^l}{l!} \\ & + \sum_{l=1}^{L-L_c} (-1)^{L_c+l-1} \binom{L-L_c}{l} \left(\frac{L_c}{l}\right)^{L_c-1} \\ & \times \frac{1 - e^{-(1+(l/L_c))(\gamma_c/\overline{\gamma})}}{1+\frac{l}{L_c}} - \sum_{m=0}^{L_c-2} \left(\frac{-l}{L_c}\right)^m \\ & \times \left(1 - e^{-\gamma_c/\overline{\gamma}} \sum_{k=0}^{m} \frac{\left(\frac{\gamma_c}{\overline{\gamma}}\right)^k}{k!} \right) \Bigg]. \end{aligned} \tag{C.2}$$

The average number of combined branches will quantify the processing power consumed by the diversity combining [5]. We denote by B_c and $\gamma_{\text{T}_{1,1}}$ the number of combined branches and the minimum required combined SNR for transmission, respectively. Then, L_c branches are combined when $\gamma_{\text{GSC}} \geq \gamma_{\text{T}_{1,1}}$, and 0 branches otherwise, i.e., the system gives up on the channel and buffers the data. The average number of GSC-combined branches is then given as

$$\overline{B}_c = L_c(1 - F_{\gamma\text{GSC}}^{(L/L_c)}(\gamma_{\text{T}_{1,1}})). \tag{C.3}$$

In Section 3, to simplify the notation we write $F_{\gamma\text{GSC}}^{(L/L_c)}(\cdot)$ and $f_{\gamma\text{GSC}}^{(L/L_c)}(\cdot)$ as $F_{\gamma_c}(\cdot)$ and $f_{\gamma_c}(\cdot)$, respectively.

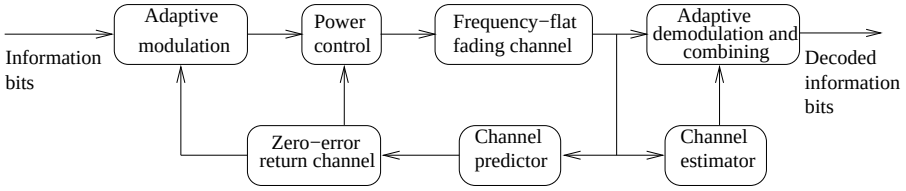

Figure C.1: Transmission system block diagram.

2.2 M-QAM Based Link Adaptation

As the baseline case we consider the constant power M-ary QAM scheme studied in [6; 5]. This scheme, denoted by η_N, consists of N signal constellations of size $M = 2^n$, where $1 \leq n \leq N$. Given a target bit error rate BER_0, the switching threshold corresponding to constellation n is given as follows[6, Eq. (4)]

$$\gamma_{\text{T}_{n,1}} = -\frac{2}{3}\ln(5\text{BER}_0)(2^n - 1). \tag{C.4}$$

The average spectral efficiency η_N of this M-QAM scheme is then found as [5, Eq. (15)]

$$\eta_N = N - \sum_{n=1}^{N} F_{\gamma\text{GSC}}^{(L/L_c)}(\gamma_{\text{T}_{n,1}}). \tag{C.5}$$

2.3 Bandwidth Efficient Scheme with MS-GSC

In MS-GSC, the *minimum* number of branches is combined with MRC weights, such that the output of the combiner is larger than or equal to a given threshold γ_T. Thus, if B_c denotes the number of branches selected out of L available branches, then B_c is the minimum number $\in \{1, 2, \cdots, L_c\}$, for which $\sum_{l=1}^{B_c} \gamma_{l:L} \geq \gamma_T$ is satisfied [7].

Our objective is to design bandwidth efficient schemes, so to maximize the spectral efficiency we employ the bandwidth efficient versions of the link adaptation and diversity schemes presented in [5]. As a consequence, the receiver tries to combine a minimum number of branches to support the highest transmission rate. When MS-GSC is combined with link adaptation in a bandwidth efficient mode, its spectral efficiency is equal to that of GSC combining [6], but at the same time MS-GSC offers a reduction in the average number of combined branches, and thus processing power savings. Therefore, we derive the optimal switching thresholds and power levels based on the GSC receiver and evaluate the power savings by utilizing these values in a MS-GSC system.

For MS-GSC, $\overline{B}_c$ can be found by generalizing [5, Eq.(14)], in which $\overline{B}_c$ is derived only for the case of $L_c = L$. To obtain $\overline{B}_c$ for $L_c \leq L$, we modify[1] [5, Eq. (14)], yielding

$$\overline{B}_c = 1 + \sum_{l=1}^{L_c-1} F_{\gamma\text{GSC}}^{L/l}(\gamma_{\text{T}_{N,1}}) - L_c F_{\gamma\text{GSC}}^{L/L_c}(\gamma_{\text{T}_{1,1}}). \tag{C.6}$$

3 Optimal Schemes for GSC-Based Systems

3.1 System Model

We consider a wireless channel with additive white gaussian noise (AWGN) and fading. Under the assumption of slow, frequency-flat fading, we may use a block-fading model to approximate the wireless fading channel by an AWGN channel within the length of a codeword [10]. Thus, the system may use codes which typically guarantee a certain target spectral efficiency within a range of SNRs on an AWGN channel.

We denote the instantaneous *pre-adaptation* combined SNR by $\gamma_c[i]$. This is the SNR that would be experienced using signal constellations of average power $\overline{S}$ without power control [2]. Assuming, as in [1], that the transmitter receives perfect channel predictions, sent over a zero-error feedback channel, we can adapt the transmit power instantaneously at time i according to a power adaptation scheme $S(\gamma_c[i])$, as shown in Fig. C.1. The received *post-adaptation* SNR at time i is then given by $\gamma_c[i]\frac{S(\gamma_c[i])}{\overline{S}}$. By virtue of a stationarity assumption, the distribution of $\gamma_c[i]$ is independent of i, and is denoted by $f_{\gamma_c}(\gamma_c)$. To simplify the notation we omit the time reference i from now on.

The transmission scheme is to be based on a set of N codes, each associated with K power levels. The choice of code and power level is at any time based on the fading channel state. Following [1; 4], we partition the range of the combined SNR γ_c into $NK + 1$ *pre-adaptation* regions, which are defined by the switching thresholds $\{\gamma_{\text{T}_{n,k}}\}$, as illustrated in Fig. C.2. Code n, with spectral efficiency R_n, is selected whenever γ_c is in the interval $[\gamma_{\text{T}_{n,1}}, \gamma_{\text{T}_{n+1,1}})$. Within this interval the transmission rate is constant, but the system can adapt the transmitted power to the channel conditions in order to maximize the average spectral efficiency. When $\gamma_c < \gamma_{\text{T}_{1,1}}$ data is buffered. For convenience, we let $\gamma_{\text{T}_{0,1}} = 0$ and $\gamma_{\text{T}_{N+1,1}} = \infty$.

[1]The upper summation limit of [5, Eq. (14)] is changed from $L-1$ to L_c-1, and the combining scheme in the last term is changed from L branch MRC to L/L_c GSC.

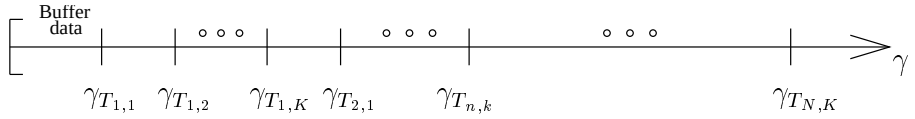

Figure C.2: The pre-adaptation SNR range is partitioned into regions where $\gamma_{\mathrm{T}_{n,k}}$ are the switching thresholds.

3.2 Spectral Efficiency Analysis

Using N distinct codes we analyze the obtainable spectral efficiencies of the L/L_c-GSC schemes, under discrete and constant transmit power adaptation. We shall assume that the fading is so slow that Shannon capacity-achieving codes for AWGN channels can be employed [2].

Now, recall that the pre-adaptation combined SNR range is divided into regions lower bounded by $\gamma_{\mathrm{T}_{n,1}}$, $1 \leq n \leq N$. Thus, we let $R_n = C_n$, where $C_n = \log_2\big(1 + \frac{S(\gamma_{\mathrm{T}_{n,1}})}{\overline{S}}\gamma_{\mathrm{T}_{n,1}}\big)$ is the highest spectral efficiency that can be supported within the range $[\gamma_{\mathrm{T}_{n,1}}, \gamma_{\mathrm{T}_{n+1,1}})$ for $1 \leq n \leq N$, after transmit power adaptation [4]. Each SNR region's contribution to the ASE of the scheme is the spectral efficiency of the nth code, times the probability $P_n = \int_{\gamma_{\mathrm{T}_{n,1}}}^{\gamma_{\mathrm{T}_{n+1,1}}} f_{\gamma_c}(\gamma_c)\,\mathrm{d}\gamma_c$ that it is employed. An upper bound ψ on the ASE —for a given set of codes/switching levels—is therefore given as

$$\psi = \sum_{n=1}^{N} \log_2\big(1 + \frac{S(\gamma_{\mathrm{T}_{n,1}})}{\overline{S}}\gamma_{\mathrm{T}_{n,1}}\big) \int_{\gamma_{\mathrm{T}_{n,1}}}^{\gamma_{\mathrm{T}_{n+1,1}}} f_{\gamma_c}(\gamma_c)\,\mathrm{d}\gamma_c, \tag{C.7}$$

subject to the average power constraint,

$$\sum_{n=1}^{N} \int_{\gamma_{\mathrm{T}_{n,1}}}^{\gamma_{\mathrm{T}_{n+1,1}}} S(\gamma_c) f_{\gamma_c}(\gamma_c)\,\mathrm{d}\gamma_c \leq \overline{S}, \tag{C.8}$$

where $\overline{S}$ denotes the average transmit power.

If arbitrarily long codewords can be used, the bound can be approached from below with arbitrary precision for an arbitrarily low BER. Our goal is now to find optimal switching levels and power adaptation schemes in order to maximize the ASE in a GSC diversity environment.

[2] The existence of such codes is guaranteed by Shannon's channel coding theorem. However, we do not address the important problem of constructing such codes, which is a research problem in itself.

3.3 Discrete-Power Transmission Scheme

For practical scenarios the resolution of power control will be limited, e.g., for the Universal Mobile Telecommunications System (UMTS) power control step sizes on the order of 1 dB are proposed [11]. Further, continuous power control is not feasible as it would require an infinite capacity feedback channel. We thus analyze discrete power adaptation, by considering the $\psi_{N\times K}$ scheme where we allow for $K \geq 1$ power regions *within* each of the N rate regions.

The optimal discrete-level power control was shown in [4] to be discretized piecewise channel inversion. Now, by defining[3] $\beta_n \triangleq \frac{S(\gamma_{\mathrm{T}_{n,1}})}{\bar{S}}\gamma_{\mathrm{T}_{n,1}}$, the ASE maximization problem can be formulated as follows [4]. Find $\{\beta_n, \gamma_{\mathrm{T}_{n,k}}\}$ to maximize

$$\psi_{N\times K} = \sum_{n=1}^{N} \log_2(1+\beta_n) \int_{\gamma_{\mathrm{T}_{n,1}}}^{\gamma_{\mathrm{T}_{n+1,1}}} f_{\gamma_c}(\gamma_c)\,\mathrm{d}\gamma_c, \tag{C.9}$$

such that

$$\sum_{n=1}^{N} \beta_n \sum_{k=1}^{K} \frac{1}{\gamma_{\mathrm{T}_{n,k}}} \int_{\gamma_{\mathrm{T}_{n,k}}}^{\gamma_{\mathrm{T}_{n,k+1}}} f_{\gamma_c}(\gamma_c)\,\mathrm{d}\gamma_c \leq 1, \tag{C.10}$$

where $\gamma_{\mathrm{T}_{n,K+1}} \triangleq \gamma_{\mathrm{T}_{n+1,1}}$. The solution is found by using constrained numerical optimization, cf. [4].

3.4 Constant-Power Transmission Scheme

When a single transmission power is used for all codes, the term *constant power transmission scheme* is used. From [4] the expression to optimize is then given by

$$\psi_N = \sum_{n=1}^{N} \log_2\Big(1 + \frac{\gamma_{\mathrm{T}_{n,1}}}{1 - F_{\gamma_c}(\gamma_{\mathrm{T}_{1,1}})}\Big) \int_{\gamma_{\mathrm{T}_{n,1}}}^{\gamma_{\mathrm{T}_{n+1,1}}} f_{\gamma_c}(\gamma_c)\,\mathrm{d}\gamma_c. \tag{C.11}$$

Now, by differentiation of (C.11), we can reduce the N-dimensional optimization to a 2-dimensional one [4], and the optimal switching thresholds follow by solving the reduced problem.

4 Numerical Results

In the following we have used $L = 7$, $L_c = 4$ and $N = 4$.

[3] β_n corresponds to the minimum post-adaptation combined SNR in the region $[\gamma_{\mathrm{T}_{n,1}}, \gamma_{\mathrm{T}_{n+1,1}})$.

Table C.1: Switching thresholds $\{\gamma_{\mathrm{T}_{n,1}}\}_{n=1}^{4}$ (dB)

$\overline{\gamma}$	η_4	ψ_4	$\psi_{4\times4}$
5 dB	5.5, 10.3, 13.9, 17.2	8.6, 10.7, 12.1, 13.5	7.2, 10.5, 12.2, 13.7
15 dB	5.5, 10.3, 13.9, 17.2	17.5, 20.2, 21.9, 23.3	16.0, 20.4, 22.3, 24.1

4.1 Switching Levels and Average Spectral Efficiencies

Table C.1 shows the optimal switching levels $\{\gamma_{\mathrm{T}_{n,1}}\}$ of the η_4, ψ_4, and $\psi_{4\times4}$ schemes for $\overline{\gamma} = \{5, 15\}$ dB. For the η_4 scheme the switching levels are independent of $\overline{\gamma}$, while the ψ schemes are adapted to the channel statistics, yielding increasing $\{\gamma_{\mathrm{T}_{n,1}}\}$ with increasing $\overline{\gamma}$, to maximize the ASE.

Fig. C.3 depicts an ASE comparison of the optimized discrete power and constant power schemes (C.9), (C.11), and the QAM scheme (C.5) operating at a target bit error rate of $\mathrm{BER}_0 = 10^{-3}$. The ASE obtained by $\psi_{4\times8}$ can be seen as an approximation to the case of variable-rate continuous-power transmission scheme [4, Section III-A]. Then it is clear from the figure that optimal power adaptation seems to yield insignificant gains over the constant power transmission schemes, contrary to the findings for a SISO link in [4].

Further, from $0 \leq \overline{\gamma}\,\mathrm{dB} \leq 10$, the four ψ schemes give an increase in spectral efficiency of approximately 2 bps/Hz over the QAM scheme. As $\overline{\gamma}$ increases the QAM scheme saturates at 4 bps/Hz, corresponding to utilizing $16-$QAM with a probability close to 1. The large gap between the QAM and the optimized schemes indicates that significant spectral efficiency gains are possible by clever system design.

4.2 Probability of No Transmission

When γ_c is less than the smallest signal constellation threshold $\gamma_{\mathrm{T}_{1,1}}$ no data is sent. The probability of no transmission $P_{\text{no tr.}}$ can then be calculated as

$$P_{\text{no tr.}} = \Pr\left(\gamma_c < \gamma_{\mathrm{T}_{1,1}}\right) = F_{\gamma_{\mathrm{GSC}}}^{(L/L_c)}(\gamma_{\mathrm{T}_{1,1}}). \tag{C.12}$$

In Fig. C.4 we have plotted $P_{\text{no tr.}}$ as a function of $\overline{\gamma}$. As expected from Table C.1, for the ψ schemes the probability of no transmission decreases both as power adaptation is introduced, as well as with increasing $\overline{\gamma}$. For the QAM scheme $P_{\text{no tr.}}$ decreases much faster than for the ψ schemes, which is due to the fact that $\gamma_{\mathrm{T}_{1,1}}$ for the QAM scheme is fixed and independent of $\overline{\gamma}$, whereas for the other schemes it is adapted to the underlying fading distribution for every value of $\overline{\gamma}$.

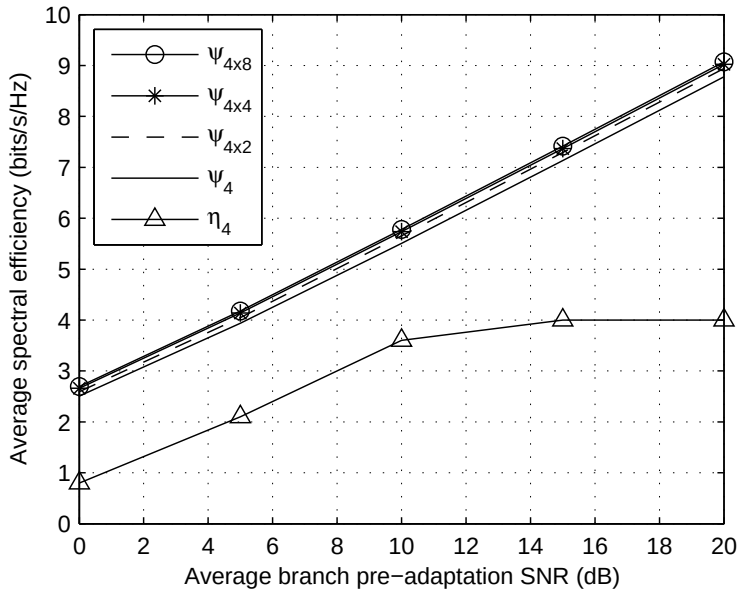

Figure C.3: Link adaptation average spectral efficiency.

It is not necessarily a disadvantage that the probability of no transmission is high. For data-centric services, the most important thing from a quality-of-service point of view is probably the total time of data downloading experienced by a user. For large data sets, this time will be minimized independently of the value $P_{\text{no tr.}}$, as long as the average spectral efficiency is maximized. However, for multimedia services with delay requirements, the probability of no transmission can be important. Thus it is interesting to see that $P_{\text{no tr.}}$ is considerably reduced when power adaptation is used.

4.3 Processing Power

For terminals with limited battery, receiver processing power is of high importance. By keeping fewer branches active, the power consumption in the receiver can be reduced [5]. Fig. C.5 shows the average number of combined branches as a function of $\overline{\gamma}$, for GSC and MS-GSC implementations of the ψ_4 and η_4 schemes. It is seen that MS-GSC reduces the average number of combined branches for both schemes over the entire SNR range. Compared to the M-QAM scheme, the optimal schemes show less reduction from an MS-GSC implementation, which is a direct consequence of the fact

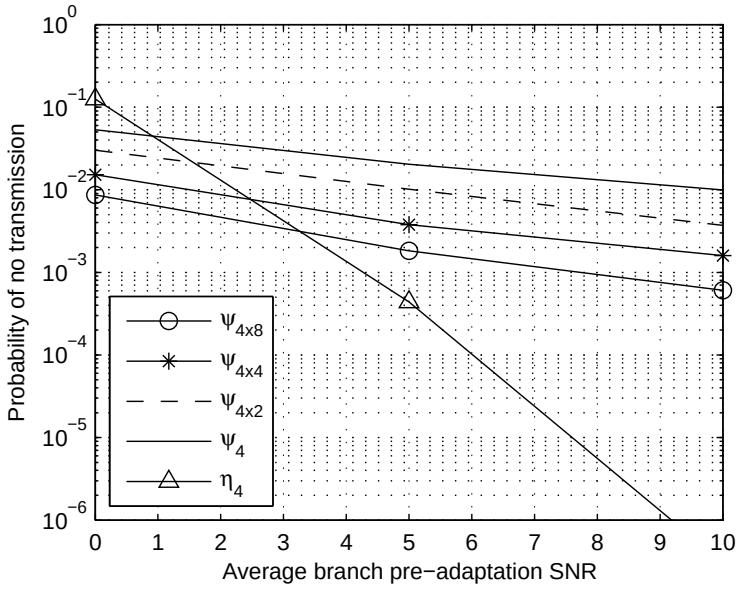

Figure C.4: Probability of no transmission as a function of average branch pre-adaptation SNR.

that the ψ schemes use the increased combined SNR at higher $\overline{\gamma}$ to facilitate higher spectral efficiencies, while the QAM saturates and will on average need to combine fewer branches.

5 Conclusions

We have analyzed optimal rate and power allocation for a joint link adaptation and adaptive combining system, under an average spectral efficiency maximization criterion and both average power and diversity combining constraints. Given the channel fading condition information the proposed schemes maximizes the obtainable channel spectral efficiency.

Compared to joint adaptive M-QAM schemes, our proposed schemes give significant ASE gains. Contrary to previous work on power control for discrete rate link adaptation, we have shown that when jointly optimized with adaptive combining, power control does not significantly increase the average spectral efficiency. However, it does significantly decrease the probability of no transmission, which is important for some multimedia networks which not only offer high-rate data-based services, but also low-rate services with real-time or low-latency requirements.

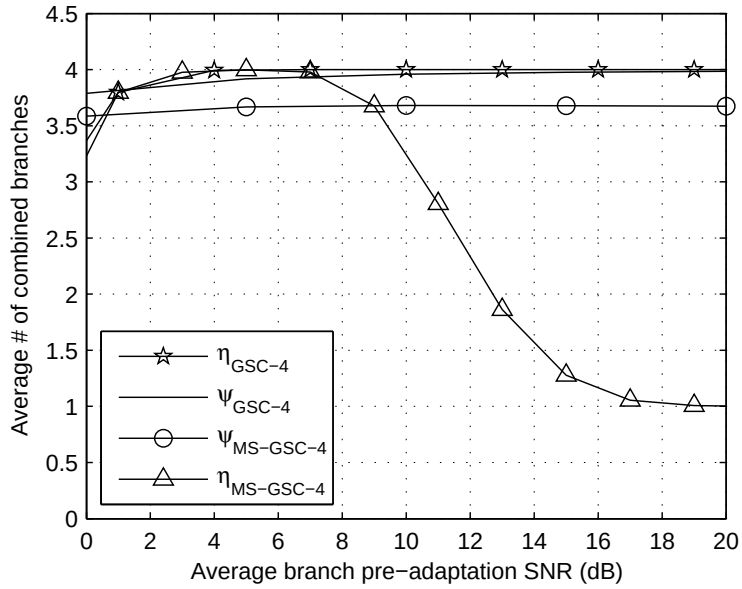

Figure C.5: Average number of combined branches for link adaptation schemes.

References

[1] A. J. Goldsmith and S.-G. Chua, "Variable-rate variable-power M-QAM for fading channels," *IEEE Transactions on Communications*, vol. 45, no. 10, pp. 1218–1230, Oct. 1997.

[2] K. J. Hole, H. Holm, and G. E. Øien, "Adaptive multidimensional coded modulation over flat fading channels," *IEEE Journal on Selected Areas in Communications*, vol. 18, no. 7, pp. 1153–1158, July 2000.

[3] A. Gjendemsjø, G. E. Øien, and H. Holm, "Optimal power control for discrete-rate link adaptation schemes with capacity-approaching coding," in *Proc. IEEE Global Telecommunications Conference*, St. Louis, MO, Nov.-Dec. 2005, pp. 3498–3502.

[4] A. Gjendemsjø, G. E. Øien, H. Holm, M. S. Alouini, D. Gesbert, K. J. Hole, and P. Orten, "Rate and power allocation for discrete-rate link adaptation," revised for the EURASIP Journal on Wireless Communications and Networking, Oct. 2007. [Online]. Available: http://www.iet.ntnu.no/~gjendems/publications

[5] H.-C. Yang, N. Belhaj, and M.-S. Alouini, "Performance analysis of joint adaptive modulation and diversity combining over fading channels," *IEEE Transactions on Communications*, vol. 55, no. 3, pp. 520–528, March 2007.

[6] N. Belhaj, N. Hamdi, M.-S. Alouini, and A. Bouallegue, "Low-power minimum estimation and combining with adaptive modulation," in *Proc. IEEE International Symposium on Signal Processing and its Applications*, Sydney, Australia, Aug. 2005, pp. 687–690.

[7] P. Gupta, N. Bansal, and R. K. Mallik, "Analysis of minimum selection GSC in Rayleigh fading," in *Proc. IEEE International Conference on Communications*, Paris, France, June 2004, pp. 3364–3368.

[8] S. W. Kim, D. S. Ha, and J. Reed, "Minimum selection GSC and adaptive low-power RAKE combining scheme," in *Proc. IEEE International Symposium on Circuits and Systems*, Bangkok, Thailand, May 2003, pp. 357–360.

[9] M.-S. Alouini and M. K. Simon, "An MGF-based performance analysis of generalized selection combining over Rayleigh fading channels," *IEEE Transactions on Communications*, vol. 48, no. 3, pp. 401–415, March 2000.

[10] R. J. McEliece and W. E. Stark, "Channels with block interference," *IEEE Transactions on Information Theory*, vol. IT-30, no. 1, pp. 44–53, Jan. 1984.

[11] *Physical Layer Procedures (TDD)*, Third Generation Partnership Project, Technical Specification Group Radio Access Network Std., Rev. TS25.224 (Release 7), March 2006.

Paper D

Binary Power Control for Sum Rate Maximization over Multiple Interfering Links

Anders Gjendemsjø, David Gesbert, Geir E. Øien, and Saad G. Kiani

To appear in the *IEEE Transactions on Wireless Communications*.

Abstract

We consider allocating the transmit powers for a wireless multi-link (N-link) system, in order to maximize the total system throughput under interference and noise impairments, and short term power constraints. Employing dynamic spectral reuse, we allow for centralized control. In the two-link case, the optimal power allocation then has a remarkably simple nature termed *binary* power control: Depending on the noise and channel gains, assign full power to one link and minimum to the other, or full power on both.

Binary power control (BPC) has the advantage of leading towards simpler or even distributed power control algorithms. For $N > 2$ we propose a strategy based on checking the corners of the domain resulting from the power constraints to perform BPC. We identify scenarios in which binary power allocation can be proven optimal also for arbitrary N. Furthermore, in the general setting for $N > 2$, simulations demonstrate that a throughput performance with negligible loss, compared to the best non-binary scheme found by geometric programming, can be obtained by BPC. Finally, to reduce the complexity of optimal binary power allocation for large networks, we provide simple algorithms achieving 99% of the capacity promised by exhaustive binary search.

Parts of this paper were presented at the 2006 International Symposium on Modeling and Optimization in Mobile, Ad Hoc, and Wireless Networks (WiOpt '06), Boston, MA, April 2006, and at the IEEE Workshop on Signal Processing Advances in Wireless communications (SPAWC'07), Helsinki, Finland, June 2007.

A. Gjendemsjø and G. E. Øien (e-mails: {gjendems,oien}@iet.ntnu.no) are with the Dept. of Electronics and Telecommunications, Norwegian University of Science and Technology (NTNU), Trondheim, Norway.

D. Gesbert and S. G. Kiani (e-mails: {gesbert,kiani}@eurecom.fr) are with the Institut Eurécom, Sophia-Antipolis, France.

1 Introduction

The need for ever higher spectrum efficiency motivates the search for system-wide optimization of the wireless resources. A key example of multi-link resource allocation is that of power control, which serves as means for both battery savings at the mobile, and for interference management. Traditional power control solutions are designed for voice-centric networks, hence aiming at guaranteeing a target signal-to-noise-and-interference ratio (SNIR) level to the users [1–3]. In modern wireless data networks, adaptive coding and modulation with power control [4; 5] is or will be implemented, and throughput maximization becomes a more relevant metric.

The simultaneous optimization of transmission rates and power with the aim of maximizing the multi-link sum capacity is a difficult problem, which perhaps explains why the problem has received relatively little attention in the past, although now it is clearly gaining interest [6; 7]. Considering the problem of optimally allocating the transmit power for N concurrent communication links, a common approach is to use a high SNIR approximation to establish convexity in the sum-throughput objective function [6; 7]. However, this approximation by construction prohibits completely turning off the power of any link at any time. This extra constraint may in fact cause the resulting power vector to steer away from the optimum solution in certain cases. Indeed one of the major points emphasized in the present work is that in the context of multi-link capacity maximization, the ability of shutting down one or more links (or transmitting at minimum allowed power > 0) in certain slots can be instrumental in approaching maximum network throughput.

By restricting the scenario to interference limited systems, i.e., neglecting noise sources, in [7] the high SNIR assumption is modified so that links contributing less than a fixed amount to the total throughput are dropped. For the remaining links the high SNIR approximation is still used. Although improvements over the schemes are presented in [6], "the proposed method is still inferior to maximization of the actual aggregate throughput" according to [7]. In [8], specializing to the case of uplink single-cell CDMA, i.e., N transmission links with a common receiver, and enforcing quality of service constraints, results on simplifying the power control search space are derived. However, in this paper we shall consider a more general system model, for which the uplink single-cell CDMA setting can be seen as a special case. Thus the results and conclusions from [8] are not in general applicable to our model.

Under a sum power constraint, the authors of [9] neglect noise sources

and use waterfilling to maximize the network capacity, while in [10], under the assumption of symmetric interference, a two-user power allocation that depends on the level of interference is derived. Due to the sum power constraint, the neglection of noise, and the symmetry-of-interference assumption these results are not applicable to our cellular system power allocation analysis. In our opinion, it is more reasonable to instead assume individual power constraints at every link, and that the received interference in general will be different for different users. Further, in [11], game-theoretic approaches are used to analyze a symmetric one-dimensional two-cell network, assuming the received power to be a function of the transmitter-receiver distance only. However, here we model any geometric setup, as well as allowing for arbitrary signal degradation, e.g., caused by path loss, multipath fading, or shadowing.

When modelling the transmission rate as a *linear* function of the received power, [12] shows that a link when active should transmit at maximum power for optimality. This result has the merit of showing potential benefits of an on/off power control, but in general, the assumed linear relationship between rate and power is however unfortunately far from the truth since the rate is known to have a $\log(\cdot)$ behavior. The proof does not extend to arbitrarily increasing rate-power relations, and the results will not in general yield throughput-optimal power allocation. Nevertheless, here we show that when using a *low SNIR approximation*, the linear relation in [12] is indeed obtained, and thus the conclusions from that paper holds in this case, and can be extended to include a minimum power constraint at each base station.

In this paper we tackle the problem of sum rate maximizing power allocation in multi-link networks with orthogonal MAC protocols without resorting to the previously described restricting assumptions of high SNIR, interference-limited systems, or interference symmetry. The application we have in mind is a wireless data access network with best-effort type of quality of service, and the total aggregate throughput (sum rate) across the network is the figure of merit. The system is assumed to be enabled with a perfect link adaptation protocol, so the user rate is adapted instantaneously as a function of the user's signal to noise and interference ratio, thus always achieving Shannon capacity in any resource slot. Extending [13], our contributions are as follows: In the two-link case, the optimal power allocation is analytically shown to be remarkably simple; transmit at full power at link 1, minimum at link 2, vice versa, or at full power at both links. Next, we consider the $N > 2$ case, and show that when either a geometric-arithmetic

mean or low-SNIR approximation is applicable, binary power control[1] is still optimal (as is always true for any SNIR in the $N = 2$ case). In the general case for $N > 2$, we utilize the mathematical framework of geometric programming [14] (GP) in order to establish a sum capacity benchmark, to compare our proposed binary power allocation with, through exhaustive simulations. Empirically, we demonstrate that the loss associated with restriction to binary power levels is negligible. On the other hand, discretizing the optimization space is highly beneficial: the feedback rate needed to communicate between network nodes is reduced, transmitter design is simplified, and finally, limiting the potential solutions to search over better facilitates distributed resource allocation [15].

For networks with a large number of links, we consider clustering groups of links as a way of lowering the power control complexity, as well as reducing the required channel knowledge. Through clustering significant complexity reduction is possible, at the cost of only a small reduction in network capacity. Finally, we propose a simple greedy approach to binary power control, and demonstrate that its throughput performance in a wide range of communication environments is virtually indistinguishable from that of exhaustive binary power search.

The remainder of the present paper is organized as follows. We introduce the wireless system model under investigation in Section 2. In Section 3 we derive optimal power control schemes that maximizes the sum throughput. Algorithms for reducing the complexity of binary power control by clustering and greedy approaches are presented in Section 4. In Section 5 numerical results are presented, and finally conclusions are given in Section 6.

2 System Model

We consider a wireless network featuring a number of transmitters and receivers, of which there are N active pairs selected for transmission by a scheduling (MAC) protocol. In order to focus solely on power control, we do not explicitly consider scheduling or MAC protocols here. However, note that the results presented in this paper are valid for any scheduling algorithm, as the effect of one such algorithm over another is simply to induce different channel statistics for the selected links [16]. We also emphasize that our analysis is valid for any geometry, even for non-cellular systems such as ad-hoc networks, as long as the sum of link capacities is

[1] On/off power control and binary power control are equivalent if the minimum transmit power is zero.

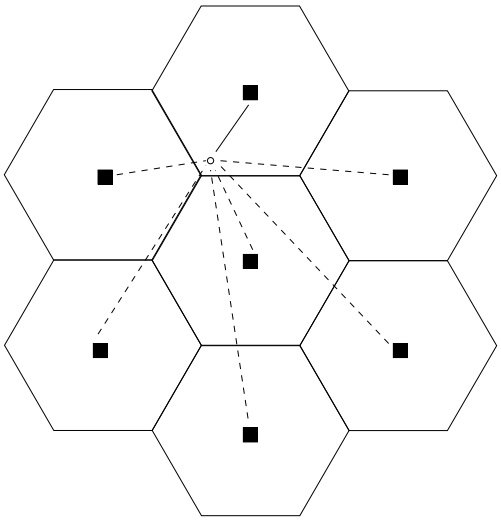

Figure D.1: N-cell wireless system model, where $N = 7$. Base stations are shown as solid squares. For the user (shown as a circle) in the top cell, the desired communication link is shown as a solid line, whereas the interference links are shown as dashed lines.

a relevant performance metric. To facilitate exposition, we shall however adopt a cellular terminology from here on; see Fig. D.1.

In the network considered, the spectral resource slots are shared by all cells, leading in general to an interference and noise impaired system. The communication links are considered to be downlink, but the results can also be generalized to an uplink scenario. The data destined for user u_n is transmitted with power P_n. Each base station is in general assumed to operate under both minimum and peak short term (per-slot) power constraints,

$$P_{\min,n} \leq P_n \leq P_{\max,n}, \quad n = 1, 2, \ldots, N. \tag{D.1}$$

Letting $P_{\min,n} > 0$ might be necessary in some scenarios to ensure that a user u_n receive a minimum transmission, such as control information or pilot symbols. Further, the different cells can be given priorities by assigning individual values of $P_{\max,n}$.

Now, denote by $G_{ni}(m)$ the channel power gain to the selected mobile user $u_n(m)$ in cell n from the cell i base station, in resource slot m. We will suppress the slot index from now on, concentrating on one arbitrary slot. The channel gains are assumed to be constant over each such resource slot, i.e., we have a block fading scenario. Note that the gains G_{nn} correspond to the desired communication links, whereas the G_{ni} for $n \neq i$ correspond

to the unwanted interference links. Assuming the transmitted symbols to be independent random variables with zero mean and a variance of P_n, the signal to noise-plus-interference ratio (SNIR) for each user is given by

$$\mathrm{SNIR}_{u_n} = \frac{P_n G_{nn}}{\sigma_n^2 + \sum_{j \neq n} P_j G_{nj}}, \tag{D.2}$$

where σ_n^2 is the variance of the independent zero-mean AWGN in cell n. Under the assumption of Gaussian distributed signal transmission in all cells, the interference terms will be Gaussian, also after being weighted by the (constant) interference gains in the current block and subsequently summed. Then channel experienced by each user within a given time slot is AWGN, and thus the capacity for each user is given by the AWGN Shannon capacity, i.e., the achievable rate (in information bits/s/Hz) for user u_n is given by

$$R_{u_n} = \log_2(1 + \mathrm{SNIR}_{u_n}). \tag{D.3}$$

From (D.2) and (D.3) the total achievable throughput (sum rate) $R = \sum_{n=1}^{N} R_{u_n}$ is then found as

$$R = \sum_{n=1}^{N} \log_2 \left(1 + \frac{P_n G_{nn}}{\sigma_n^2 + \sum_{j \neq n} P_j G_{nj}} \right). \tag{D.4}$$

Finally, we note that our system model with (possibly different) noise levels $\{\sigma_n^2\}_{n=1}^{N}$ also accommodates the modeling of additional interfering sources disturbing the users differently, contrary to previous works. As will be discussed later, one important application of this is when, for complexity reduction, joint multi-cell power allocation is undertaken over a subnet (cluster) of neighboring cells only. In this case σ_i^2 represents the combined effect of noise and interference received from out-of-cluster cells by the i^{th} user.

3 Transmit Power Analysis

This section presents the general optimal power allocation scheme $\mathbf{P}^* = (P_1^*, \ldots, P_N^*)$, which has as inputs the channel gains $\{G_{ni} > 0\}$, and the AWGN variances $\{\sigma_n^2 > 0\}$. We search for the optimal power allocation by approaching the following optimization problem,

$$\mathbf{P}^* = \arg \max_{\mathbf{P} \in \Omega^N} R, \tag{D.5}$$

where $\Omega^N = \{\mathbf{P} |\ P_{\min,n} \leq P_n \leq P_{\max,n},\ n = 1, \ldots, N\}$ is the feasible set and R is given in (D.4). Since Ω^N is a closed and bounded set and $R : \Omega^N \to \mathbb{R}$

is continuous, (D.5) has a solution [17, Theorem 0.3]. Before we proceed, we note the following lemma.

Lemma D.1
The optimal transmit power vector will have at least one component equal to $P_{max,n}$.

Proof: From (D.4) we have that, for $\beta > 1$ and $\mathbf{P} \in \Omega^N$:

$$R(\beta\mathbf{P}) = \log_2\Big(\prod_{n=1}^{N}(1 + \frac{P_n G_{nn}}{\frac{\sigma_n^2}{\beta} + \sum_{j\neq n} P_j G_{nj}})\Big) > R(\mathbf{P}). \tag{D.6}$$

Thus, we can increase the sum throughput R, by increasing all components of $\mathbf{P}$ by a factor β, until one component hits the boundary $P_{\max,n}$. Hence, the solution of (D.5) will have at least one component equal to $P_{\max,n}$. The interpretation of (D.6) is that increasing all the transmit powers by a factor β, is equivalent to reducing the noise in each cell by the same factor. □
Note that for one or more $P_{\min,n} = 0$, Ω^N admits solutions where some base stations shut down the power completely. Since one or more of the N base stations may then be turned off in a resource slot, from a cellular engineering point of view this scheme can be interpreted as a form of dynamic channel reuse. Allowing the network to completely turn off base stations will be sum-throughput optimal, but this optimality comes at the expense of fairness between the users in the various cells. Fairness can be restored by increasing $P_{\min,n}$, achieving full fairness at $P_{\min,n} = P_{\max,n}$, $\forall n$, analogously to the time horizon parameter in proportional fair scheduling [18]. Additionally, fairness can be targeted through introducing appropriate scheduling criteria [16].

3.1 Trivial Solutions

By inspection of (D.4) we can identify some trivial (not necessarily unique) solutions of (D.5). Firstly, if the system is noise limited, i.e., the interference can be neglected, then $\mathbf{P}^* = (P_{\max,1}, \ldots, P_{\max,N})$. Secondly, for the case of an interference limited system (noise set to zero), we see that $R \to \infty$ if any one of the base stations is turned on with any power $P_{\min,n} \leq P_n \leq P_{\max,n}$. However, in our analysis we will assume that noise is present, as in all practical systems.

3.2 The 2-Cell Case

We shall deal with the 2-cell case separately, as it allows us to derive analytically the optimal power allocation. By Lemma D.1, the optimal power allocation is found among the following alternatives:

- Extremal points on the boundaries of Ω^2: I.e., for $P_2 = P_{\max,2}$, P_1's corresponding to $\frac{\partial R(P_1,P_{\max,2})}{\partial P_1} = 0$, or for $P_1 = P_{\max}$, P_2's such that $\frac{\partial R(P_{\max,1},P_2)}{\partial P_2} = 0$.
- Corner points of Ω^2: $(P_{\max,1}, P_{\min,2})$, or $(P_{\min,1}, P_{\max,2})$, or $(P_{\max,1}, P_{\max,2})$.

Since the logarithm is a monotonically increasing function, we can look for extreme points on the boundary by considering the function $J(P_1, P_2) \triangleq (1 + \text{SNIR}_{u_1})(1 + \text{SNIR}_{u_2})$, i.e.,

$$J(P_1, P_2) = \big(1 + \frac{P_1 G_{11}}{\sigma_1^2 + P_2 G_{12}}\big)\big(1 + \frac{P_2 G_{22}}{\sigma_2^2 + P_1 G_{21}}\big). \tag{D.7}$$

Now, by differentiating $J(P_1, P_{\max,2})$ with respect to P_1 we find

$$\frac{\partial J}{\partial P_1} = \frac{CP_1^2 + 2DP_1 + E}{F}, \tag{D.8}$$

where

$$C = G_{11}G_{21}^2 > 0, \quad D = G_{11}G_{21}\sigma_2^2 > 0, \tag{D.9a}$$

$$E = -P_{\max,2}G_{21}G_{22}(\sigma_1^2 + P_{\max,2}G_{12}) + G_{11}\sigma_2^2(\sigma_2^2 + P_{\max,2}G_{22}), \tag{D.9b}$$

$$F = (\sigma_1^2 + P_{\max,2}G_{12})(\sigma_2^2 + P_1 G_{21})^2 > 0. \tag{D.9c}$$

Since F is always strictly positive, a P_1 such that $\frac{\partial J}{\partial P_1} = 0$ can be found as the solution to $CP_1^2 + 2DP_1 + E = 0$. Now, since also $C, D > 0$, this quadratic equation either has no zero for $P_1 \in [P_{\min,1}, P_{\max,1}]$, or has one zero there, and changes sign from $-$ to $+$. In either case it is clear that the maximum is attained at a boundary point $P_{\min,1}$ or $P_{\max,1}$. Due to symmetry, the above analysis also hold for P_2. Thus, we can conclude that (P_1^*, P_2^*) is found in the set of corner points of the feasible domain, $\Delta\Omega^2 = \{(P_{\max,1}, P_{\min,2}), (P_{\min,1}, P_{\max,2}), (P_{\max,1}, P_{\max,2}).\}$. Hence, we have the following theorem.

Theorem D.1
For the two-cell case, the sum throughput maximizing power allocation is binary[2]*. Mathematically,*

$$\arg \max_{(P_1,P_2)\in\Delta\Omega^2} R(P_1, P_2) = \arg \max_{(P_1,P_2)\in\Omega^2} R(P_1, P_2). \tag{D.10}$$

[2]For the case of $P_{\min,n} = 0$, $\forall n$, this result was independently reported both by the authors in [13], and in [19; 20].

Proof: See above. □

Inspecting (D.10) we see that, for zero minimum powers, of the two users in question, the user with the highest signal to noise ratio (SNR), defined as $\frac{P_{\max,n}G_{nn}}{\sigma_n^2}$, will always receive transmission at full power $P_{\max,n}$. For $(P_1, P_2) = (P_{\max,1}, P_{\max,2})$ this is trivially true. Furthermore, from (D.4), the decision of $(P_1, P_2) = (P_{\max,1}, 0)$ or $(0, P_{\max,2})$ is decided by each user's SNR alone, since there will be no interference for these power allocations.

3.3 Binary Power Control in the N-Cell Case

For $N > 2$, analytical treatment of the optimization problem (D.5) proves to be challenging, because of the lack of convexity and the fact that the above analysis from the two-cell case does not generalize to N cells. However, motivated by the optimality of binary power allocation for the two-cell case, reduced feedback requirements, and as well as by its potential as the key simplification in design of simple or even distributed algorithms, we will investigate the properties of binary power control also in the N-cell case.

Binary power control for N cells is done by evaluating $R(\mathbf{P})$ at the corners of Ω^N, and picking the maximum value. Mathematically formulated,

$$\mathbf{P}_{\text{bin}} = \arg \max_{\mathbf{P} \in \Delta\Omega^N} R(\mathbf{P}), \tag{D.11}$$

where $\Delta\Omega^N$ is the set of $2^N - 1$ corner points of Ω, excluding the all-$P_{\min,n}$ point.

Unfortunately, a seemingly pessimistic theoretical result is obtained there: It can be shown that binary power allocation is no longer optimal for $N > 2$. However, as we shall see it appears to still be very well approximating the capacity obtained by the optimal solution resulting from continuous power control, as indicated by the example below.

Example 2 *We simulated a $N = 3$ cell network with the following parameters. Common peak and minimum power constraints of $P_{max} = 10^{-3}$, and $P_{min} = 0$, respectively, assuming identical noise figures for the different receivers, the AWGN power is found as kT_0B, where k is Boltzmann's constant, $T_0 = 290$ Kelvin is the ambient temperature, and $B = 1$ MHz is the equivalent noise bandwidth, i.e., $\sigma_1^2 = \sigma_2^2 = \sigma_3^2 = 4.0039 \times 10^{-15}$. As an example of the randomly generated channel gain matrix, based on path loss, shadowing and multipath effects we have*

$$G = 10^{-9} \times \begin{pmatrix} 0.0432 & 0.0106 & 0.0012 \\ 0.0004 & 0.2770 & 0.0043 \\ 0.0045 & 0.0137 & 0.1050 \end{pmatrix}.$$

Then, by the best binary power allocation $(P_1, P_2, P_3) = (1, 1, 1)P_{max}$*, a sum throughput of* 9.4555 *bits/s/Hz is obtained, while by assigning the optimal powers* $(P_1, P_2, P_3) = (1, 0.8595, 1)P_{max}$ *we get a throughput of* 9.4590 *bits/s/Hz. As we will see later, this example is quite typical in the sense that binary power control, though suboptimal, very often yields a throughput close to that obtained by optimally allocating the powers. While achieving only marginally higher sum throughput under the given power constraints, optimal continuous control can however offer some savings in terms of sum transmit power.*

We shall now consider binary power control for N cells in three cases, 1) approximation by the arithmetic-geometric means inequality, 2) the low-SNIR regime, and 3) the general case.

3.3.1 Arithmetic mean-geometric mean approximation

From the *arithmetic - geometric means inequality* we have, for positive numbers $x_1, \cdots, x_N$ [21],

$$G_N = \left(\prod_{n=1}^{N} x_n \right)^{\frac{1}{N}} \leq \frac{1}{N} \sum_{n=1}^{N} x_n = A_N, \tag{D.12}$$

where G_N and A_N are the geometric mean (GM) and arithmetic mean (AM) of $x_1, \cdots, x_N$, respectively. Equality in (D.12) can be obtained if and only if $x_1 = \cdots = x_N$. Writing (D.4) as a log of products, and letting $x_n = (1 + \text{SNIR}_n)$, we can apply the above inequality to obtain

$$\begin{aligned} R(\mathbf{P}) &= \log_2 \left(\prod_{n=1}^{N} 1 + \frac{P_n G_{nn}}{\sigma_n^2 + \sum_{j \neq n} P_j G_{nj}} \right) \\ &\leq N \log_2 \left(1 + \frac{1}{N} \sum_{n=1}^{N} \frac{P_n G_{nn}}{\sigma_n^2 + \sum_{j \neq n} P_j G_{nj}} \right). \end{aligned} \tag{D.13}$$

Now, in scenarios where the right hand side of the above inequality can be used as an *approximation* of $R(\mathbf{P})$, i.e., $R(\mathbf{P}) \approx N \log_2 \left(1 + \frac{1}{N} \sum_{n=1}^{N} \frac{P_n G_{nn}}{\sigma_n^2 + \sum_{j \neq n} P_j G_{nj}} \right)$, the optimization problem (D.5) simplifies to

$$\mathbf{P}^* = \arg \max_{\mathbf{P} \in \Omega^N} N \log_2 \left(1 + \frac{1}{N} \sum_{n=1}^{N} \frac{P_n G_{nn}}{\sigma_n^2 + \sum_{j \neq n} P_j G_{nj}} \right), \tag{D.14}$$

and we can analytically find a closed form solution. As is always true in the two-cell case, the optimal power control in the N-cell case is binary when the AM-GM approximation is accurate.

Theorem D.2
The solution $\mathbf{P}^*$ *from* (D.14) *is binary, i.e.,* $\mathbf{P}^* \in \Delta\Omega^N$.

Proof: Due to the monotonicity of the log-function, we establish the result by showing that the argument of the logarithm in the cost function of (D.14) is convex in each variable P_k.

$$\frac{\partial^2}{\partial P_k^2}\left(1+\frac{1}{N}\sum_{n=1}^{N}\frac{P_n G_{nn}}{\sigma_n^2+\sum_{j\neq n}P_j G_{nj}}\right)=\frac{1}{N}\sum_{n\neq k}\frac{2P_n G_{nn}G_{nk}^2}{(\sigma_n^2+\sum_{j\neq n}P_j G_{nj})^3}\geq 0. \tag{D.15}$$

Now, for any $\mathbf{P}$ where at least one of its components is not an endpoint of its interval, there is another point $\mathbf{P}'$ with $R(\mathbf{P}')\geq R(\mathbf{P})$ such that one more component is at an endpoint of its interval. □

An obvious question is for which scenarios the sum throughput is well approximated using the AM-GM inequality. The quality of the approximation can in general be quantified by inspecting the difference between the right hand and left hand side of (D.13), which can be written as

$$\begin{aligned}&N\log_2\left(1+\frac{1}{N}\sum_{n=1}^{N}\frac{P_n G_{nn}}{\sigma_n^2+\sum_{j\neq n}P_j G_{nj}}\right)-\log_2\left(\prod_{n=1}^{N}1+\frac{P_n G_{nn}}{\sigma_n^2+\sum_{j\neq n}P_j G_{nj}}\right)\\&=N\log_2\left(\frac{A_N}{G_N}\right).\end{aligned} \tag{D.16}$$

From (D.12), $\log_2\left(\frac{A_N}{G_N}\right)\geq 0$, and using Specht's ratio $S(h)$ [22] we find

$$\frac{A_N}{G_N}\leq S(h)\triangleq\frac{(h-1)h^{\frac{1}{h-1}}}{e\ln h}, \tag{D.17}$$

where $h\triangleq\max_{1\leq j,k\leq N}\frac{x_k}{x_j}$. Using these bounds together we have the following result:

$$0\leq\log_2\left(\frac{A_N}{G_N}\right)\leq\log_2\left(\frac{(h-1)h^{\frac{1}{h-1}}}{e\ln h}\right). \tag{D.18}$$

Inspecting (D.18), we see that the quality of the approximation largely depends on the spread of the x_n values; indeed the more concentrated the $(1+\text{SNIR}_n)$ factors are, the better the approximation is, reaching equality between the arithmetic and geometric mean with all SNIRs equal. As an example application, consider the case of low SNIR. Then, by default the SNIR is low in all cells, providing concentrated values of $\{x_n\}_{n=1}^N$, and the optimal power control in this scenario is binary.

3.3.2 Low-SNIR regime

The optimality of binary power control in the low-SNIR case can also be derived using another argument as we now investigate. In the low-SNIR regime we can apply an approximation of the achievable rate of each user, thus simplifying the problem. Specifically, when the SNIR is low, the following approximation obtained by Taylor expansion holds [23]: $\log_2(1+\text{SNIR}) \approx \frac{\text{SNIR}}{\ln 2}$. Thus, we have

$$R(\mathbf{P}) = \sum_{n=1}^{N} \log_2(1+\text{SNIR}_{u_n}) \approx \frac{1}{\ln 2} \sum_{n=1}^{N} \frac{P_n G_{nn}}{\sigma_n^2 + \sum_{j \neq n} P_j G_{nj}}, \tag{D.19}$$

and again find that binary power control is optimal, which is easily seen from the proof of Theorem D.2[3]. In fact, the objective function obtained by both the low-SNIR approximation and the arithmetic-geometric means approximation is maximized by the same binary power values.

In the low-SNIR case the binary power allocation is also optimal for a weighted sum rate criterion, $R_{\text{w}} = \sum_{n=1}^{N} w_n R_n, w_n \geq 0$, which we state as a corollary.

Corollary 1 *In the low-SNIR regime, for a weighted sum rate criterion, the sum throughput maximizing power control is binary.*

Proof: The result follows by the rules of differentiation. □

3.3.3 General case

In general, when none of the above approximations hold, unfortunately we have not found mathematical relations establishing the performance of binary power control, and hence we resort to exhaustive numerical simulations, trying to cover typical settings for cellular networks. To evaluate the performance of our proposed binary power control against a non-binary benchmark we capitalize on recent developments in geometric programming [14; 24], as discussed in the next subsection.

Independent of whether any of the above approximations hold, we still have to solve the discrete maximization (D.11), which has a worst-case complexity of $O(2^N)$ for exhaustive search. For small to moderate values of N, the globally optimal solution to (D.11) can easily be found by simply

[3]For the case of $P_{\min,n} = 0$, $\forall n$, and identical peak power constraints, this was independently reported also by the authors in [19; 20]. Further, in [12], also with $P_{\min,n} = 0$, $\forall n$, the optimization problem (D.5) with R as a linear function of the received power, similar to (D.19), is considered and an alternative proof for on/off power control is given.

checking the corner points. For large N, since the cost function is non-linear and the optimization search space is spanned by binary variables, (D.11) may be approached using $0-1$ nonlinear programming [25], clustering, or greedy approaches. We discuss clustering and greedy approaches in Section 4.

Currently, there is also ongoing research on finding simple, distributed solutions to the present power control problem (also including scheduling) [15]. Finally, we note that the previously mentioned and more general case where the objective function to be maximized is a sum of weighted rates is also an interesting problem, but this is a subject for future research[4].

3.4 Geometric Programming Power Control for N Cells

As mentioned above, to evaluate the performance of binary power control, we will use power control by geometric programming as the yardstick[5]. First, we therefore provide a brief background on geometric programming [14]. A *monomial* is a function $f : \mathbf{R}^n_{++} \rightarrow \mathbf{R}$: $g(\mathbf{P}) = cP_1^{a^{(1)}} P_2^{a^{(2)}} \cdots P_n^{a^{(n)}}$, where $\mathbf{R}^n_{++}$ is the strictly positive quadrant of $\mathbf{R}^n$, $c > 0$ is a constant, and $a^{(i)} \in \mathbf{R}$, $i = 1, \ldots, n$. A sum of monomials is called a *posynomial*:

$$f(\mathbf{P}) = \sum_{k=1}^{K} c_k P_1^{a_k^{(1)}} P_2^{a_k^{(2)}} \cdots P_n^{a_k^{(n)}}. \tag{D.20}$$

Then, a geometric program (GP) in standard form is written as:

$$\begin{aligned} &\text{minimize} && f_0(\mathbf{P}), \\ &\text{subject to} && f_i(\mathbf{P}) \leq 1,\ i = 1, \ldots, I \\ &&& g_m(\mathbf{P}) = 1,\ m = 1, \ldots, M, \end{aligned} \tag{D.21}$$

where f_i, $i = 0, \ldots, I$ are posynomials and g_m, $m = 1 \ldots M$ are monomials.

Using the results in [24], the optimization problem in (D.5) can be writ-

[4]The weighted sum solution presented in [24] is only valid in the high-SNIR regime.

[5]The content in this section is largely based on [26; 24], where geometric power control for wireless networks is given a formal mathematical treatment.

ten as follows[6]:

$$\begin{aligned} \text{minimize} \quad & \prod_{n=1}^{N} \frac{1}{1+\text{SNIR}_{u_n}}, \\ \text{subject to} \quad & \frac{P_n}{P_{\max,n}} \leq 1,\ n = 1,\ldots,N, \\ & \frac{P_{\min,n}}{P_n} \leq 1,\ n = 1,\ldots,N. \end{aligned} \tag{D.22}$$

Inspecting (D.22), we see that the constraints are monomials (and hence posynomials), but the objective function is a *ratio* of posynomials, as shown by

$$\prod_{n=1}^{N} \frac{1}{1+\text{SNIR}_{u_n}} = \prod_{n=1}^{N} \frac{\sigma_n^2 + \sum_{j\neq n} G_{nj}P_j}{\sigma_n^2 + \sum_{j=1}^{N} G_{nj}P_j}, \tag{D.23}$$

and the fact that posynomials are closed under multiplication. Hence, (D.22) is not a GP in standard form, but a *signomial* programming (SP) problem [14]. Following the iterative procedure from [24], (D.22) is solved by constructing a series of GPs, each of which can easily be solved. The GP in iteration l of the series is constructed by approximating the denominator posynomial (D.23) by a monomial, using the value of $\mathbf{P}$ from the previous iteration, while the series is initialized by any feasible $\mathbf{P}$. Specifically, denote the denominator posynomial of (D.23) as $g(\mathbf{P})$. Since a posynomial is a sum of monomials, write $g(\mathbf{P}) = \sum_i u_i(\mathbf{P})$ where $u_i(\mathbf{P})$ is a monomial. Then, in iteration l, $g(\mathbf{P})$ is approximated by a monomial $\tilde{g}_l(\mathbf{P})$ as follows [24]:

$$g(\mathbf{P}) \geq \tilde{g}_l(\mathbf{P}) = \prod_i \Big(\frac{u_i(\mathbf{P})}{\alpha_i^l}\Big)^{\alpha_i^l}, \tag{D.24}$$

where $\alpha_i^l = u_i(\mathbf{P}_{l-1})/g(\mathbf{P}_{l-1})$, and $\mathbf{P}_l$ is the value of $\mathbf{P}$ in iteration l. By using (D.24), (D.23) is now a ratio of a posynomial and a monomial. This ratio is again a posynomial, and hence (D.22) is approximated and transformed to standard form, and can be solved using GP techniques. The iteration is terminated at the l'th loop if $||\mathbf{P}_l - \mathbf{P}_{l-1}|| < \epsilon$, where ϵ is the error tolerance. This procedure is provably convergent and empirically almost always computes the optimal power allocation [24], and thus represents an upper bound against which we can measure the performance of binary power control.

[6]For $P_{\min,n} = 0$, in theory the strictly positive quadrant assumption can be violated. However, numerically this is not a problem in practice as the geometric programs are solved using interior-point methods, searching *inside* the feasible domain [26].

4 Low-complexity Power Control Algorithms

Despite the promise of binary power control in terms of near throughput optimality and key implementation simplifications, solving the exhaustive binary power allocation problem (D.11) for large networks presents the system designer with an exponentially complex task. In this section we study two approaches towards reducing the search complexity.

The underlying idea behind lowering the complexity in both approaches is to split the original problem into smaller subproblems, each of which can easily be solved. However, since the problem does not exhibit an *optimal substructure property*, i.e., an optimal solution to the problem does not contain within it optimal solutions to subproblems [27], in general, we will not be able to derive simple algorithms for finding the globally optimal binary solution. As such, our algorithms seek to a achieve a good performance versus complexity compromise, rather than obtaining a global performance optimum.

4.1 Grouping Clusters of Cells

We now investigate a setting where the total number of N cells in the network are clustered into groups of $K << N$ cells, and each cell either transmits with full or minimum power. For a given cluster Q, the interference from the remaining $N-K$ cells will simply contribute as noise, i.e. the sum throughput of the cells in Q is given as

$$R_{\text{cluster, }Q} = \sum_{q \in Q} \log_2\big(1 + \frac{P_q G_{qq}}{\sigma_q^2 + \sigma_{\mathrm{I}_q}^2 + \sum_{\substack{j \in Q \\ j \neq q}} P_j G_{qj}}\big), \tag{D.25}$$

where $\sigma_{\mathrm{I}_q}^2 = \sum_{j \notin Q} P_j G_{qj}$ is the interference from cells in the network which are *not* part of the cluster. Assuming that this interference term can be estimated or averaged from the knowledge of the power activity in other clusters, the idea is to do power control only *locally* within each cluster. Hence, the following problem is solved for each cluster Q,

$$\mathbf{P}_Q = \arg \max_{\mathbf{P} \in \Delta\Omega^K} R_{\text{cluster, }Q}. \tag{D.26}$$

To solve the cluster based maximization problem, we have to investigate $\frac{N}{K}$ subproblems each with maximally 2^K evaluations, hence yielding a complexity in N and K of $O(N\,2^K)$, while keeping K fixed, the complexity is $O(N)$. Also, since we only need to know the sum of the out-of-cluster interference, not its terms, compared to the exhaustive binary search problem (D.11), the required channel knowledge is reduced.

Algorithm 1: Greedy power control

1: $\mathbf{P}_0 = \mathbf{P}_{\min}$, $R_0 = R(\mathbf{P}_0)$, $S = \emptyset$
2: **for** $l = 1$ to N **do**
3: $\quad \mathbf{P}_l = \mathbf{P}_{l-1}$
4: $\quad n^* = \arg\max_{n \notin S} R\big((\mathbf{P}_l)_n = P_{\max,n}, (\mathbf{P}_l)_{j \neq n} = (\mathbf{P}_l)_j\big)$
5: $\quad (\mathbf{P}_l)_{n^*} = P_{\max,n}$
6: $\quad S = S + \{n^*\}$
7: $\quad R_l = R(\mathbf{P}_l)$
8: **end for**
9: $\mathbf{P}^* = \mathbf{P}_{\substack{\arg\max R_l \\ 1 \leq l \leq N}}$

4.2 A Greedy Approach to Power Control

Now, consider approaching the binary power control problem by a greedy method, i.e., we are looking for a simple and efficient algorithm which in each step makes the choice that appears best at the moment. This greedy algorithm belongs to the class of "local search" methods, popular due to its wide range of applications in non-linear integer programming problems [25], an example being allocating traffic channels in OFDMA systems [28].

A key point in a greedy algorithm is the *selection function* which chooses the best candidate to be added to the solution. Here, we start with all cells assigned minimum power $P_{\min,n}$, and look for candidate cells which should have maximum power $P_{\max,n}$. Inspecting (D.4), and denoting the set of cells assigned maximum power as S, we note that at each stage, in deciding whether a cell $n \notin S$ should be operated at maximum power, an obvious selection function is the capacity that would be obtained by letting cell n transmit at maximum power $P_{\max,n}$, while keeping the transmit powers obtained in the previous stages fixed. Summarizing, we arrive at Algorithm 1 looping once over N cells, where R_l and $(\mathbf{P}_l)_j$ respectively denote the sum throughput and the j'th component of the power allocation vector $\mathbf{P}_l$, at step l. After traversing the N cells, the power allocation vector is found by inspecting at which step the sum rate achieved its maximum.

Complexitywise, the proposed greedy algorithm makes N choices, and needs to solve the optimization problem in line 4, with complexity $O(N)$. Thus, it runs in $O(N^2)$ time, achieving a significant reduction compared to the exhaustive search.

Table D.1: Cellular System Parameters

Parameter	Suburban Macro	Urban Macro	Urban Micro LOS
Cell layout	Hexagonal	Hexagonal	Hexagonal
Carrier frequency	1900 MHz	1900 MHz	1900 MHz
$P_{\max,n}, \forall n$	10 W	10W	1 W
$P_{\min,n}, \forall n$	0 W	0 W	0 W
BS to BS distance	3000 m	3000 m	1000 m
Exclusion disc radius	35 m	35 m	20 m
Operating temperature	290 Kelvin	290 Kelvin	290 Kelvin
Shadowing st. dev.	8 dB	8 dB	4 dB
Equiv. noise BW	1 MHz	1 MHz	1 MHz

5 Numerical Results

In this section we present numerical results on the achievable sum network capacities for an N-cell wireless system utilizing the various schemes of power control we have analyzed.

5.1 Simulation Model

Based on the system model described in Section 2, we will now evaluate a cellular system through Monte Carlo simulations, assuming that the user distribution is uniform in each cell. To most accurately model a typical cellular system we follow the spatial channel models for use in system level simulations developed by the 3GPP-3GPP2 working group [29]. Specifically the following environments are considered: the suburban macrocell, the urban macrocell, and the urban microcell line of sight (LOS). In the macrocell environments the base station antennas are above rooftop height, while for the urban microcell setting it is at rooftop height. Depending on the model, BS-to-user distances should exceed $20-35$ meters, thus we exclude users from being located in a circular disk of radius $20-35$ m around each base station. Further simulation details can be found in Table D.1.

5.2 Description of Transmission Schemes

We consider two link adaptation schemes; adaptive coded modulation using capacity-achieving codes with, and without, power control. Without power control, the power at all base stations is held constant at $P_{\max,n}$, $\forall n$. Based on the current received SNIR level the modulation and coding rates are then selected. Allowing for power control, adaptive coded modulation is used to transmit at power levels that are optimized respectively accord-

Table D.2: Network capacity statistics

	Average pr. cell capacity $\frac{R}{N}$ (bits/s/Hz/cell) shown in (GP, Binary, Full) triplets		
Number of cells (N)	Suburban Macro	Urban Macro	Urban Micro
1	(6.02, 6.02, 6.02)	(5.13, 5.13, 5.13)	(11.96, 11.96, 11.96)
2	(4.93, 4.93, 4.74)	(4.40, 4.40, 4.27)	(6.64, 6.64, 4.54)
3	(4.41, 4.40, 4.02)	(4.03, 4.03, 3.75)	(6.03, 6.03, 3.39)
4	(4.03, 4.01, 3.53)	(3.70, 3.69, 3.33)	(4.66, 4.65, 2.91)
5	(3.98, 3.95, 3.45)	(3.68, 3.67, 3.28)	(3.88, 3.85, 2.75)
6	(3.81, 3.78, 3.25)	(3.54, 3.53, 3.11)	(3.41, 3.36, 2.58)
7	(3.67, 3.64, 3.08)	(3.42, 3.41, 2.97)	(3.06, 3.00, 2.40)

ing to GP power control (D.5), binary power control (D.11), the clustering approach (D.26), and greedy power control.

5.3 Network Capacity Statistics

To obtain the system throughput statistics for an average user in each cell, we ran 10000 independent trials, in each trial drawing user locations and path gain matrices from their corresponding distributions. Table D.2 depicts the average per-cell capacity, defined as $\frac{R}{N}$, for the three simulation settings, in bits/s/Hz versus the number of cells. It is clear that introducing power control improves the throughput performance for $N \geq 2$, in particular for the urban microcell environment. However, note the only marginal improvement in going from binary power control to optimal GP power control based on geometric programming. As seen from the table, the average per cell capacity decreases as the number of cells increase. This is to be expected since all cells share the same spectral resources. As an example of how instrumental it is to be able to operate some cells at minimum power, we see that the *system capacity* in the urban microcell environment is less for two cells than for one cell when using full power. However, using binary and GP power control, we observe an *increase* in system capacity when going from one to two cells, due to better management of interference.

In Fig. D.2 we have plotted the frequency of optimality of binary power control, i.e., the percentage of simulations where binary power control is still optimal. It is seen that for one and two cells, binary power control is indeed always optimal, while for more than two cells it is optimal only in a certain fraction of the cases. When the number of cells increases, binary power allocation is more seldom optimal. However, as shown in Table D.2,

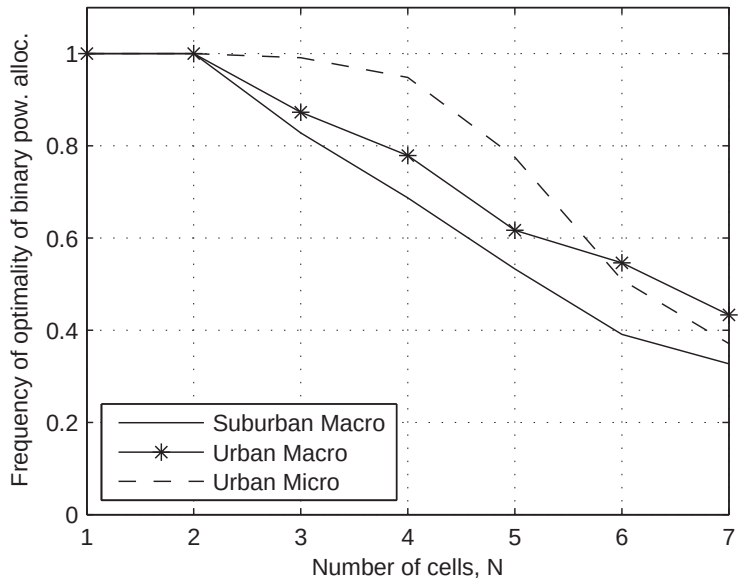

Figure D.2: Frequency of optimality of binary power allocation, relative to optimal (GP) power allocation, plotted versus the number of cells N for all three simulation environments.

the gap between the optimal (GP) power control and the suboptimal binary power control is still marginal. This demonstrated near-optimality of binary power control has several potential implications in the design and analysis of wireless networks. Firstly, the complexity of the transmitter design is reduced, since only a two-level power control is required. Secondly, binary power control provides a key simplification of the problem by enabling *distributed* control of the power allocation [15].

5.4 Average transmit power

To improve further our understanding of the power control problem, in Fig. D.3 we have plotted the average transmit power for the suburban macrocell and the urban microcell environments, as a function of the number of cells. In the macrocell setup, we see that the average transmit power of binary and GP power allocation are approximately the same, and that on average for a 7-cell network, 4 cells should be on. On the other hand, for the LOS microcell setup, significantly fewer cells should be turned on. This is due to the fact that the cells are much smaller, combined with a lower

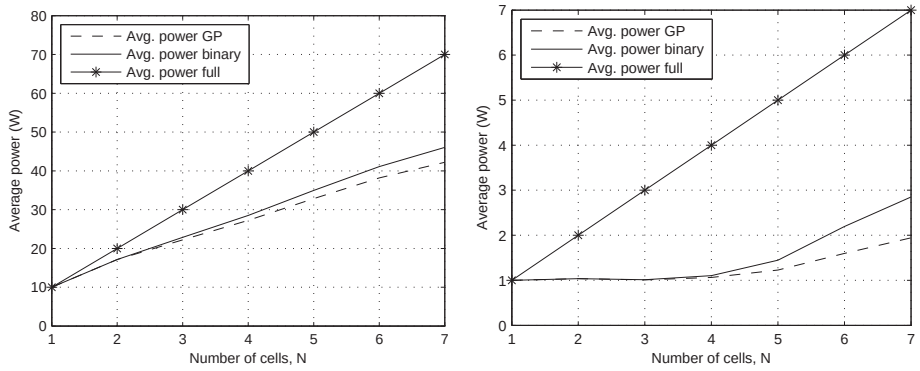

(a) Suburban macrocell environment. Maximum transmit power per cell $P_{\max,n} = 10\,\mathrm{W}, \forall n$

(b) Urban microcell environment. Maximum transmit power per cell $P_{\max,n} = 1\,\mathrm{W}, \forall n$.

Figure D.3: Average sum transmit power for macro and microcell setups versus the number of cells N.

path loss due to a line of sight environment, hence the interference caused by turning on a cell dominate more. Also, we note that for increasing N, the GP power control uses less transmit power than binary control. Hence, even though there are no significant throughput gains in using continuous power control in these settings, it is possible to reduce the average transmit power, while achieving the same network capacity.

5.5 Reducing Complexity by Clustering Cells and Greedy Power Control

Now, we consider the results obtained by grouping the total number of cells in a large system into smaller clusters of neighboring cells[7]. In Table D.3 the *normalized capacity* from (D.26), i.e., the capacity obtained by using binary power allocation in clusters of size K relative to a binary exhaustive search over the total network of 19 cells, is plotted versus the number of cells in the clusters. It is seen that even with small clusters of 3 cells more than 90% of the capacity can be achieved. Increasing the cluster size K yields improvements in sum throughput. Although not shown here, it is clear that as $K \to N$, the clustering scheme will be identical to that of the binary exhaustive search.

[7]Clustering by grouping neighboring cells is not claimed to be optimal; indeed optimal clustering is a research problem in itself, beyond the scope of this paper.

Table D.3: Network Capacity Statistics for Complexity Reduced Schemes, $N = 19$

	Normalized capacity relative to binary exhaustive search								
	Clusters of K cells							Greedy	Binary exhaustive
	1	2	3	4	5	6	7		
Suburb. Macro	0.82	0.88	0.91	0.93	0.95	0.96	0.95	0.997	1
Urban Macro	0.84	0.89	0.92	0.94	0.95	0.96	0.96	0.998	1
Urban Micro	0.84	0.87	0.9	0.92	0.93	0.95	0.94	0.994	1

Table D.4: Average Number of Cells Turned On for Complexity Reduced Schemes, $N = 19$

	Average number of cells turned on								
	Clusters of K cells							Greedy	Binary exhaustive
	1	2	3	4	5	6	7		
Suburb. Macro	19	16.88	15.19	14.55	13.99	13.47	13.5	11.3	11.3
Urban Macro	19	16.98	15.38	14.79	14.21	13.75	13.75	11.7	11.7
Urban Micro	19	17.93	16.45	15.72	15.1	14.23	14.26	10.7	10.5

Finally, we evaluate the results of the greedy power control scheme. As seen from Table D.3, the greedy scheme performs extremely well, achieving more than 99% of the capacity from binary exhaustive search in all simulation environments. Using the previously derived running time expressions, we see that the complexity is reduced by a factor of $\frac{N^2}{2^N} = \frac{19^2}{2^{19}}$, or equivalently 99.99% complexity reduction, while sacrificing less than 1% of the network capacity. Comparing the clustering approach to the greedy approach, it is clear the greedy algorithm yields better results, which is to be expected, and can be explained as follows. While the greedy approach is a fully centralized scheme, the clustering based power control operates locally in clusters using an interference average from the other clusters, and has also for a fixed cluster size lower complexity. Also, from Table D.4 we see the average number of cells turned on by the clustering, greedy, and binary exhaustive schemes. We see as the number of cells in a cluster K increases, the fraction of cells turned on decreases. For the greedy and binary exhaustive search less cells are on, which helps explain their strong performance. Nonetheless, we see that the promised benefits of discretizing the power levels can be achieved at a low complexity.

6 Conclusions

We have analyzed transmit power allocation for an N-cell wireless system under a sum-capacity maximization criterion and minimum and peak power constraints at each base station. Assuming perfect channel gain information to be available, we have investigated the system capacity without power control, with binary power control, and with GP-based power control. We show that the optimal power control is binary for two cells, as well as when the network throughput can be approximated either by a geometric-arithmetic means inequality or by a low-SNIR assumption. In the general case when $N > 2$, it was demonstrated by extensive computer simulations that a restriction to binary power levels yields only a negligible capacity loss.

To reduce the complexity of exhaustively searching for the optimal binary power allocation for large networks, simple algorithms based on clustering and greedy approaches were derived. Using these algorithms a significant complexity reduction is possible at only a small penalty in network capacity. For practical systems, these results are of importance since the transmitter design is simplified, overhead feedback signalling is reduced, and the search for distributed algorithms becomes more manageable. Finally, we note that power control should complemented with scheduling to further improve the performance of the system. In certain scenarios this has previously been explored in [15; 30].

Acknowledgement

The authors wish to thank Dr. Prasanna Chaporkar for insightful discussions and feedback on the manuscript, and finally the anonymous reviewers for comments which improved the quality of the paper.

References

[1] J. Zander, "Performance of optimum transmitter power control in cellular radio systems," *IEEE Transactions on Vehicular Technology*, vol. 41, no. 1, pp. 57–62, Feb. 1992.

[2] G. J. Foschini and Z. Miljanic, "A simple distributed autonomous power control algorithm and its convergence," *IEEE Transactions on Vehicular Technology*, vol. 42, no. 4, pp. 641–646, Nov. 1993.

[3] Y.-H. Lin and R. L. Cruz, "Power control and scheduling for interfering links," in *Proc. IEEE Information Theory Workshop*, San Antonio, TX, Oct. 2004, pp. 288–291.

[4] A. Gjendemsjø, G. E. Øien, and H. Holm, "Optimal power control for discrete-rate link adaptation schemes with capacity-approaching coding," in *Proc. IEEE Global Telecommunications Conference*, St. Louis, MO, Nov.-Dec. 2005, pp. 3498–3502.

[5] A. Gjendemsjø, G. E. Øien, and P. Orten, "Optimal discrete-level power control for adaptive coded modulation schemes with capacity-approaching component codes," in *Proc. IEEE International Conference on Communications*, Istanbul, Turkey, June 2006, pp. 5047–5052.

[6] X. Qiu and K. Chawla, "On the performance of adaptive modulation in cellular systems," *IEEE Transactions on Communications*, vol. 47, no. 6, pp. 884–895, June 1999.

[7] A. Babaei and B. Abolhassani, "A new iterative method for joint power and modulation adaptation in cellular systems," in *Proc. IFIP International Conference on Wireless and Optical Communications Networks*, Dubai, United Arab Emirates, Mar. 2005, pp. 94–97.

[8] S.-J. Oh and A. C. K. Soong, "QoS-constrained information-theoretic sum capacity of reverse link CDMA systems," *IEEE Transactions on Wireless Communications*, vol. 5, no. 1, pp. 3–7, Jan. 2006.

[9] K. L. Baum, T. A. Kostas, P. J. Sartori, and B. K. Classon, "Performance characteristics of cellular systems with different link adaptation strategies," *IEEE Transactions on Vehicular Technology*, vol. 52, no. 6, pp. 1497–1507, Nov. 2003.

[10] T. Park, J. Jang, O.-S. Shin, and K. B. Lee, "Transmit power allocation for a downlink two-user interference channel," *IEEE Communication Letters*, vol. 9, no. 1, pp. 13–15, Jan. 2005.

[11] C. Zhou, M. L. Honig, and S. Jordan, "Utility-based power control for a two-cell CDMA data network," *IEEE Transactions on Wireless Communications*, vol. 4, no. 6, pp. 2764–2776, Nov. 2005.

[12] A. Bedekar, S. Borst, K. Ramanan, P. Whiting, and E. Yeh, "Downlink scheduling in CDMA data networks," in *Proc. IEEE Global Telecommunications Conference*, Rio de Janeiro, Brazil, Dec. 1999, pp. 2653–2657.

[13] A. Gjendemsjø, D. Gesbert, G. E. Øien, and S. G. Kiani, "Optimal power allocation and scheduling for two-cell capacity maximization," in *Proc. Modeling and Optimization in Mobile, Ad Hoc, and Wireless Networks*, Boston, MA, April 2006, pp. 1–6.

[14] S. Boyd, S. J. Kim, L. Vandenberghe, and A. Hassibi, "A tutorial on geometric programming," *Optimization and Engineering*, vol. 8, no. 1, pp. 67–127, March 2007.

[15] S. G. Kiani, G. E. Øien, and D. Gesbert, "Maximizing multi-cell capacity using distributed power allocation and scheduling," in *Proc. IEEE Wireless Communications and Networking Conference*, Hong Kong, China, March 2007, pp. 1690 – 1694.

[16] M. Andrews, K. Kumaran, K. Ramanan, A. Stoylar, P. Whiting, and R. Vijayakumar, "Providing quality of service over a shared wireless link," *IEEE Communications Magazine*, vol. 39, no. 2, pp. 150–154, Feb. 2001.

[17] J. L. Troutman, *Variational calculus and optimal control: Optimization with elementary convexity*, 2nd ed. New York: Springer-Verlag, 1996.

[18] D. Gesbert and M.-S. Alouini, "Selective multi-user diversity," in *International Symposium on Signal Processing and Information Technology*, Darmstadt, Germany, Dec. 2003, pp. 162–165.

[19] M. Ebrahimi, M. A. Maddah-Ali, and A. K. Khandani, "Power allocation and asymptotic achievable sum-rates in single-hop wireless networks," in *Proc. Conference on Information Sciences and Systems*, Princeton, NJ, March 2006, pp. 498–503.

[20] ——, "Throughput scaling in decentralized single-hop wireless networks with fading channels," submitted to IEEE Transactions on Information Theory, 2006.

[21] P. Bullen, D. Mitronivic, and P. Vasic, *Means and Their Inequalities*. D. Reidel Publ. Company, Dordrecht-Boston-Lancaster-Tokyo, 1988.

[22] M. Fujii, J. Micic, J. Pecaric, and Y. Seo, "Reverse inequalities on chaotically geometric mean via Specht ratio, ii," *Journal of Inequalities in Pure and Applied Mathematics*, vol. 4(2), Art. 40, pp. 1–8, 2003.

[23] C. H. Edwards and D. E. Penney, *Calculus with analytic geometry*. Upper Saddle River, NJ: Prentice Hall, 1998.

[24] M. Chiang, C. W. Tan, D. P. Palomar, D. O'Neill, and D. Julian, "Power control by geometric programming," *IEEE Transactions on Wireless Communications*, vol. 6, no. 7, pp. 2640–2651, July 2007.

[25] D. Li and X. Sun, *Nonlinear Integer Programming*. New York: Springer, 2006.

[26] M. Chiang, "Geometric programming for communications systems," *Foundations and Trends in Communications and Information Theory*, vol. 2, no. 1/2, pp. 1–156, Aug. 2005.

[27] T. H. Cormen, C. E. Leiserson, R. L. Rivest, and C. Stein, *Introduction to Algorithms*, 2nd ed. MIT Press, 2001.

[28] G. Li and H. Liu, "Downlink radio resource allocation for multi-cell OFDMA system," *IEEE Transactions on Wireless Communications*, vol. 5, no. 12, pp. 3451–3459, Dec. 2006.

[29] Spatial Channel Model AHG, "Spatial channel model text description," 3GPP-3GPP2, Tech. Rep., 2003.

[30] D. Gesbert, S. G. Kiani, A. Gjendemsjø, and G. E. Øien, "Adaptation, coordination and distributed resource allocation in interference-limited wireless networks," *Proc. of the IEEE, Special Issue on Adaptive Transmission*, (Invited Paper), to appear Dec. 2007. [Online]. Available: http://www.iet.ntnu.no/~gjendems/publications/

Paper E

Joint Adaptive Modulation and Diversity Combining with Downlink Power Control

Anders Gjendemsjø, Hong-Chuan Yang, Geir E. Øien, and Mohamed-Slim Alouini

To appear in the *IEEE Transactions on Vehicular Technology*.

Abstract

We consider the problem of finding low-complexity, bandwidth-efficient, and processing-power efficient transmission schemes for a downlink scenario under the framework of diversity combining. Capitalizing on recent results for joint adaptive modulation and diversity combining schemes (AMDC), we design and analyze two AMDC schemes that utilize power control to reduce the radiated power, and thus the potential interference to other systems/users. Based on knowledge of the channel fading, the proposed schemes adaptively select the signal constellation, diversity combiner structure, and transmit power level. We show that the novel schemes also provide significant average transmit power gains compared to existing joint adaptive QAM and diversity schemes. In particular, over a large signal to noise ratio range, the transmitted power is reduced by $30 - 50\%$, yielding a substantial decrease in interference to co-existing systems/users, while maintaining high average spectral efficiency, low combining complexity, and compliance with bit error rate constraints.

Parts of this paper were presented at the IEEE Wireless Communications and Networking Conference, Hong-Kong, China, March 2007.

A. Gjendemsjø and G. E. Øien (e-mails: {gjendems,oien}@iet.ntnu.no) are with the Dept. of Electronics and Telecommunications, Norwegian University of Science and Technology (NTNU), Trondheim, Norway.

H. -C. Yang (e-mail: hyang@uvic.ca) is with the Dept. of ECE, University of Victoria, Victoria, Canada.

M. -S. Alouini (e-mail: alouini@qatar.tamu.edu) is with the Dept. of ECE, Texas A&M University-Qatar, Education City, Doha, Qatar.

1 Introduction

The need for ever higher spectrum efficiency for power limited mobile users motivates further optimization of the use of wireless resources. Resource management in wireless communications is a difficult task due to user mobility and highly time-variant propagation environments, thus implying adaptive solutions. Key adaptive techniques are those of adaptive modulation [1], power control [2], and adaptive combining [3–6].

In [7; 8] novel jointly adaptive modulation and combining schemes are introduced. As the schemes utilize a constant-power variable-rate setup, for a finite number of rates, these schemes transmit with a higher average power than what is necessary to fulfill the bit error rate (BER) constraint. Specifically, for a multi-link (e.g., in cellular or ad-hoc networks) communications environment, higher transmit power implies higher interference to co-existing links, which in turn can impose significant network capacity reductions. Further, in [9], adaptive combining and power control were studied for constant-rate transmission. Hence, for the purpose of interference reduction in variable-rate systems, we extend the schemes of [7; 8], by introducing power control, and [9; 10], by introducing adaptive modulation. The transmission schemes we consider here are directed towards implementation, contrasting the more theoretical work in [11], where capacity-achieving codes were used for spectral efficiency maximization.

There is a rich literature on diversity combining schemes, e.g., [12; 4; 3; 5; 13]. In generalized selection combining (GSC), the receiver will combine a fixed number of the resolvable paths with the highest signal-to-noise ratio (SNR), reducing the complexity relative to the optimal maximum ratio combining (MRC) scheme. However, both the GSC and MRC combining schemes always combine the maximum number of allowed branches, even if combining fewer branches would satisfy the transmission requirements. Proposed in [5], the *minimum selection* GSC (MS-GSC) attempts to solve this by combining the smallest possible number of highest-SNR branches such that the combined SNR is above a given threshold. On the average MS-GSC combines less branches, and hence uses less processing power than GSC [4; 3; 6], making it ideal for a downlink scenario where the mobile unit is power and size limited.

In this paper, we consider joint adaptive modulation and diversity combining (AMDC) for downlink transmission, where it is of interest to have low processing costs at the battery powered mobile unit (hence, to combine the fewest number of branches). Additionally, reducing the transmitted power from the base stations is beneficial, as this will introduce less interference to other users and systems, and as such increase the overall system

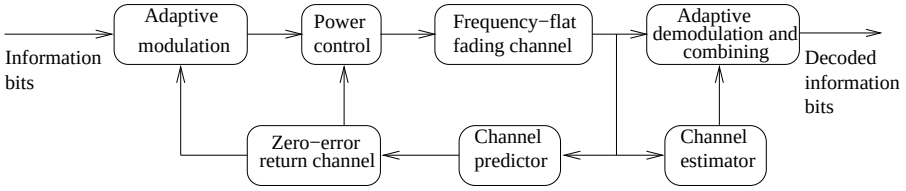

Figure E.1: Transmission system block diagram.

capacity. Depending on the key purpose of the design, we arrive at either a processing-power efficient or a bandwidth-efficient scheme. Based on a mathematical analysis, we evaluate the average spectral efficiency, BER, diversity combining complexity, and transmit power gain performance of these schemes. We show that the new power controlled AMDC schemes simultaneously achieve low processing complexity and reduced radiated power, as well as high average spectral efficiency (ASE) and compliance with BER constraints. Specifically, over a large SNR range the transmitted power is reduced by $30 - 50\%$.

The remainder of the present correspondence is organized as follows. In Section 2, we introduce the system model and describe the joint adaptive transmission schemes. Performance analysis of the proposed schemes is carried out in Section 3. Numerical examples and plots are given in Section 4. Finally, we conclude in Section 5.

2 Models and Mode of Operation

2.1 System And Channel Model

We study a generic diversity system as shown in Fig. E.1, assuming that there are L available diversity branches. While the proposed schemes and corresponding analytical framework are in general applicable to generic fading distributions, we limit ourselves to an independent identically distributed (iid) Rayleigh fading scenario to obtain closed-form results. Hence, we assume that the received signal on each diversity branch experiences iid Rayleigh fading. Additionally, the wireless channel is affected by additive white gaussian noise (AWGN). Under the assumption of frequency-flat fading, we may use a block-fading model to approximate the wireless fading channel by an AWGN channel within the length of one coherence time [14]. Further, as in [1], we assume that there is a reliable feedback path between the receiver and the transmitter. Within a guard period in the transmitted signal, the receiver is able to perform path esti-

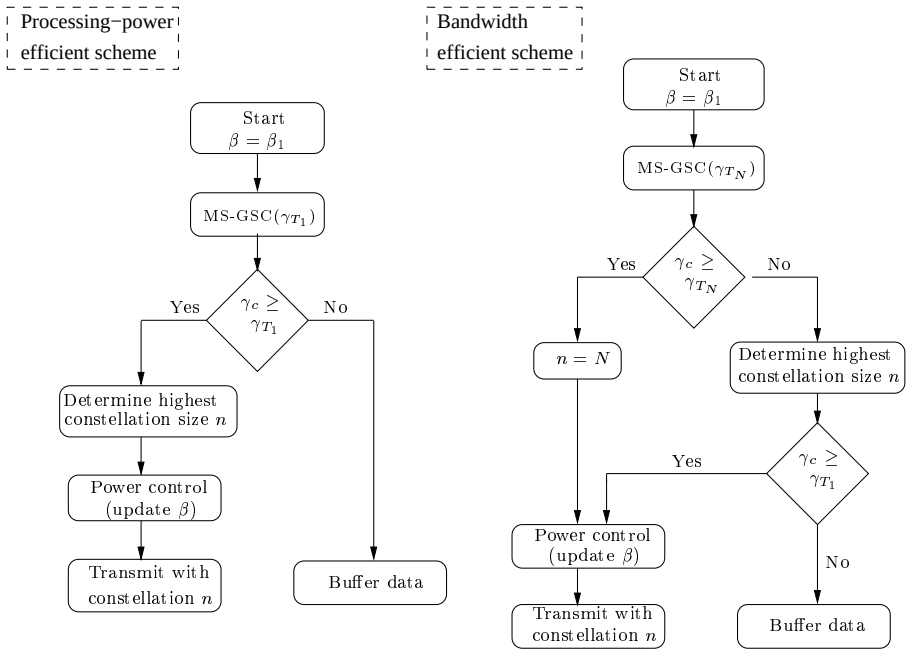

Figure E.2: Mode of operation for the proposed joint adaptive schemes. To the left the processing-power efficient scheme is shown, and to the right is the bandwidth efficient scheme.

mation, decide on a diversity structure and signal constellation, and finally select the power to be used for transmission. Once the settings are found, the transmitter and receiver will use them for the subsequent data burst, lasting up to one fading block.

2.2 M-QAM Based Link Adaptation

We consider the constant power M-ary adaptive QAM scheme studied in [7; 8]. This scheme consists of N signal constellations of size $M = 2^n$, where $1 \leq n \leq N$. Mode selection is based on a partitioning of the combined SNR range into $N + 1$ regions, defined by the switching thresholds $\{\gamma_{\mathrm{T}_n}\}_{n=1}^{N}$, defining $\gamma_{\mathrm{T}_0} = 0$ and $\gamma_{\mathrm{T}_{N+1}} = \infty$ for convenience. Constellation n is used for transmission if the combined SNR is in the interval $[\gamma_{\mathrm{T}_n}, \gamma_{\mathrm{T}_{n+1}})$. The BER of 2^n-QAM constellations over an AWGN channel with SNR γ can be well approximated by [1]

$$\mathrm{BER}_n(\gamma) = \frac{1}{5} \exp\left(\frac{-3\gamma}{2(2^n - 1)}\right), \; n = 1, \ldots, N. \tag{E.1}$$

Now, given a target bit error rate BER_0, the switching thresholds $\{\gamma_{\mathrm{T}_n}\}$ are found from (E.1) as:

$$\gamma_{\mathrm{T}_n} = -\frac{2}{3}\ln(5\,\mathrm{BER}_0)(2^n - 1),\ n = 1, \ldots, N. \tag{E.2}$$

2.3 Processing-Power Efficient AMDC Scheme

The idea of the processing-power efficient AMDC scheme (PES) is to combine the fewest branches possible, while achieving the required SNR for the lowest signal constellation, and still benefiting from rate adaptivity. The left flowchart in Fig. E.2 shows the mode of operation for the PES AMDC scheme. For each data burst, the base station initially transmits a training sequence using the highest available power level. The mobile subsequently tries to increase the output SNR above the threshold for the lowest constellation size by performing MS-GSC[1] with γ_{T_1} as output threshold. When the combined output SNR γ_c is above γ_{T_1}, the mobile stops and determines the highest feasible constellation index n for the given γ_c. This index might be larger than the lowest rate index 1, since the combining procedure yields discrete steps in SNR when the number of combined branches increases. Next, the mobile asks the base station to i) reduce its power level maximally such that this constellation is still usable and, ii) transmit with the chosen constellation. Hence, this scheme can still benefit from the availability of higher rates should the channel be in a good enough state. This feature is especially desirable for the transmission of multimedia streams. If the combined SNR is still smaller than γ_{T_1} after combining all L paths, the base station buffers the data, and will not transmit for the next time interval.

For the PES, the probability density function (pdf) of the received SNR using the highest power level is[8]

$$f_{\gamma_c}(\gamma_c) = f_{\gamma_c}^{\mathrm{MSC}(\gamma_{\mathrm{T}_1})}(\gamma_c)u(\gamma_c - \gamma_{\mathrm{T}_1}) + F_{\gamma_c}^{\mathrm{MSC}(\gamma_{\mathrm{T}_1})}(\gamma_{\mathrm{T}_1})\delta(\gamma_c), \tag{E.3}$$

where $u(\cdot)$, $\delta(\cdot)$, $F(\cdot)$ are respectively, the unit step function, the delta function, and the cumulative distribution function (cdf). $f_{\gamma_c}^{\mathrm{MSC}(\gamma_{\mathrm{T}_1})}$ denotes the pdf of the combined SNR with L-branch MS-GSC combining, using γ_{T_1} as the output threshold, and is given for the iid Rayleigh fading case as [6, Eq.

[1] For a detailed explanation and analysis of MS-GSC, please see [6].

(34)]:

$$f_{\gamma_c}^{\mathrm{MSC}(\gamma)} = \begin{cases} \frac{L}{\overline{\gamma}}\left(1-e^{-\frac{\gamma}{\overline{\gamma}}}\right)^{L-1} e^{-\frac{\gamma}{\overline{\gamma}}} + \sum_{i=2}^{L}\Bigg\{ \frac{L!}{(L-i)!(i-1)!i!\overline{\gamma}} e^{-\frac{\gamma}{\overline{\gamma}}} \left(\frac{i\gamma_{\mathrm{T}_1}-(i-1)\gamma}{\overline{\gamma}}\right)^{i-1} \\ + \sum_{j=1}^{L-i} \frac{L!(-1)^{j-i+1}}{(L-i-j)!i!j!\overline{\gamma}} \left(\frac{i}{j}\right)^{i-1} \\ \times \left[1 - e^{-\frac{j((i-1)\gamma - i\gamma_{\mathrm{T}_1})}{i\overline{\gamma}}} \sum_{k=0}^{i-2} \frac{1}{k!}\left(\frac{j((i-1)\gamma - i\gamma_{\mathrm{T}_1})}{i\overline{\gamma}}\right)\right]\Bigg\} \\ \times \left(u(\gamma-\gamma_{\mathrm{T}_1}) - u(\gamma - \frac{i}{i-1}\gamma_{\mathrm{T}_1})\right), & \gamma \geq \gamma_{\mathrm{T}_1}, \\ e^{-\frac{\gamma}{\overline{\gamma}}}\left(\frac{\gamma^{L-1}}{\overline{\gamma}^L(L-1)!}\right), & 0 \leq \gamma < \gamma_{\mathrm{T}_1}. \end{cases} \tag{E.4}$$

Inspecting (E.4), we see that for $0 \leq \gamma < \gamma_{\mathrm{T}_1}$, the pdf is equivalent to the well known pdf for maximum ratio combining [12, Eq. (17)], while for $\gamma \geq \gamma_{\mathrm{T}_1}$, the pdf carefully takes into account that only the minimum number of branches required to reach the threshold γ_{T_1} should be combined. Similarly, $F_{\gamma_c}^{\mathrm{MSC}(\cdot)}$ is found in [6, Eq. (24)].

2.4 Bandwidth-Efficient AMDC Scheme

Whereas the previous scheme strives to minimize the number of combined branches for a minimum rate requirement, the bandwidth-efficient scheme (BES) is primarily designed to maximize the spectral efficiency. In this scheme the receiver thus performs diversity combining aiming for the highest signal constellation, however with a side look to transmit power reduction. As illustrated to the right in Fig. E.2, the mobile tries to facilitate the highest constellation by performing MS-GSC with γ_{T_N} as output threshold. Whenever the output SNR goes above γ_{T_N}, the mobile asks the base station to transmit using the lowest possible power level such that the highest constellation is still usable. If the combined SNR is still smaller than γ_{T_N}, even after combining all L paths, the mobile will determine the highest feasible constellation size. Next, the mobile asks the base station to i) reduce its power level such that this constellation is still usable, and ii) transmit with the chosen constellation. If even the lowest constellation size is not feasible, data is buffered, and there is no transmission for the next time interval.

For the BES, the pdf of the received SNR using the highest power level is [8]

$$f_{\gamma_c}(\gamma_c) = f_{\gamma_c}^{\mathrm{MSC}(\gamma_{\mathrm{T}_N})}(\gamma_c)u(\gamma_c - \gamma_{\mathrm{T}_1}) + F_{\gamma_c}^{\mathrm{MSC}(\gamma_{\mathrm{T}_N})}(\gamma_{\mathrm{T}_1})\delta(\gamma_c). \tag{E.5}$$

2.5 Power Control

In an ideal adaptive power control scheme, the transmitted power can be varied continuously to follow the channel variations, establishing an upper bound on the transmit power gain. However, continuous power control is not realistic as it would require an infinite capacity feedback channel. In addition, it is not likely that the transmitter is able to transmit at a very large (infinite) number of power levels. For practical scenarios the resolution of power control is limited, e.g., in UMTS power control steps are on the order of 1 dB [15]. Thus, we analyze both continuous and discrete power adaptation.

For a combined SNR of γ_c, we denote the post-adaptation SNR by ${\gamma_c}' = \frac{\gamma_c}{\beta}$, where β is the power control parameter. Specifically, for continuous power control, $\beta \in [1, \infty)$, while for the discrete level power control, the system can choose between M power parameters, $\{\beta_1 = 1 < \beta_2 < \cdots < \beta_M\}$. The range of the power control must be limited such that once a signal constellation n has been chosen, the BER constraint is not violated. For continuous power control this implies that the SNR is reduced to γ_{T_n}, while for discrete control we enforce

$$\beta_M \leq \min_{1 \leq n \leq N} \frac{\gamma_{\mathrm{T}_{n+1}}}{\gamma_{\mathrm{T}_n}}. \tag{E.6}$$

Using discretized power levels, the mobile is only required to feed back an indexed rate and power pair for each fading block. Indexing $N+1$ SNR regions and M power levels requires at most $\log_2(N+1+M)$ bits, thus implying a manageable feedback load.

Before we proceed, note that both the BES and PES schemes can be applied directly to uplink transmission. However, in an uplink setting, the processing power cost of diversity combining is likely to be less important, and hence GSC should be used in place of MS-GSC.

3 Performance Analysis

3.1 Transmit Power Gains

Let us assume that, using full transmit power and MS-GSC diversity combining, the system has obtained a combined SNR of γ_c, and decides to operate with constellation n. Now, the constellation n requires a SNR of at least γ_{T_n} to operate within the BER requirement. Thus, there is an SNR surplus of $\frac{\gamma_c}{\gamma_{\mathrm{T}_n}}$.

3.1.1 Continuous Power Control

Using continuous power control we are able to reduce the SNR surplus maximally, i.e. to zero, hence maximally reducing the interference. For $\gamma_{\mathrm{T}_n} \leq \gamma_c < \gamma_{\mathrm{T}_{n+1}}$, the power gain is thus given by $\frac{\gamma_c}{\gamma_{\mathrm{T}_n}}$, yielding an average transmit power gain in decibels of

$$\begin{aligned}\overline{G}_{\mathrm{dB}} &= \sum_{n=1}^{N} \int_{\gamma_{\mathrm{T}_n}}^{\gamma_{\mathrm{T}_{n+1}}} 10\log_{10}\left(\frac{\gamma_c}{\gamma_{\mathrm{T}_n}}\right) f_{\gamma_c}(\gamma_c)\,\mathrm{d}\gamma_c \\ &= \sum_{n=1}^{N} \int_{\gamma_{\mathrm{T}_n}}^{\gamma_{\mathrm{T}_{n+1}}} 10\log_{10}(\gamma_c) f_{\gamma_c}(\gamma_c)\,\mathrm{d}\gamma_c \\ &\quad - \sum_{n=1}^{N} 10\log_{10}(\gamma_{\mathrm{T}_n})\big(F_{\gamma_c}(\gamma_{\mathrm{T}_{n+1}}) - F_{\gamma_c}(\gamma_{\mathrm{T}_n})\big).\end{aligned} \tag{E.7}$$

3.1.2 Discrete Power Control

For discrete level power control, the choice of the power parameter β will quantify the transmit power gain, and can be summarized as follows. For $\gamma_{\mathrm{T}_n} \leq \gamma_c < \gamma_{\mathrm{T}_{n+1}}$, $n \geq 1$,

$$\begin{aligned}&\beta = \beta_M \text{ iff } \frac{\gamma_c}{\gamma_{\mathrm{T}_n}} \geq \beta_M, \\ &\beta = \beta_{M-1} \text{ iff } \frac{\gamma_c}{\gamma_{\mathrm{T}_n}} \geq \beta_{M-1} \text{ and } \frac{\gamma_c}{\gamma_{\mathrm{T}_n}} < \beta_M, \\ &\quad\vdots \\ &\beta = \beta_2 \text{ iff } \frac{\gamma_c}{\gamma_{\mathrm{T}_n}} \geq \beta_2 \text{ and } \frac{\gamma_c}{\gamma_{\mathrm{T}_n}} < \beta_3, \\ &\beta = 1, \text{ iff } \frac{\gamma_c}{\gamma_{\mathrm{T}_n}} < \beta_2.\end{aligned} \tag{E.8}$$

Introducing the power level switching thresholds $\gamma_{\mathrm{T}_{n,m}}$, which for $m \neq M+1$ are given as $\gamma_{\mathrm{T}_{n,m}} = \gamma_{\mathrm{T}_n}\beta_m$, while $\gamma_{\mathrm{T}_{n,M+1}} = \gamma_{\mathrm{T}_{n+1}}$, we can calculate the average transmit power gain from (E.8) as

$$\begin{aligned}\overline{G}_{\mathrm{dB}} &= \sum_{n=1}^{N} \int_{\gamma_{\mathrm{T}_n}}^{\gamma_{\mathrm{T}_{n+1}}} 10\log_{10}\left(\frac{\gamma_c}{\gamma_c/\beta}\right) f_{\gamma_c}(\gamma_c)\,\mathrm{d}\gamma_c \\ &= \sum_{n=1}^{N} \int_{\gamma_{\mathrm{T}_n}}^{\gamma_{\mathrm{T}_{n+1}}} 10\log_{10}(\beta) f_{\gamma_c}(\gamma_c)\,\mathrm{d}\gamma_c \\ &= \sum_{n=1}^{N} \sum_{m=2}^{M} 10\log_{10}(\beta_m)\big(F_{\gamma_c}(\gamma_{\mathrm{T}_{n,m+1}}) - F_{\gamma_c}(\gamma_{\mathrm{T}_{n,m}})\big).\end{aligned} \tag{E.9}$$

3.2 Average Spectral Efficiency and Number of Combined Branches

Based on the results of [8], we can evaluate the average spectral efficiency, denoted by η, for both schemes as:

$$\eta = \begin{cases} N - \sum_{n=1}^{N} F_{\gamma_c}^{\mathrm{MSC}(\gamma_{\mathrm{T}_1})}(\gamma_{\mathrm{T}_n}), \text{ PES}, \\ N - \sum_{n=1}^{N} F_{\gamma_c}^{\mathrm{MSC}(\gamma_{\mathrm{T}_N})}(\gamma_{\mathrm{T}_n}), \text{ BES}. \end{cases} \tag{E.10}$$

Next, the average number of combined branches ($\overline{B}_c$) is found as [8]:

$$\overline{B}_c = \begin{cases} 1 + \sum_{i=1}^{L-1} F_{\gamma_c}^{L/i-\mathrm{GSC}}(\gamma_{\mathrm{T}_1}) - L F_{\gamma_c}^{L-\mathrm{MRC}}(\gamma_{\mathrm{T}_1}), \text{ PES}, \\ 1 + \sum_{i=1}^{L-1} F_{\gamma_c}^{L/i-\mathrm{GSC}}(\gamma_{\mathrm{T}_N}) - L F_{\gamma_c}^{L-\mathrm{MRC}}(\gamma_{\mathrm{T}_1}), \text{ BES}, \end{cases} \tag{E.11}$$

where $F_{\gamma_c}^{L-\mathrm{MRC}}(\cdot)$ is the cdf of the combined SNR using L-branch MRC combining [12, Eq. (29)].

3.3 Statistics of The Combined SNR After Power Control

To analyze the BER performance of the proposed schemes, we need a statistical characterization of the combined SNR after power control, which we now derive based on the mode of operation described in Section 2.

3.3.1 Continuous Power Control

The continuous power control allows the system to use the smallest power possible, after a signal constellation has been chosen. The pdf of the combined SNR after power control, $\gamma_c{}'$, is then simply given as

$$f_{\gamma_c{}'}(\gamma_c{}') = \left(F_{\gamma_c}(\gamma_{\mathrm{T}_{n+1}}) - F_{\gamma_c}(\gamma_{\mathrm{T}_n})\right) \delta(\gamma_c{}' - \gamma_{\mathrm{T}_n}),\ 0 \le n \le N, \tag{E.12}$$

The cumulative distribution function is then found, for $0 \le n \le N$, as

$$F_{\gamma_c{}'}(\gamma_c{}') = \begin{cases} 0, & \gamma_c{}' < 0, \\ F_{\gamma_c}(\gamma_{\mathrm{T}_{n+1}}), & \gamma_{\mathrm{T}_n} \le \gamma_c{}' < \gamma_{\mathrm{T}_{n+1}}. \end{cases} \tag{E.13}$$

3.3.2 Discrete Power Control

Utilizing discrete-level power control we will, for a fixed constellation n, obtain a combined SNR in the range $[\gamma_{\mathrm{T}_n}, \max\{\gamma_{\mathrm{T}_n}\beta_2, \gamma_{\mathrm{T}_{n+1}}/\beta_M\})$. In the following derivation we assume that all the power control steps are of equal

length (in dB)[2], i.e., $\frac{\beta_{p+1}}{\beta_p} = \Delta\beta$, $1 \leq p \leq M-1$. Depending on the length of the interval $[\gamma_{\mathrm{T}_n}, \gamma_{\mathrm{T}_{n+1}}]$ and the power parameter β_M, the post-adaptation SNR can be in one of two regions. Specifically, if $\gamma_{\mathrm{T}_n}\beta_M\beta_2 \geq \gamma_{\mathrm{T}_{n+1}}$, the combined SNR after power adaptation will be in $[\gamma_{\mathrm{T}_n}, \gamma_{\mathrm{T}_n}\beta_2)$, while if this condition is not satisfied, it is *also* possible to have a post-adaptation SNR in the region $[\gamma_{\mathrm{T}_n}\beta_2, \gamma_{\mathrm{T}_{n+1}}/\beta_M)$. Thus, for $\gamma_{\mathrm{T}_n} \leq y < \gamma_{\mathrm{T}_n}\beta_2, n \geq 1$,

$$\begin{aligned}\Pr\left(\gamma_c{}' \leq y\right) &= \Pr\left(\gamma_c \leq y\right) \\ &+ \Pr\left(\gamma_{\mathrm{T}_n}\beta_2 \leq \gamma_c < y\Delta\beta\right) + \cdots + \Pr\left(\gamma_{\mathrm{T}_n}\beta_M \leq \gamma_c < \min\left\{y\Delta\beta, \gamma_{\mathrm{T}_{n+1}}\right\}\right).\end{aligned} \tag{E.14}$$

Now, if $\gamma_{\mathrm{T}_n}\beta_M\Delta\beta < \gamma_{\mathrm{T}_{n+1}}$, we have for $\gamma_{\mathrm{T}_n}\beta_2 \leq y < \gamma_{\mathrm{T}_{n+1}}/\beta_M$,

$$\Pr\left(\gamma_c{}' \leq y\right) = \Pr\left(\gamma_{\mathrm{T}_n}\beta_M\Delta\beta \leq \gamma_c < y\beta_M\right) + \Pr\left(\gamma_c{}' \leq \gamma_{\mathrm{T}_n}\beta_2\right). \tag{E.15}$$

Finally, for $\max\{\gamma_{\mathrm{T}_n}\beta_2, \gamma_{\mathrm{T}_{n+1}}/\beta_M\} \leq y < \gamma_{\mathrm{T}_{n+1}}$:

$$\Pr\left(\gamma_c{}' \leq y\right) = \Pr\left(\gamma_c{}' \leq \max\{\gamma_{\mathrm{T}_n}\beta_2, \gamma_{\mathrm{T}_{n+1}}/\beta_M\}\right). \tag{E.16}$$

Then, by differentiation we obtain the pdf as follows:

$$f_{\gamma_c{}'}(\gamma_c{}') = \begin{cases} f_{\gamma_c}(\gamma_c{}') + \sum_{j=2}^{M}\beta_j f_{\gamma_c}(\gamma_c{}'\beta_j), & \gamma_{\mathrm{T}_n} \leq \gamma_c{}' < \gamma_{\mathrm{T}_n}\beta_2, \\ & \& \ \gamma_c{}'\beta_M \leq \gamma_{\mathrm{T}_{n+1}}, \\ f_{\gamma_c}(\gamma_c{}') + \sum_{j=2}^{M-1}\beta_j f_{\gamma_c}(\gamma_c{}'\beta_j), & \gamma_{\mathrm{T}_n} \leq \gamma_c{}' < \gamma_{\mathrm{T}_n}\beta_2, \\ & \& \ \gamma_c{}'\beta_M > \gamma_{\mathrm{T}_{n+1}}, \\ \beta_M f_{\gamma_c}(\gamma_c{}'\beta_M), & \gamma_{\mathrm{T}_n}\beta_2 \leq \gamma_c{}' < \frac{\gamma_{\mathrm{T}_{n+1}}}{\beta_M}, \\ & \& \ \gamma_{\mathrm{T}_n}\beta_M\Delta\beta \leq \gamma_{\mathrm{T}_{n+1}}, \\ 0, & \text{otherwise.} \end{cases} \tag{E.17}$$

3.4 Bit Error Rate

The average bit error rate for the proposed schemes can be calculated as [1]

$$\overline{\mathrm{BER}} = \frac{1}{\eta}\sum_{n=1}^{N} n\overline{\mathrm{BER}}_n, \tag{E.18}$$

where $\overline{\mathrm{BER}}_n$ is the average bit error rate for constellation n, found by utilizing (E.1) as:

$$\overline{\mathrm{BER}}_n = \int_{\gamma_{\mathrm{T}_n}}^{\gamma_{\mathrm{T}_{n+1}}} \mathrm{BER}_n(\gamma_c{}') f_{\gamma_c{}'}(\gamma_c{}')\,\mathrm{d}\gamma_c{}', \ n = 1, \ldots, N. \tag{E.19}$$

[2]This is not claimed to be optimal, but accurately reflects practical power control settings used in e.g. UMTS [15].

Hence, using the probability distributions derived in the previous subsections, we can calculate the bit error rate performance of the proposed schemes as follows:

$$\overline{\mathrm{BER}} = \frac{\sum_{n=1}^{N} n \int_{\gamma_{\mathrm{T}_n}}^{\gamma_{\mathrm{T}_{n+1}}} \mathrm{BER}_n(\gamma_c{}') f_{\gamma_c{}'}(\gamma_c{}') \, \mathrm{d}\gamma_c{}'}{\eta}. \tag{E.20}$$

Using continuous power allocation, we have from the analysis above:

$$\begin{aligned} \overline{\mathrm{BER}} &= \frac{1}{N - \sum_{n=1}^{N} F_{\gamma_c}^{\mathrm{MSC}(\gamma_{\mathrm{T}})}(\gamma_{\mathrm{T}_n})} \sum_{n=1}^{N} n \int_{\gamma_{\mathrm{T}_n}}^{\gamma_{\mathrm{T}_{n+1}}} \frac{1}{5} \exp\left(\frac{-3\gamma_c{}'}{2(2^n-1)}\right) \\ &\quad \times \left(F_{\gamma_c}^{\mathrm{MSC}(\gamma_{\mathrm{T}})}(\gamma_{\mathrm{T}_{n+1}}) - F_{\gamma_c}^{\mathrm{MSC}(\gamma_{\mathrm{T}})}(\gamma_{\mathrm{T}_n})\right) \delta(\gamma_c{}' - \gamma_{\mathrm{T}_n}) \, \mathrm{d}\gamma_c{}' \\ &\overset{\text{a)}}{=} \mathrm{BER}_0 \frac{\sum_{n=1}^{N} n \left(F_{\gamma_c}^{\mathrm{MSC}(\gamma_{\mathrm{T}})}(\gamma_{\mathrm{T}_{n+1}}) - F_{\gamma_c}^{\mathrm{MSC}(\gamma_{\mathrm{T}})}(\gamma_{\mathrm{T}_n})\right)}{N - \sum_{n=1}^{N} F_{\gamma_c}^{\mathrm{MSC}(\gamma_{\mathrm{T}})}(\gamma_{\mathrm{T}_n})} = \mathrm{BER}_0, \end{aligned} \tag{E.21}$$

where $\gamma_{\mathrm{T}} = \gamma_{\mathrm{T}_1}$ or $\gamma_{\mathrm{T}} = \gamma_{\mathrm{T}_N}$, and a) follows from using the sifting property of the Delta function [16] and (E.2). Thus, from (E.21), we see that for both schemes the average bit error rate using continuous power control is, as expected, equal to the bit error rate constraint, independent of the (average) SNR per branch.

Finally, in the case of very large average branch SNR and discrete level power control, the proposed schemes will always use the largest constellation size with the lowest transmit power level. Therefore, the average BER performance of the proposed schemes asymptotically approaches that of a 2^N-QAM constellation with transmit power scaled down by a factor of β_M from the maximum power level when SNR becomes large. If the size of the largest constellation N also increases, the proposed schemes will enjoy even higher spectral efficiency but with a non-diminishing average BER.

4 Numerical Results

In this section, we set the number of available diversity branches $L = 3$, the number of signal constellations $N = 4$, and the bit error rate constraint as $\mathrm{BER}_0 = 10^{-3}$.

4.1 Average Spectral Efficiency and Number of Combined Branches

Using Eqs. (E.10), (E.11) we plot the average spectral efficiency and the number of combined branches, as shown in Fig. E.3. The average num-

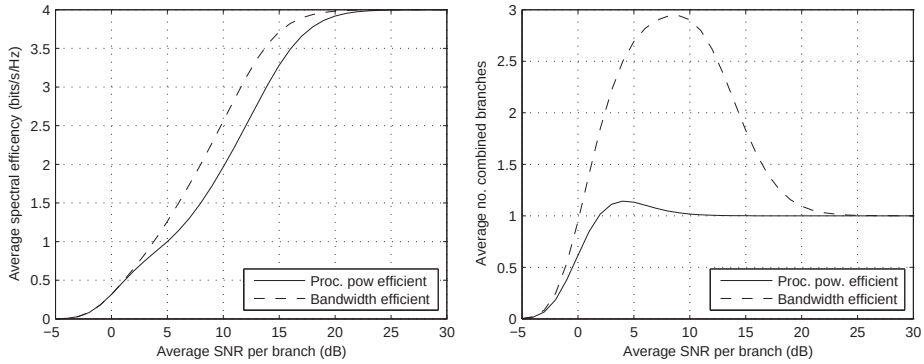

(a) (b)

Figure E.3: Average spectral efficiency and combining complexity versus the average SNR per branch.

ber of combined branches is roughly proportional to the receiver processing power, since every branch need a separate processing chain. For average branch SNRs between $5 - 20\,\mathrm{dB}$, there is a clear trade-off between processing power and spectral efficiency. For branch SNRs above 20 dB, one branch is enough to utilize the highest signal constellation (16-QAM), and the two schemes are for all practical purposes equivalent.

4.2 Transmit Power Gains

In Figs. E.4 and E.5 we depict the average transmit power gains (E.7), (E.9) for the proposed schemes. Although both figures exhibit a non-monotonic behavior, it is clear that introducing power control significantly reduces the average radiated power. Figs. E.4 and E.5 can be explained as follows. The power gains are due to a surplus of SNR relative to the selected constellation. From Fig. E.3a, at very low SNR data is buffered, hence no transmit power gain is possible. Increasing the branch SNR, we observe a steady increase in transmit power gain. In the intermediate range we see a slight decrease in the power gain, due to a combination of that i) the increased branch SNRs are used to facilitate larger constellations, and ii) the two intermediate intervals for constellations $n = 2, 3$ are shorter than the interval for $n = 1$, as seen from

$$\{\gamma_{\mathrm{T}_1}^{\mathrm{dB}}, \gamma_{\mathrm{T}_2}^{\mathrm{dB}}, \gamma_{\mathrm{T}_3}^{\mathrm{dB}}, \gamma_{\mathrm{T}_4}^{\mathrm{dB}}\} = \{5.48, 10.25, 13.93, 17.24\}. \tag{E.22}$$

Now, recall that the maximum reduction for discrete level transmit power control is limited by the shortest interval according to (E.6).

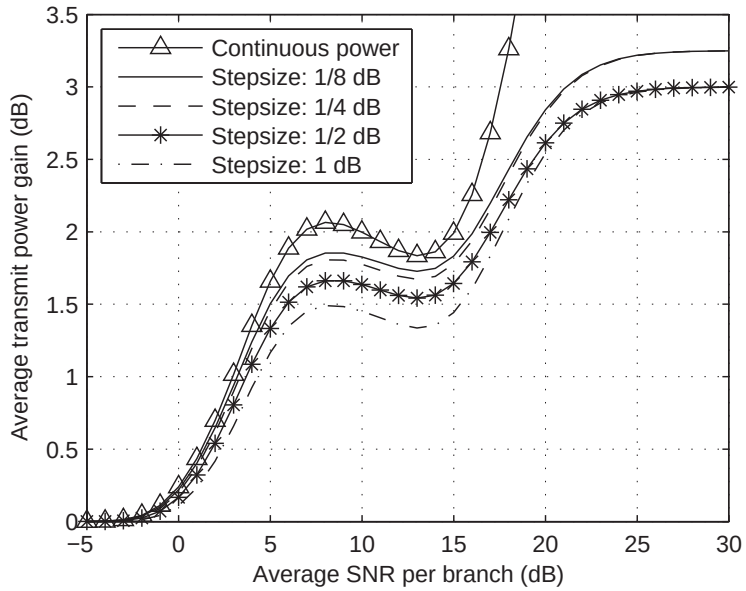

Figure E.4: Average transmit power gain for the processing-power efficient AMDC scheme versus the average SNR per branch.

From (E.6) and (E.22), the potential for power reduction using discrete level control is 3.31 dB. Thus, as expected when increasing the branch SNRs further, the average transmit power gain saturates at 3 dB for the step sizes $\Delta\beta_{\mathrm{dB}} = \{1, 1/2\}$ dB, while using step sizes of $\Delta\beta_{\mathrm{dB}} = \{1/4, 1/8\}$ dB allows for further increasing the average transmit power gain. Finally, the transmit power gain using continuous power control is unbounded, since there is no limitation on the maximum reduction in this case.

4.3 BER Performance

The bit error rate performance of the proposed schemes are shown in Fig. E.6. In the low-SNR range, the bandwidth-efficient scheme has slightly better error performance than the processing-power efficient scheme, due to combining more branches, as seen in Fig. E.3b. For reference, we also have included the BER performances of the two schemes using constant full power and continuous power control (E.21). As expected, the schemes using full power have better error performance, showing the tradeoff between transmit power gain and BER.

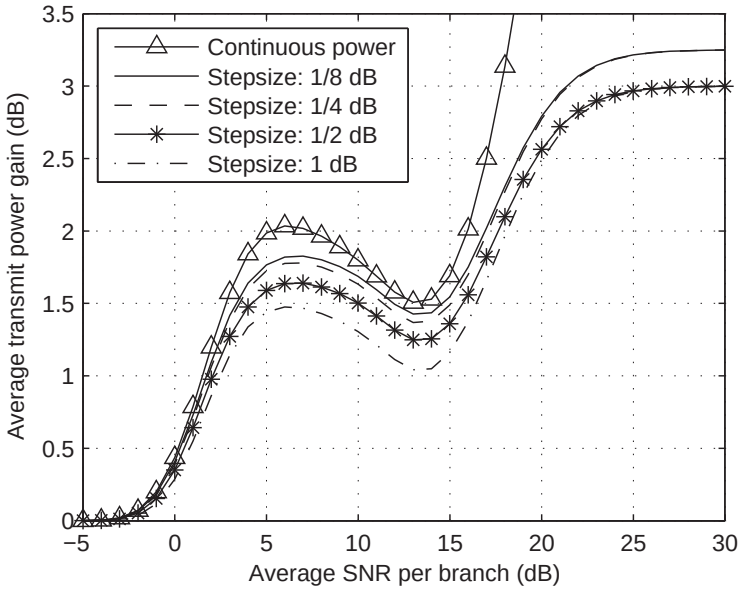

Figure E.5: Average transmit power gain for the bandwidth-efficient AMDC scheme versus the average SNR per branch.

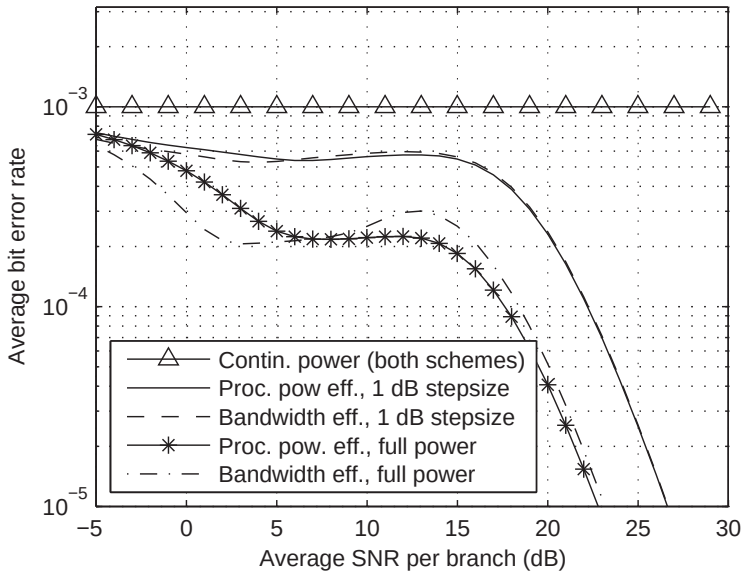

Figure E.6: Average bit error rate versus average SNR per branch. (BER constraint $\mathrm{BER}_0 = 10^{-3}$.)

5 Conclusions

We have investigated joint adaptive modulation and diversity combining for a downlink scenario. Specifically, we have introduced and analyzed a processing-power efficient scheme and a bandwidth-efficient scheme, both of which jointly determine the signal constellation and diversity combiner structure based on the channel fading condition and a bit error rate requirement. Furthermore, to reduce the interference to co-existing systems and users, transmit power control is applied. The statistics of the combined SNR after power control are derived, and both schemes are analyzed in terms of spectral efficiency, combiner complexity and bit error rate. For both schemes, a reduction of transmitted power on the order of $30 - 50\%$ is feasible over a large SNR range, thus significantly decreasing the level of interference to co-existing systems/users, making them ideal in a multi-link scenario, while upholding high spectral efficiency, maintaining low diversity combining complexity, and satisfying the BER constraints.

References

[1] M.-S. Alouini and A. J. Goldsmith, "Adaptive modulation over Nakagami fading channels," *Kluwer J. Wireless Communications*, vol. 13, pp. 119–143, May 2000.

[2] A. Gjendemsjø, G. E. Øien, and P. Orten, "Optimal discrete-level power control for adaptive coded modulation schemes with capacity-approaching component codes," in *Proc. IEEE International Conference on Communications*, Istanbul, Turkey, June 2006, pp. 5047–5052.

[3] R. K. Mallik, P. Gupta, and Q. T. Zhang, "Minimum selection GSC in independent Rayleigh fading," *IEEE Transactions on Vehicular Technology*, vol. 54, no. 3, pp. 1013–1021, May 2005.

[4] P. Gupta, N. Bansal, and R. K. Mallik, "Analysis of minimum selection H-S/MRC in Rayleigh fading," *IEEE Transactions on Communications*, vol. 53, no. 5, pp. 780–784, May 2005.

[5] S. W. Kim, D. S. Ha, and J. Reed, "Minimum selection GSC and adaptive low-power RAKE combining scheme," in *Proc. IEEE International Symposium on Circuits and Systems*, Bangkok, Thailand, May 2003, pp. 357–360.

[6] H.-C. Yang, "New results on ordered statistics and analysis of minimum-selection generalized selection combining (GSC)," *IEEE Transactions on Wireless Communications*, vol. 5, no. 7, pp. 1876–1885, July 2006.

[7] N. Belhaj, N. Hamdi, M.-S. Alouini, and A. Bouallegue, "Low-power minimum estimation and combining with adaptive modulation," in *Proc. IEEE International Symposium on Signal Processing and its Applications*, Sydney, Australia, Aug. 2005, pp. 687–690.

[8] H.-C. Yang, N. Belhaj, and M.-S. Alouini, "Performance analysis of joint adaptive modulation and diversity combining over fading channels," *IEEE Transactions on Communications*, vol. 55, no. 3, pp. 520–528, March 2007.

[9] N. Belhaj, M.-S. Alouini, and K. A. Qaraqe, "Minimum selection GSC with down-link power control," in *Proc. IEEE Vehicular Technology Conference*, Melbourne, Australia, May 2006, pp. 1821–1825.

[10] S. S. Nam, M.-S. Alouini, and K. A. Qaraqe, "Diversity combining with up-link power control," in *Proc. IEEE International Symposium on Personal, Indoor and Mobile Radio Communications*, Helsinki, Finland, Sept. 2006, pp. 1–5.

[11] A. Gjendemsjø, H.-C. Yang, M.-S. Alouini, and G. E. Øien, "Joint adaptive transmission and combining with optimized rate and power allocation," in *Proc. IEEE Workshop on Signal Processing Advances in Wireless Communications*, Cannes, France, July 2006, pp. 1–5.

[12] M.-S. Alouini and M. K. Simon, "An MGF-based performance analysis of generalized selection combining over Rayleigh fading channels," *IEEE Transactions on Communications*, vol. 48, no. 3, pp. 401–415, March 2000.

[13] M. K. Simon and M.-S. Alouini, *Digital Communication over Fading Channels*, 2nd ed. Wiley-IEEE Press, 2005.

[14] R. J. McEliece and W. E. Stark, "Channels with block interference," *IEEE Transactions on Information Theory*, vol. IT-30, no. 1, pp. 44–53, Jan. 1984.

[15] *Physical Layer Procedures (TDD)*, Third Generation Partnership Project, Technical Specification Group Radio Access Network Std., Rev. TS25.224 (Release 7), March 2006.

[16] E. W. Weisstein. Delta function. From MathWorld - A Wolfram web resource. [Online]. Available: http://mathworld.wolfram.com/DeltaFunction.html

Paper F

Joint Adaptive Modulation, Diversity Combining, and Power Control in Two-cell Wireless Networks

Anders Gjendemsjø, Hong-Chuan Yang, Mohamed-Slim Alouini, and Geir E. Øien

Under revision for possible publication in the *IEEE Transactions on Wireless Communications*.

Abstract

We consider the joint application of power control, adaptive modulation, and diversity combining in a two-cell wireless network. The goal is to derive practical low-complexity, bandwidth-efficient, and battery-power-efficient transmission schemes addressing the challenges of uplink and downlink transmission. Employing dynamic spectral reuse, we allow for coordination of the transmit power levels, thus managing interference to co-existing systems and cells. For uplink transmission, we minimize the sum transmit power in order to save valuable battery lifetime, and in the downlink setting we investigate spectral efficiency improving power control, taking into account the limited processing power of a mobile unit. The proposed schemes are evaluated by analyzing the spectral efficiency, transmit power, and diversity combiner complexity. Under a bit error rate constraint, we show that the novel transmission schemes significantly reduce the transmit power (uplink), and increase the spectral efficiency while achieving a low combining complexity (downlink), compared to reference schemes.

Parts of this paper will be presented at the IEEE International Symposium on Wireless Communication Systems (ISWCS'07), Trondheim, Norway, October 2007, and at the Asilomar Conference on Signals, Systems, and Computers (Asilomar '07) (invited paper), Pacific Grove, CA, USA, November 2007.

A. Gjendemsjø (contact author, e-mail: gjendems@iet.ntnu.no) and G. E. Øien are with the Dept. of Electronics and Telecommunications, Norwegian University of Science and Technology (NTNU), Trondheim, Norway.

H.-C. Yang (e-mail: hyang@ece.uvic.ca) is with the Dept. of ECE, University of Victoria, Victoria, Canada.

M.-S. Alouini (e-mail: alouini@qatar.tamu.edu) is with the Dept. of ECE, Texas A&M University-Qatar, Education City, Doha, Qatar.

1 Introduction

The demand for high system efficiency with limited available spectral and power resources presents the cellular system designer with tough challenges. Resource management in wireless communications is a difficult task due to user mobility and highly time-variant propagation environments, thus implying adaptive solutions. Key adaptive techniques are those of: i) *Adaptive modulation* increasing the spectral efficiency by adapting the signal constellation to the fading state [1; 2], ii) *power control* providing battery savings at the mobile unit and interference management [3; 4], and iii) (adaptive) *diversity combining* improving link quality by utilizing multiple signal paths for communication [5–7].

Recently, diversity combining and power control were studied for constant rate transmission in [8; 9] and for adaptive modulation in [10], however in both cases restricted to the single link case. Generalizing the system to multiple links adds the problem of inter-link interference. Hence, for the purpose of battery lifetime maximization, improved interference management, and increased spectral efficiency in variable-rate cellular systems, we extend the schemes of [8–10], by considering both uplink and downlink transmission in a two-cell network with a dynamic frequency reuse. A practical use of this two-cell setup to larger systems, would be to cluster the cells into (carefully chosen) groups of two cells over which the proposed scheme is employed.

The transmission between a mobile user and a base station in a cellular system is characterized by distinctive features. First, the mobile user has a very limited battery capacity. This battery limitation imposes important challenges; in the uplink the transmit power should be minimized subject to fulfilling the relevant quality of service constraints. In the downlink, when the mobile user is equipped with a receiver for diversity combining, the combining complexity is a significant source of power use, and should also be optimized. Second, the limited available radio spectrum inevitably leads to a high frequency reuse, and thus co-channel interference, which for both uplink and downlink can be managed by power control.

There is a rich literature on diversity combining schemes, e.g., [11; 5; 6; 12–15]. In *generalized selection combining* (GSC), the receiver will adaptively combine a fixed number of the resolvable paths with the highest signal-to-noise ratio (SNR)[1], reducing the complexity relative to the optimal *maximum ratio combining* (MRC) scheme. Further, since GSC receivers exclude the weakest branches from the combining process, they are more robust to-

[1] In the case of cellular systems, signal-to-noise-and-interference ratio (SNIR).

ward channel estimation errors. However, both the GSC and MRC combining schemes always combine the maximum number of allowed branches, even if combining fewer branches would also satisfy the transmission requirements. Proposed in [12], the *minimum selection* GSC (MS-GSC) attempts to solve this by combining the smallest possible number of highest-SNR branches such that the combined SNR is above a given threshold. On the average MS-GSC combines less branches, and hence uses less processing power than GSC [13–15], making it ideal for a downlink scenario where the mobile unit is power and size limited. Optimum diversity combining techniques from the perspective of a single cell experiencing co-channel interference were derived in [11]; however power control and adaptive modulation were not considered.

To address the particular challenges faced in up- and downlink transmission, in this paper we propose and analyze two different practical adaptive modulation and diversity combining schemes targeted at two-cell networks. In this scenario, and assuming dynamic frequency spectrum reuse, coordinated transmit power levels are used to i) reduce the transmitted power to extend the battery lifetime of the mobile user (uplink), ii) increase the spectral efficiency (downlink), and iii) minimize the interference to co-existing systems and cells. The proposed schemes are evaluated in terms of average spectral efficiency, transmit power, and number of combined branches, all based on a mathematical analysis. We show that the novel schemes achieve significant reductions in sum transmitted power compared to two benchmarking schemes (uplink), as well as high average spectral efficiency (ASE) and low combining complexity (downlink), as well as compliance with the bit error rate (BER) constraints.

The remainder of the present paper is organized as follows. In Section 2, we introduce the cellular, diversity combining, and adaptive modulation models. The novel schemes for uplink and downlink transmission are described and mathematically analyzed in Sections 3 and 4, respectively. Numerical examples and plots are given in Section 5. Finally, we conclude and discuss directions for future work in Section 6.

2 System Model

2.1 Cellular Setup

We consider both uplink and downlink transmission between mobile terminals and base stations in two neighboring cells, as depicted in Fig. F.1. We assume an orthogonal intra-cell multiple access scheme, such that in any given *spectral resource slot* (where resource slots can be time or fre-

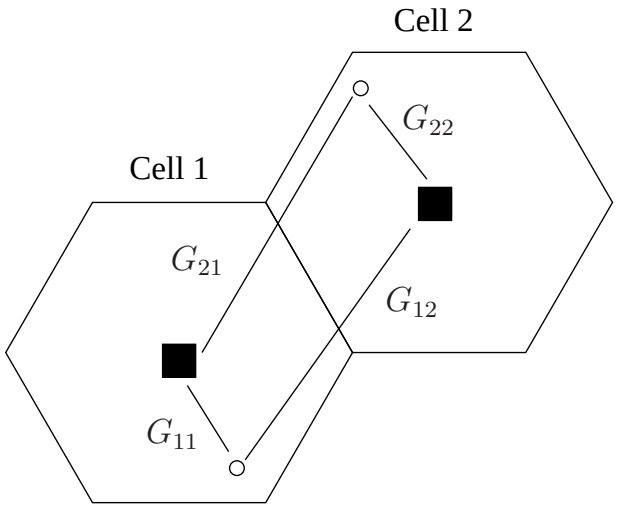

Figure F.1: Two-cell wireless system model (exemplified with hexagonal and perfectly aligned cells). Base stations (BS) are shown as solid squares and users as circles. For each link the associated channel gain G_{ji} is shown, where j corresponds to the BS index and i to the user index.

quency slots in TDMA/FDMA, or codes in orthogonal CDMA) two users are selected for transmission by a medium access control (MAC) protocol. The spectral resource slots are shared by both cells, leading in general to an interference and noise impaired system. Scheduling policies can, in principle, also be incorporated by suitably modifying the users' channel statistics [16]. However, in order to focus solely on the problem of joint adaptive modulation, power control, and diversity combining, we do not explicitly consider scheduling or MAC protocols here. Furthermore, although a hexagonal cell layout is shown for illustrational purposes in Fig. F.1, we emphasize that our analysis is valid for any pair of interfering links, even for non-cellular systems such as ad-hoc networks. However, to facilitate exposition a cellular terminology is adopted.

2.2 Diversity Model

In each receiver, we consider a generic diversity combiner where there are L available diversity branches, and assume that the received signal on each diversity branch experiences independent identically distributed (iid) Rayleigh fading. We assume that due to hardware complexity considerations, a maximum of L_c branches can be combined at the receiver side ($L_c \leq L$). Additionally, the wireless channel is affected by additive white

Gaussian noise (AWGN).

Denote by $G_{ji}(m) > 0$ the channel power gain between the mobile user $u_j(m)$ in cell j and the cell i base station, in resource slot m, after diversity combining. We will suppress the slot index from now on, concentrating on one arbitrary slot. Note that the gains G_{jj} correspond to the desired communication links, whereas the G_{ji} for $j \neq i$ correspond to the unwanted interference links. The channel gains are assumed to be independent across cells.

Assuming that the transmitters are enabled with a power control facility, we denote the *pre-adaptation* combined signal to noise-plus-interference ratio (SNIR) in cell j by γ_j^c, $j = 1, 2$. These are the SNIRs that would be experienced using signal constellations of power $P_{\max}$ in both cells. Adapting the transmitted power based on the channel state information, the SNIR after power control, termed *post-adaptation* SNIR and denoted by γ_j^{pc}, $j = 1, 2$, are given by:

$$\text{Uplink:} \quad \gamma_1^{\text{pc}} = \frac{P_1 G_{11}}{\sigma_1^2 + P_2 G_{21}}, \quad \gamma_2^{\text{pc}} = \frac{P_2 G_{22}}{\sigma_2^2 + P_1 G_{12}}, \tag{F.1a}$$

$$\text{Downlink:} \quad \gamma_1^{\text{pc}} = \frac{P_1 G_{11}}{\sigma_1^2 + P_2 G_{12}}, \quad \gamma_2^{\text{pc}} = \frac{P_2 G_{22}}{\sigma_2^2 + P_1 G_{21}}, \tag{F.1b}$$

where P_j and σ_j^2 are, respectively, the transmit powers and the variance of the independent zero-mean AWGN in cell j. It is seen from (F.1) that $\gamma_j^c = \gamma_j^{\text{pc}}|_{P_1 = P_2 = P_{\max}}$.

Assuming that the receivers have no explicit interference cancellation ability, the interference can be considered as noise, and in a Rayleigh fading environment this noise has a Gaussian distribution [11]. In this paper, the increase of noise power due to interference will be assumed to be the same across the branches and to be proportional to the transmitted power of the interferer. Hence in cell j, there is AWGN with a variance of $\sigma_j^2 + P_i G_{ji}, j \neq i$ for downlink, and similarly $\sigma_j^2 + P_i G_{ij}, j \neq i$ for uplink. In this setting, combining as per the rules of MRC is optimal [11].

Finally, we note that our system model with (possibly different) noise levels σ_1^2, σ_2^2 also accommodates the modeling of additional interfering sources disturbing the users differently. One important application of this is when, for complexity reduction, joint multi-cell power allocation is undertaken over a subnet (cluster) of two neighboring cells only. In this case σ_j^2 represents the combined effect of noise and interference received from the remaining out-of-cluster cells by the j^{th} user.

2.3 M-QAM Based Link Adaptation

We consider an adaptive QAM scheme consisting of N signal constellations of size 2^n, where $1 \leq n \leq N$. The mode selection is based on the channel state and the bit error rate requirement. Using the results of [1], the BER of 2^n-QAM constellations over an AWGN channel with a SNIR of γ, assuming coherent detection, can be well approximated by

$$\mathrm{BER}_n(\gamma) = \frac{1}{5}\exp\left(\frac{-3\gamma}{2(2^n-1)}\right),\ n = 1,\ldots,N. \tag{F.2}$$

Now, given a target bit error rate BER_0, the minimum SNIR threshold for utilizing constellation n is found by inverting (F.2):

$$\gamma_{\mathrm{T}_n} = -\frac{2}{3}\ln(5\,\mathrm{BER}_0)(2^n-1),\ n = 1,\ldots,N. \tag{F.3}$$

(F.3) represents a partition of the SNIR range into $N+1$ regions, defined by the switching thresholds $\{\gamma_{\mathrm{T}_n}\}_{n=1}^{N}$. Constellation n is selected for transmission if the SNIR is in the interval $[\gamma_{\mathrm{T}_n}, \gamma_{\mathrm{T}_{n+1}})$.

3 Uplink Transmission

3.1 Mode of Operation

The flowchart in Fig. F.2 shows the mode of operation for the proposed scheme. During a guard period, for each data burst, both mobiles transmit a training sequence using the highest available power level $P_{\max}$, permitting the channel power gains to be estimated at the base stations. The base station in cell j subsequently perform GSC diversity combining to achieve a pre-adaptation combined SNIR of γ_j^c. After combining, the receiver checks whether the combined SNIR is greater than γ_{T_1}. If so, the highest feasible constellation index for the given γ_j^c is determined. Following this, i) a centralized power control is invoked to minimize the sum transmit power of both cells, subject to the constraint that both constellations are still usable under the BER constraints, ii) the mobile is informed about the power level and constellation, and finally, iii) transmission occurs with the chosen constellation. If the combined SNIR is smaller than γ_{T_1}, the data are buffered and there will be no transmission in cell j in the next time interval.

Treating the interference as noise, and extending the results of [17] to GSC, the pdf of the pre-adaptation SNIR in cell j is found as:

$$f_{\gamma_j^c}(\gamma_j^c) = f_{\gamma_j^c}^{L/L_c-\mathrm{GSC}}(\gamma_j^c)u(\gamma_j^c - \gamma_{\mathrm{T}_1}) + F_{\gamma_j^c}^{L/Lc-\mathrm{GSC}}(\gamma_{\mathrm{T}_1})\delta(\gamma_j^c), \tag{F.4}$$

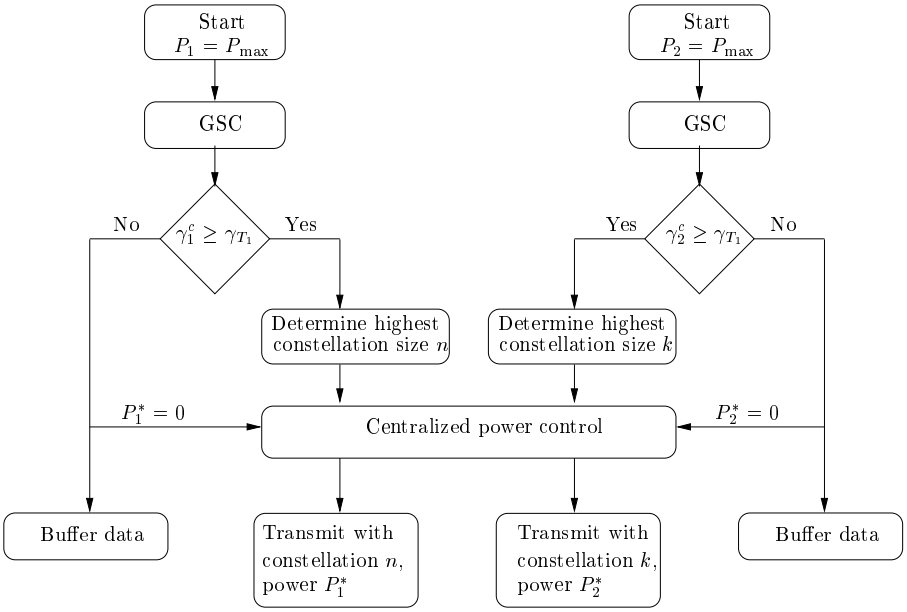

Figure F.2: Mode of operation for the *uplink* two-cell adaptive modulation, diversity combining and power control scheme.

where $u(\cdot)$, $\delta(\cdot)$, $F(\cdot)$ are, respectively, the unit step function, the delta function, and the cumulative density function (cdf). $f_{\gamma_j^c}^{L/L_c-\mathrm{GSC}}(\cdot)$ denotes the pdf of the combined SNIR with an L/L_c-GSC combining scheme, and is given in closed form for the iid Rayleigh fading case in [6, Eq. (16)]. Similarly, $F_{\gamma_j^c}^{L/Lc-\mathrm{GSC}}(\cdot)$ is found in [6, Eq. (24)].

3.2 Transmit Power Control

Following the mode of operation outlined above, after diversity combining, the centralized power control will minimize the sum transmit power subject to the constraint that the selected constellations are still usable. To establish upper bounds on the performance of the considered scheme, we consider the use of continuous power control. In general, we have pre-adaptation combined SNIRs of $\gamma_{\mathrm{T}_n} \leq \gamma_1^c < \gamma_{\mathrm{T}_{n+1}}$ and $\gamma_{\mathrm{T}_k} \leq \gamma_2^c < \gamma_{\mathrm{T}_{k+1}}$, and the power control proceeds by finding powers P_1^*, P_2^*, minimizing the sum transmit power, as the solution to the following constrained optimization problem[2]:

[2]Note that the problem can easily be extended to a weighted sum minimization.

$$\begin{aligned} &\text{minimize} && P_1 + P_2, \\ &\text{subject to} && \gamma_1^{\text{pc}} \geq \gamma_{\text{T}_n},\ \gamma_2^{\text{pc}} \geq \gamma_{\text{T}_k} \\ & && 0 \leq P_1, P_2 \leq P_{\max}. \end{aligned} \tag{F.5}$$

Writing out the constraints from (F.5) we find:

$$P_1 G_{11} - \gamma_{\text{T}_n}(\sigma_1^2 + P_2 G_{21}) \geq 0, \tag{F.6a}$$

$$P_2 G_{22} - \gamma_{\text{T}_k}(\sigma_2^2 + P_1 G_{12}) \geq 0, \tag{F.6b}$$

$$0 \leq P_1, P_2 \leq P_{\max}. \tag{F.6c}$$

Clearly, when considering *continuous* power control this is a convex optimization problem, and as such it has a global minimum. In fact the problem is a linear programming problem, which can be solved analytically. From the constraints in (F.6) and the mode of operation described in Section 3.1, we can identify four different events that might occur.

- Event A: Both cells achieve a pre-adaptation SNIR greater than or equal to the minimum threshold for communication γ_{T_1}, i.e., $\gamma_1^c, \gamma_2^c \geq \gamma_{\text{T}_1}$. In this case, the thresholds of the selected constellations, $\gamma_{\text{T}_n}, \gamma_{\text{T}_k} > 0$. Now, defining

$$b_1 = \frac{\gamma_{\text{T}_n} G_{21}}{G_{11}}, \quad b_2 = \frac{\gamma_{\text{T}_k} G_{12}}{G_{22}}, c_1 = \frac{\gamma_{\text{T}_n}\sigma_1^2}{G_{11}}, \quad c_2 = \frac{\gamma_{\text{T}_k}\sigma_2^2}{G_{22}}, \tag{F.7}$$

  and inspecting the feasible domain spanned by the constraints (F.6a), (F.6b), (F.6c) the solution to (F.5) is obtained as follows:

$$P_1^* = \frac{b_1 c_2 + c_1}{1 - b_1 b_2}, \quad P_2^* = c_2 + b_2 P_1^*, \tag{F.8}$$

  where it can be shown that $0 < b_1 b_2 < 1$.
- Event B: Cell 1 achieves a sufficient pre-adaptation SNIR for transmission, and selects constellation n. However, cell 2 cannot satisfy the transmission requirements. Hence, cell 2 is shut down, and the user in cell 1 will not experience any interference. Then P_1^* is found as the minimum power required to transmit using constellation n without interference, i.e.,

$$P_1^* = \frac{\gamma_{\text{T}_n}\sigma_1^2}{G_{11}}, \quad P_2^* = 0. \tag{F.9}$$

- Event C: Similar to Event B, just change all indices $1 \rightarrow 2$, and $n \rightarrow k$.

- Event D: Neither of the cells can achieve transmission, i.e., both $\gamma_1^c, \gamma_2^c < \gamma_{\mathrm{T}_1}$. Hence, both cells are turned off and we have

$$P_1^* = 0, \quad P_2^* = 0. \tag{F.10}$$

The power control above admits solutions where a mobile user shuts down completely. Since one or more of the mobile users may then be turned off in a resource slot, from a cellular engineering point of view this scheme can be interpreted as a form of *dynamic spectrum reuse*.

3.3 Average Transmit Power

Starting with initial powers $P_{\max}$ at both mobiles, after power control the powers are reduced to P_1^* and P_2^*. Now, based on the (mutually exclusive) events described in Section 3.2, we can derive the average per-cell transmit power $\overline{P}$ for the proposed scheme as follows:

$$\overline{P} = \frac{1}{2}\Big(E\{P_1^* + P_2^*, A\} + E\{P_1^* + P_2^*, B\} + E\{P_1^* + P_2^*, C\} + E\{P_1^* + P_2^*, D\}\Big). \tag{F.11}$$

To calculate the expectations we need the joint probability density function of γ_1^c, γ_2^c, which by the independence assumption in Section 2.1 is given as the product of the two marginal pdfs $f_{\gamma_1^c}(\cdot)$ and $f_{\gamma_2^c}(\cdot)$. Then, for given values of G_{12} and G_{21},

$$E\{P_1^* + P_2^*, A\} = \frac{1}{2}\sum_{n=1}^{N}\sum_{k=1}^{K}\int_{\gamma_{\mathrm{T}_n}}^{\gamma_{\mathrm{T}_{n+1}}}\int_{\gamma_{\mathrm{T}_k}}^{\gamma_{\mathrm{T}_{k+1}}}(P_1^* + P_2^*) f_{\gamma_1^c}(\gamma_1^c) f_{\gamma_2^c}(\gamma_2^c)\,\mathrm{d}\gamma_1^c\,\mathrm{d}\gamma_2^c, \tag{F.12}$$

where P_1^*, P_2^* are given in (F.8). Next, using P_1^* from (F.9) we arrive at

$$\begin{aligned} E\{P_1^* + P_2^*, B\} &= \frac{1}{2}\sum_{n=1}^{N}\int_{\gamma_{\mathrm{T}_n}}^{\gamma_{\mathrm{T}_{n+1}}} P_1^* f_{\gamma_1^c}(\gamma_1^c)\,\mathrm{d}\gamma_1^c \int_0^{\gamma_{\mathrm{T}_1}} f_{\gamma_2^c}(\gamma_2^c)\,\mathrm{d}\gamma_2^c \\ &= \frac{F_{\gamma_2^c}(\gamma_{\mathrm{T}_1})}{2}\sum_{n=1}^{N}\int_{\gamma_{\mathrm{T}_n}}^{\gamma_{\mathrm{T}_{n+1}}} P_1^* f_{\gamma_1^c}(\gamma_1^c)\,\mathrm{d}\gamma_1^c, \end{aligned} \tag{F.13}$$

and similarly for $E\{P_1^* + P_2^*, C\}$, while $E\{P_1^* + P_2^*, D\}$ is obviously zero.

3.4 Average Spectral Efficiency

The average per-cell spectral efficiency, denoted by η, is given by

$$\eta = \frac{1}{2}\left(\sum_{n=1}^{N} n p_{1,n} + \sum_{k=1}^{N} k p_{2,k}\right), \tag{F.14}$$

where $p_{1,n}$ is the probability that the nth constellation is used for transmission in cell 1, and similarly $p_{2,k}$ for constellation k in cell 2. Extending the single cell framework from [17] to a two-cell network, (F.14) can be evaluated as

$$\eta = N - \frac{1}{2}\sum_{n=1}^{N}\left(F_{\gamma_1^c}^{L/L_c-\mathrm{GSC}}(\gamma_{\mathrm{T}_n}) + F_{\gamma_2^c}^{L/L_c-\mathrm{GSC}}(\gamma_{\mathrm{T}_n})\right). \tag{F.15}$$

4 Downlink Transmission

Whereas the previous scheme targets minimization of transmit power for uplink transmission, we now consider a bandwidth-efficient scheme, primarily designed for high spectral efficiency downlink transmission. For battery powered mobile units, the combining complexity, measured as the (average) number of combined branches, is also an important issue. Hence, in this scheme the receiver thus performs MS-GSC[3] diversity combining aiming for the highest signal constellation, combined with a centralized power control seeking to increase the spectral efficiency.

4.1 Mode of Operation

As illustrated in Fig. F.3, in the bandwidth efficient downlink scheme, both base stations transmit a training sequence using the highest power level. Then, the mobile receivers estimate the channel power gains, and try to facilitate reception of the highest available constellation by performing MS-GSC with γ_{T_N} as output threshold. Following this, the channel power gains and the pre-adaptation constellations sizes are fed back the base stations, allowing for a centralized control. Now, if both mobiles can receive the highest constellation, the base stations use transmit power coordination to transmit using the lowest possible sum power such that the highest constellations are still usable. Otherwise, if the combined SNIR in one or both cells is still smaller than γ_{T_N}, even after combining all L_c paths, the centralized power control tries to increase the spectral efficiency (constellation size), subject to the BER constraints. After power control, the mobiles are informed about the chosen constellations and data transmission starts. If, for a given cell, even the lowest constellation size is not feasible, data are buffered, and there is no transmission for the next time interval.

Using MS-GSC, the number of combined branches is adapted to both the channel conditions and the target SNIR. And again, as in the uplink

[3]For a detailed explanation and analysis of MS-GSC, please see [15].

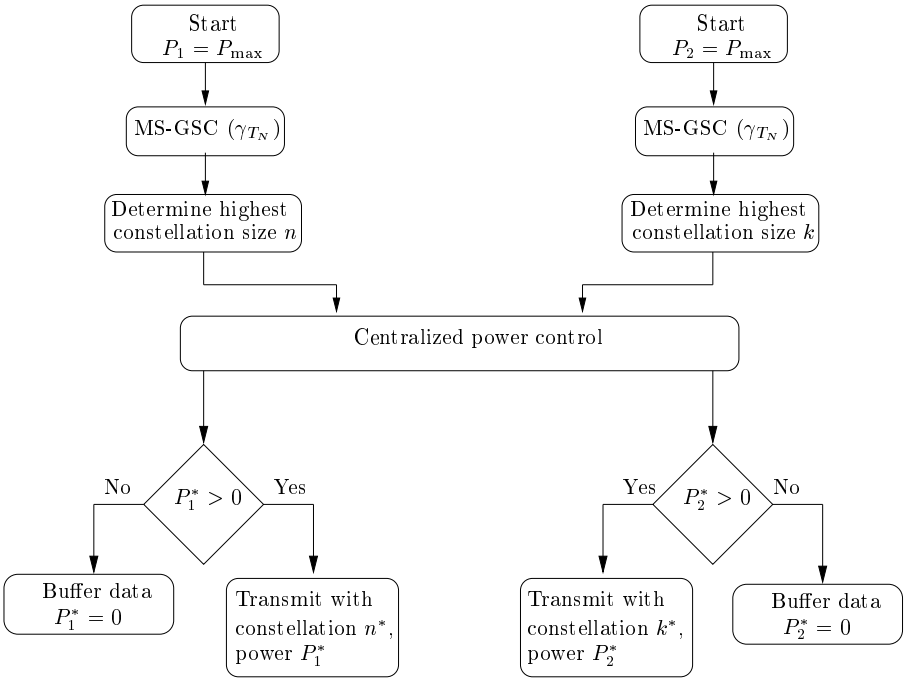

Figure F.3: Mode of operation for the *downlink* two-cell adaptive modulation, diversity combining and power control scheme.

case, when the interference is treated as noise, by means of [17] the pdf of the pre-adaptation SNIR in cell j using the bandwidth efficient scheme is found as

$$f_{\gamma_j^c}(\gamma_j^c) = f_{\gamma_j^c}^{\mathrm{MSC}(\gamma_{\mathrm{T}_N})}(\gamma_j^c)u(\gamma_j^c - \gamma_{\mathrm{T}_1}) + F_{\gamma_j^c}^{\mathrm{MSC}(\gamma_{\mathrm{T}_N})}(\gamma_{\mathrm{T}_1})\delta(\gamma_j^c), \qquad \text{(F.16)}$$

where $f_{\gamma_c}^{\mathrm{MSC}(\gamma_{\mathrm{T}})}$ denotes the pdf of the combined SNIR with L_c/L-branch MS-GSC combining, using γ_{T} as the output threshold, and is given for the iid Rayleigh fading case in [15, Eq. (34)]. Similarly, $F_{\gamma_c}^{\mathrm{MSC}(\cdot)}$ is found in [15, Eq. (24)].

4.2 Power Control Strategy

Following the mode of operation outlined above, the power control we propose minimizes the transmit power should both mobiles achieve a pre-adaptation SNIR $\geq \gamma_{\mathrm{T}_N}$. If not, the coordinated power control tries to increase the constellation sizes n and k to n^* and k^*, respectively.

As a starting point for the design of a practical spectral efficiency increasing power control scheme, we use the following result.

Lemma F.1
Starting with the maximum transmit power P_{max} in both cells, no power control strategy can be increase the SNIR in both cells simultaneously.

Proof: The idea of the proof is to show that no matter how we reduce powers P_1 and P_2 from their maximum values, at least one cell will decrease its SNIR level. Denote by $0 \leq \alpha = \frac{P_1}{P_{\max}}$, $\beta = \frac{P_2}{P_{\max}} \leq 1$, $\sigma_{j'}^2 = \frac{\sigma_j^2}{P_{\max}}$. Then, the post-adaptation SNIR in cell 1 can be written as

$$\gamma_1^c = \frac{\alpha G_{11}}{\sigma_{1'}^2 + \beta G_{12}}. \tag{F.17}$$

Lowering the transmit power in only one cell will obviously not increase the SNIRs of both cells, thus consider reducing the transmit powers such that $0 \leq \alpha \leq \beta < 1$, we obtain a SNIR in cell 1 as

$$\frac{\alpha G_{11}}{\sigma_{1'}^2 + \beta G_{12}} \leq \frac{\beta G_{11}}{\sigma_{1'}^2 + \beta G_{12}} < \frac{G_{11}}{\sigma_{1'}^2 + G_{12}} = \gamma_1^c, \tag{F.18}$$

where the far right hand side γ_1^c is the SNIR obtained by $\alpha = \beta = 1$, i.e., full power in both cells. Then, by symmetry, the same arguments hold for cell 2. □

Equipped with Lemma F.1, we cannot increase the constellation sizes of both cells simultaneously, and thus in the case of $n \neq k$, we give preference to the cell with the lowest constellation, i.e., reduce the power in the cell having the largest constellation, thus decreasing the interference to the other cell, and hence increasing the SNIR-level in the other cell. For the case of $n = k < N$, preference is given to the cell with the largest SNIR level, hoping to achieve a higher constellation. Summarizing, we have listed in Table F.1 the relevant cases we need to consider in order to analyze the proposed scheme. Due to symmetry, we only detail the analysis for events E, F, H, and J.

First, for event E, the two cells achieve $\gamma_1^c, \gamma_2^c \geq \gamma_{\mathrm{T}_N}$, and, similar to the uplink scheme, power control is carried out by finding powers P_1^*, P_2^*, minimizing the sum transmit power, as the solution to the following constrained optimization problem:

$$\begin{aligned} \text{minimize} \quad & P_1 + P_2, \\ \text{subject to} \quad & \gamma_1^{\mathrm{pc}} \geq \gamma_{\mathrm{T}_N},\ \gamma_2^{\mathrm{pc}} \geq \gamma_{\mathrm{T}_N} \\ & 0 \leq P_1, P_2 \leq P_{\max}. \end{aligned} \tag{F.19}$$

Table F.1: Events, Downlink Transmission

Event	Pre-adaptation		Post-adap.
	Constellations	SNIR	Constellations
E	N,N	γ_1^c, γ_2^c	N, N
F	$n > k$	$\gamma_1^c \geq \gamma_2^c$	$n^* = n$, $k^* \geq k$
G	$k > n$	$\gamma_2^c \geq \gamma_1^c$	$n^* \geq n$, $k^* = k$
H	$1 \leq n = k < N$	$\gamma_2^c \geq \gamma_1^c$	$n^* = n$, $k^* \geq k$
I	$1 \leq n = k < N$	$\gamma_1^c \geq \gamma_2^c$	$n^* \geq n$, $k^* = k$
J	$n = k = 0$	$\gamma_2^c \geq \gamma_1^c$	$n^* = n$, $k^* \geq k$
K	$n = k = 0$	$\gamma_1^c \geq \gamma_2^c$	$n^* \geq n$, $k^* = k$

Following (F.7) and (F.8), the solution to (F.19), can be obtained as follows:

$$P_1^* = \frac{c_4 b_3 + c_3}{1 - b_3 b_4}, \quad P_2^* = c_4 + b_4 P_1^*, \tag{F.20}$$

where we have defined

$$b_3 = \frac{\gamma_{\mathrm{T}_N} G_{12}}{G_{11}},\ b_4 = \frac{\gamma_{\mathrm{T}_N} G_{21}}{G_{22}},\ c_3 = \frac{\gamma_{\mathrm{T}_N} \sigma_1^2}{G_{11}},\ c_4 = \frac{\gamma_{\mathrm{T}_N} \sigma_2^2}{G_{22}}. \tag{F.21}$$

Next, for both events F and H, we want to reduce the power maximally in cell 1 in order to aid a spectral efficiency increase in cell 2, under the constraint that the constellation n can still be used for cell 1. I.e., we enforce $\gamma_1^{\mathrm{pc}} = \gamma_{\mathrm{T}_n}$, yielding

$$P_1^* = \frac{\gamma_{\mathrm{T}_n}}{G_{11}} \left(\sigma_1^2 + P_2 G_{12} \right). \tag{F.22}$$

Then, P_2^* is found as the power level that maximizes γ_2^{pc} subject to the peak power constraint. Using (F.22), we have

$$\gamma_2^{\mathrm{pc}} = \frac{P_2 G_{22}}{\sigma_2^2 + \frac{\gamma_{\mathrm{T}_n}}{G_{11}} \left(\sigma_1^2 + P_2 G_{12} \right) G_{21}}. \tag{F.23}$$

By differentiation of (F.23), we find

$$\frac{\mathrm{d}\, \gamma_2^{\mathrm{pc}}}{\mathrm{d}\, P_2} = \frac{G_{22} G_{11} (\sigma_2^2 G_{11} + \gamma_{\mathrm{T}_n} \sigma_1^2)}{(\sigma_2^2 G_{11} + \gamma_{\mathrm{T}_n} \sigma_1^2 + \gamma_{\mathrm{T}_n} P_2 G_{12})^2} > 0, \tag{F.24}$$

i.e., γ_2^{pc} is a strictly increasing function of P_2, and hence over the range of $0 \leq P_2 \leq P_{\max}$ the SNIR in cell 2 is maximized by letting $P_2 = P_{\max}$. Thus, we have the following power levels for events F and H:

$$P_1^* = \frac{\gamma_{\mathrm{T}_n} (\sigma_1^2 + P_{\max} G_{12})}{G_{11}}, \quad P_2^* = P_{\max}. \tag{F.25}$$

Finally, for event J cell 1 shuts down, i.e., $P_1^* = 0$, and there is no interference. Cell 2 will then operate at maximum power if any constellation can be achieved and turned off otherwise, hence the power allocation is given as

$$P_1^* = 0, \quad P_2^* = \begin{cases} P_{\max} & \frac{P_{\max} G_{22}}{\sigma_2^2} \geq \gamma_{\mathrm{T}_1}, \\ 0 & \frac{P_{\max} G_{22}}{\sigma_2^2} < \gamma_{\mathrm{T}_1}. \end{cases} \tag{F.26}$$

Events G, I, K, which are not explicitly discussed above follow easily by symmetry.

4.3 Average Transmit Power

Starting with initial powers $P_{\max}$ at both base stations, after power control the power is reduced to P_1^* and P_2^*. Now, based on the above analysis and the events listed in Table F.1, we can derive the average per-cell transmit power $\overline{P}$ as follows:

$$\overline{P} = \frac{1}{2} \sum_{\text{event} \in \{E,\ldots,K\}} E\{P_1^* + P_2^*, \text{event}\}. \tag{F.27}$$

Starting with event E, where both cells achieve a pre-adaption SNIR $\geq \gamma_{\mathrm{T}_N}$, we have

$$E\{P_1^* + P_2^*, E\} = \int_{\gamma_{\mathrm{T}_N}}^{\infty} \int_{\gamma_{\mathrm{T}_N}}^{\infty} (P_1^* + P_2^*) f_{\gamma_1^c}(\gamma_1^c) f_{\gamma_2^c}(\gamma_2^c) \, \mathrm{d}\gamma_1^c \, \mathrm{d}\gamma_2^c, \tag{F.28}$$

where P_1^*, P_2^* are given in (F.20). Proceeding to events F and H, and using P_1^* and P_2^* from (F.25), we find

$$\begin{aligned} E\{P_1^* + P_2^*, F\} &= \sum_{n=1}^{N} P_{\max}(\gamma_{\mathrm{T}_{n+1}} + 1) \int_{\gamma_{\mathrm{T}_n}}^{\gamma_{\mathrm{T}_{n+1}}} \int_0^{\gamma_{\mathrm{T}_n}} \frac{1}{\gamma_1^c} f_{\gamma_1^c}(\gamma_1^c) f_{\gamma_2^c}(\gamma_2^c) \, \mathrm{d}\gamma_1^c \, \mathrm{d}\gamma_2^c \\ &= \sum_{n=1}^{N} P_{\max}(\gamma_{\mathrm{T}_{n+1}} + 1) F_{\gamma_2^c}(\gamma_{\mathrm{T}_n}) \int_{\gamma_{\mathrm{T}_n}}^{\gamma_{\mathrm{T}_{n+1}}} \frac{1}{\gamma_1^c} f_{\gamma_1^c}(\gamma_1^c) \, \mathrm{d}\gamma_1^c. \end{aligned} \tag{F.29}$$

$$\begin{aligned} E\{P_1^* + P_2^*, H\} &= \sum_{n=1}^{N} P_{\max}(\gamma_{\mathrm{T}_{n+1}} + 1) \int_{\gamma_{\mathrm{T}_n}}^{\gamma_{\mathrm{T}_{n+1}}} \int_{\gamma_1^c}^{\gamma_{\mathrm{T}_{n+1}}} \frac{1}{\gamma_1^c} f_{\gamma_1^c}(\gamma_1^c) f_{\gamma_2^c}(\gamma_2^c) \, \mathrm{d}\gamma_1^c \, \mathrm{d}\gamma_2^c \\ &= \sum_{n=1}^{N} P_{\max}(\gamma_{\mathrm{T}_{n+1}} + 1) \int_{\gamma_{\mathrm{T}_n}}^{\gamma_{\mathrm{T}_{n+1}}} \frac{1}{\gamma_1^c} \left(F_{\gamma_2^c}(\gamma_{\mathrm{T}_{n+1}}) - F_{\gamma_2^c}(\gamma_1^c) \right) f_{\gamma_1^c}(\gamma_1^c) \, \mathrm{d}\gamma_1^c. \end{aligned} \tag{F.30}$$

Finally, for event J, using the power levels of (F.31),

$$\begin{aligned} E\{P_1^* + P_2^*, J\} &= P_{\max} \int_{\frac{\gamma_{\mathrm{T}_1}\sigma_2^2}{\sigma_2^2 + P_{\max}G_{21}}}^{\gamma_{\mathrm{T}_1}} \int_0^{\gamma_2^c} f_{\gamma_1^c}(\gamma_1^c) f_{\gamma_2^c}(\gamma_2^c)\, \mathrm{d}\gamma_1^c\, \mathrm{d}\gamma_2^c \\ &= P_{\max} \int_{\frac{\gamma_{\mathrm{T}_1}\sigma_2^2}{\sigma_2^2 + P_{\max}G_{21}}}^{\gamma_{\mathrm{T}_1}} F_{\gamma_1^c}(\gamma_2^c) f_{\gamma_2^c}(\gamma_2^c)\, \mathrm{d}\gamma_2^c. \end{aligned} \tag{F.31}$$

4.4 Average Spectral Efficiency

Based on the mode of operation of the proposed downlink scheme and the events described in Table F.1, we are now ready to analyze the per-cell average spectral efficiency η. Recalling that the obtained constellations after power control in cell 1 and 2 are denoted by n^* and k^*, respectively, we have:

$$\eta = \frac{1}{2} \sum_{\text{event} \in \{E,\ldots,K\}} E\{n^* + k^*, \text{event}\}. \tag{F.32}$$

As in the previous subsection, we analyze the events separately, and find

$$\begin{aligned} E\{n^* + k^*, E\} &= 2N \int_{\gamma_{\mathrm{T}_N}}^{\infty} f_{\gamma_1^c}(\gamma_1^c)\, \mathrm{d}\gamma_1^c \int_{\gamma_{\mathrm{T}_N}}^{\infty} f_{\gamma_2^c}(\gamma_2^c)\, \mathrm{d}\gamma_2^c \\ &= 2N \left(1 - F_{\gamma_1^c}(\gamma_{\mathrm{T}_N})\right) \left(1 - F_{\gamma_2^c}(\gamma_{\mathrm{T}_N}\right). \end{aligned} \tag{F.33}$$

Next, for events F and H, we use γ_2^{pc} obtained by inserting $P_2 = P_{\max}$ in (F.23), to find

$$E\{n^* + k^*, \mathrm{F}\} = \sum_{n^*=1}^{N} \sum_{k^*=0}^{N} (n^* + k^*) \mathcal{I}_{n^*,k^*}^{\mathrm{F}} \tag{F.34}$$

where

$$\begin{aligned} &\mathcal{I}_{n^*,k^*}^{\mathrm{F}} = \Pr\left\{\gamma_{\mathrm{T}_{n^*}} \le \gamma_1^c < \gamma_{\mathrm{T}_{n^*+1}}, \gamma_2^c < \gamma_{\mathrm{T}_n}, \gamma_{\mathrm{T}_{k^*}} \le \gamma_2^{\mathrm{pc}} < \gamma_{\mathrm{T}_{k^*+1}}\right\} \\ &= \begin{cases} \int_{\gamma_{\mathrm{T}_{n^*}}}^{\gamma_{\mathrm{T}_{n^*+1}}} f_{\gamma_1^c}(\gamma_1^c) \left(F_{\gamma_2^c}(\min\{w, \gamma_{\mathrm{T}_n}\}) - F_{\gamma_2^c}(v)\right) \mathrm{d}\gamma_1^c, & v \le \min\{w, \gamma_{\mathrm{T}_n}\}, \\ 0, \quad \text{otherwise}, \end{cases} \end{aligned} \tag{F.35}$$

and

$$v = \gamma_{\mathrm{T}_{k^*}} \frac{\sigma_2^2 + \frac{\gamma_{\mathrm{T}_{n^*}} G_{21} P_{\max}}{\gamma_1^c}}{\sigma_2^2 + P_{\max} G_{21}}, \; w = \gamma_{\mathrm{T}_{k^*+1}} \frac{\sigma_2^2 + \frac{\gamma_{\mathrm{T}_{n^*}} G_{21} P_{\max}}{\gamma_1^c}}{\sigma_2^2 + P_{\max} G_{21}}. \tag{F.36}$$

Proceeding to event H we obtain

$$E\{n^*+k^*,H\} = \sum_{n^*=1}^{N-1}\sum_{k^*=1}^{N}(n^*+k^*)\mathcal{I}^{\mathrm{H}}_{n^*,k^*}, \tag{F.37}$$

where

$$\begin{aligned}\mathcal{I}^{\mathrm{H}}_{n^*,k^*} &= \Pr\left\{\gamma_{\mathrm{T}_{n^*}} \le \gamma_1^c < \gamma_{\mathrm{T}_{n^*+1}}, \gamma_1^c \le \gamma_2^c < \gamma_{\mathrm{T}_{n+1}}, \gamma_{\mathrm{T}_{k^*}} \le \gamma_2^{\mathrm{pc}} < \gamma_{\mathrm{T}_{k^*+1}}\right\} \\ &= \begin{cases} \int_{\gamma_{\mathrm{T}_{n^*}}}^{\gamma_{\mathrm{T}_{n^*+1}}} f_{\gamma_1^c}(\gamma_1^c)\left(F_{\gamma_2^c}(\min\{w,\gamma_{\mathrm{T}_{n+1}}\}) - F_{\gamma_2^c}(\max\{v,\gamma_1^c\})\right)\mathrm{d}\gamma_1^c, \\ \qquad\qquad \max\{v,\gamma_1^c\} \le \min\{w,\gamma_{\mathrm{T}_{n+1}}\}, \\ 0, \quad \text{otherwise}, \end{cases}\end{aligned} \tag{F.38}$$

with v, w again being found from (F.36).

Finally, for case J, we have

$$E\{n^*+k^*,J\} = \sum_{k^*=1}^{N} k^*\mathcal{I}^{\mathrm{J}}_{k^*}, \tag{F.39}$$

and

$$\begin{aligned}\mathcal{I}^{\mathrm{J}}_{n^*,k^*} &= \Pr\left\{\gamma_2^c < \gamma_{\mathrm{T}_1}, \gamma_1^c \le \gamma_2^c, \gamma_{\mathrm{T}_{k^*}} \le \gamma_2^{\mathrm{pc}} < \gamma_{\mathrm{T}_{k^*+1}}\right\} \\ &= \begin{cases} \int_0^{\gamma_{\mathrm{T}_1}} f_{\gamma_1^c}(\gamma_1^c)\left(F_{\gamma_2^c}(\min\{y,\gamma_{\mathrm{T}_1}\}) - F_{\gamma_2^c}(\max\{x,\gamma_1^c\})\right)\mathrm{d}\gamma_1^c, \\ \qquad\qquad \max\{x,\gamma_1^c\} \le \min\{y,\gamma_{\mathrm{T}_1}\}, \\ 0, \quad \text{otherwise} \end{cases}\end{aligned} \tag{F.40}$$

where

$$x = \frac{\gamma_{\mathrm{T}_{k^*}}\sigma_2^2}{\sigma_2^2 + P_{\max}G_{21}},\ y = \frac{\gamma_{\mathrm{T}_{k^*+1}}\sigma_2^2}{\sigma_2^2 + P_{\max}G_{21}}. \tag{F.41}$$

4.5 Average Number of Combined Branches

By building on the single link results from [17], we can find the average per-cell number of combined branches $\overline{B}_c$ in the downlink when using MS-GSC with a threshold of γ_{T_N}. Denote by $F^{L/i-\mathrm{GSC}}_{\gamma^c}(\cdot)$ the cdf of the combined

pre-adaptation SNIR obtained with a L/i GSC scheme. Then;

$$\begin{aligned}\overline{B}_c = 1 + \frac{1}{2}\sum_{i=1}^{L_c-1}\left(F_{\gamma_1^c}^{L/i-\mathrm{GSC}}(\gamma_{\mathrm{T}_N}) + F_{\gamma_2^c}^{L/i-\mathrm{GSC}}(\gamma_{\mathrm{T}_N})\right) \\ - \frac{L_c}{2}\Bigg(F_{\gamma_1^c}^{L/L_c-\mathrm{GSC}}(\gamma_{\mathrm{T}_1}) + F_{\gamma_2^c}^{L/L_c-\mathrm{GSC}}(\gamma_{\mathrm{T}_1}) \\ - \sum_{n=1}^{N}(\mathcal{J}_{n,1}+\mathcal{J}_{n,2}) - (\mathcal{K}_1+\mathcal{K}_2)\Bigg),\end{aligned} \tag{F.42}$$

where

$$\mathcal{J}_{n,1} = \begin{cases}\int_{\gamma_{\mathrm{T}_n}}^{\gamma_{\mathrm{T}_{n+1}}} f_{\gamma_1^c}(\gamma_1^c)\int_{v|_{k^*=1}}^{\gamma_{\mathrm{T}_1}} f_{\gamma_2^c}(\gamma_2^c),\mathrm{d}\gamma_2^c\,\mathrm{d}\gamma_1^c, & v|_{k^*=1} \le \gamma_{\mathrm{T}_1}, \\ 0, \quad \text{otherwise,}\end{cases} \tag{F.43}$$

$$\mathcal{K}_1 = \begin{cases}\int_0^{\gamma_{\mathrm{T}_1}} f_{\gamma_1^c}(\gamma_1^c)\int_{\max\{x|_{k^*=1},\gamma_1^c\}}^{\gamma_{\mathrm{T}_1}} f_{\gamma_2^c}(\gamma_2^c)\,\mathrm{d}\gamma_2^c\,\mathrm{d}\gamma_1^c, & \max\{x|_{k^*=1},\gamma_1^c\} \le \gamma_{\mathrm{T}_1} \\ 0, \quad \text{otherwise,}\end{cases} \tag{F.44}$$

and v, x are given in (F.36) and (F.41), respectively. Note that $\mathcal{J}_{n,1}$ represents the probability that in the downlink of cell 2 a pre-adaptation SNIR below γ_{T_1} is achieved, and where the power control leads to an inreased SNIR in cell 2 such that transmission with a constellation $k^* \ge 1$ is possible, while the mobile in cell 1 can receive a constellation of size n. Similarly, for pre-adaptation SNIRs $\gamma_1^c \le \gamma_2^c < \gamma_{\mathrm{T}_1}$, $\mathcal{K}_1$ is the probabilty that the power control makes it feasible for the base station in cell 2 to transmit using constellation $k^* \ge 1$. The corresponding expressions for $\mathcal{J}_{n,2}$ and $\mathcal{K}_2$ are easily derived by symmetry.

Before we proceed we note that the power control applied for uplink transmission can be applied a posteriori also in the downlink setting to facilitate less sum transmitted power. And finally, that even though the schemes are presented in, and primarily motivated for, either a downlink or uplink scenario, they are interchangeable, e.g., the spectral efficiency increasing downlink scheme may well be applied also for uplink.

5 Numerical results

To accurately model an interference-dominated cellular system we follow the spatial channel model for use in system level simulations developed by the 3GPP-3GPP2 working group [18], using the parameters listed in Table F.2, and taking the pre-adaptation SNIR to be identically distributed

Table F.2: Cellular System Parameters

Scenario	Urban Microcell
Cell layout	Hexagonal
Carrier frequency	1900 MHz
$P_{\max}$	1 W
BS to BS distance	1000 m
Operating temperature	290 Kelvin
Equiv. noise BW	100 KHz

across cells. To better evaluate the proposed schemes, we will benchmark them against some reference schemes. These are briefly explained Sections 5.1 and 5.2 below, with the necessary mathematical details provided in the Appendix.

In the following numerical examples, for the downlink scenario, we set the number of available diversity branches $L = 3$, and the maximum number of combined branches $L_c = 2$. For uplink transmission, we assume $L = 5$ and $L_c = 4$. Common for both up- and downlink is that the number of signal constellations $N = 4$, i.e., the signal constellations are 2-QAM (BPSK), 4-QAM, 8-QAM, and 16-QAM, and finally a bit error rate constraint of $\text{BER}_0 = 10^{-3}$.

5.1 Average Spectral Efficiency and Number of Combined Branches

By means of (F.15) and (F.32), we plot the average spectral efficiency as a function of the average pre-adaptation SNIR, as shown in Fig. F.4. As expected the ASE increases with the average pre-adaptation SNIR, and saturates at 4 bits/s/Hz/cell, corresponding to utilizing, in each cell, 16-QAM with a probability close to 1. In Fig. F.4b, we have also plotted the ASE of a reference scheme (F.45), employing MS-GSC, but without a spectral efficiency increasing power control. It is seen that introducing power control improves the spectral efficiency over the entire pre-adaptation SNIR range. The ASE gain is most pronounced for low SNIRs, which is due to the fact that when none of the cells can achieve a pre-adaptation SNIR above γ_{T_1}, the power control considers the possibility of having only one cell on.

Turning to the average number of combined branches, from Fig. F.5 the proposed uplink scheme using GSC always combines $L_c = 4$ branches,

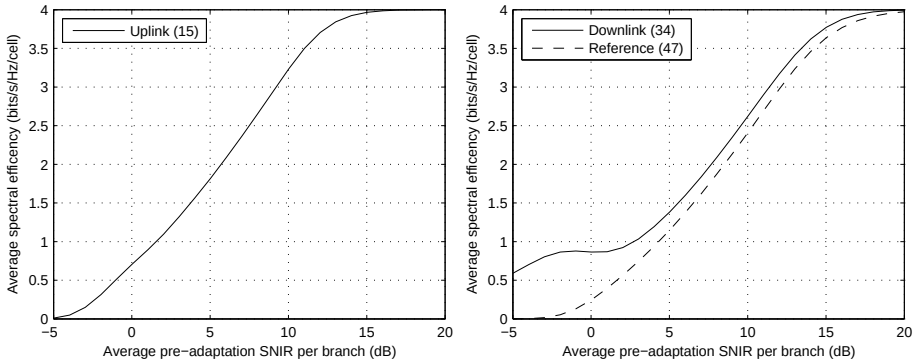

(a) Uplink (b) Downlink

Figure F.4: Average spectral efficiency per cell versus the average pre-adaptation SNIR per branch.

while the downlink scheme benefits from the MS-GSC combining. Comparing the proposed downlink scheme to the reference scheme we see that the increased spectral efficiency comes at a price of a higher number of combined branches at low SNIR. Since every branch need a separate processing chain, the average number of combined branches is roughly proportional to the receiver processing power, and thus there is a spectral efficiency versus processing power trade-off.

5.2 Average Transmit Power

Fig. F.6 depicts the average normalized per-cell transmit power, $\frac{\overline{P}}{P_{\max}}$, versus the average SNIR per branch. For both uplink and downlink, we will compare the transmit power consumption to two benchmark schemes: i) the *on/off* scheme (F.47), which transmits with full power in a cell as long as the pre-adaptation SNIR level is above γ_{T_1}, and ii) the *extended single-cell* scheme (F.49), denoted Ex. s-c in Fig. F.6, which is an extended version of the single-cell continuous power control scheme developed and analyzed in [10], where the extension is to use the scheme in each cell without centralized coordination.

In the uplink scenario, from Fig. F.6a, we see that compared to both the proposed scheme and extended single-cell, the coordinated scheme proposed in the present paper provides an extensive reduction of transmitted power. Further, it is clear that when allowing for coordinated power control, we obtain an additional significant reduction over the non-coordinated

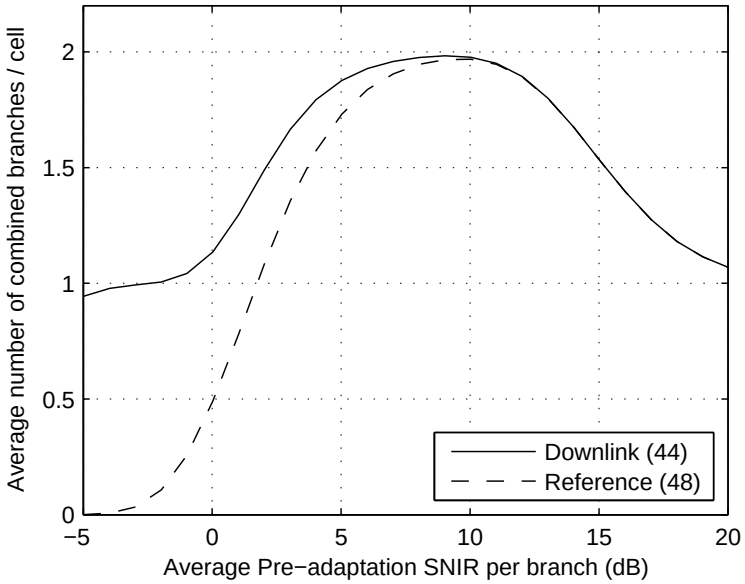

Figure F.5: Average per cell number of combined branches versus the average pre-adaptation SNIR per branch.

scheme. These gains can be explained as follows: The non-coordinated scheme must always assume worst case interference from both cells, and adjust its power levels to facilitate the chosen constellations under such conditions; on the other hand for the coordinated scheme, power control can be done in collaboration, thus opening a door to further savings.

For low pre-adaptation SNIRs in a downlink transmission setting, the situation is different. Indeed, Fig. F.6b shows that the proposed downlink scheme uses more transmitted power than both reference schemes, thus explaining the spectral efficiency gains already seen in Fig F.4b. In this SNIR range, the normalized per-cell average transmit power $\frac{\overline{P}}{P_{\max}} \approx \frac{1}{2}$, corresponding to operating one out of two cells at a maximum power $P_{\max}$, in agreement with (F.26). As the channel state improved, i.e., in the medium to high-SNIR range, the proposed downlink scheme uses significantly less transmit power than both reference schemes, while still providing a higher spectral efficiency.

In both up- and downlink scenarios, it should be noted that the difference between the coordinated scheme over the non-coordinated is due to the presence of co-channel interference; without such interference both schemes would perform identically.

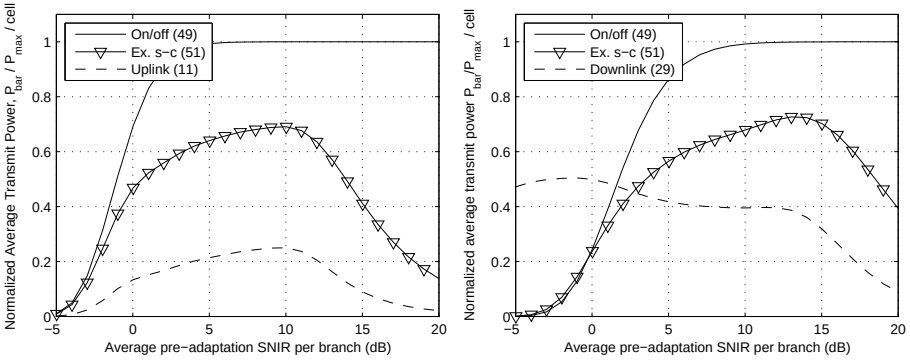

(a) Uplink (b) Downlink

Figure F.6: Normalized average transmit power for the proposed scheme using coordination (Cord.) versus average pre-adaptation SNIR. The cases of on/off power control and the continuous power control without coordination are shown for reference.

6 Conclusions

We have investigated joint adaptive modulation, diversity combining, and power control in a dynamic frequency reuse two-cell network. Specifically, we have introduced and analyzed two practical bandwidth and battery-power efficient schemes that attack the challenges faced in up- and downlink transmission, respectively. The schemes jointly determine the signal constellation, diversity combining structure, and power levels based on coordination between the transmitters, and on the channel state. For both schemes, we detailed the mode of operation, and through a mathematical analysis we quantified the key performance indicators: spectral efficiency, transmit power and number of combined branches.

Our results show that there is a tradeoff between the combiner complexity, transmit power and the spectral efficiency. Comparing to reference schemes, we demonstrated that the novel uplink scheme yields a significant reduction in average transmit power, thus extending the battery lifetime, and decreasing the level of interference to co-existing systems and cells, while upholding spectral efficiency. Taking into account the power consumption from diversity combining, the proposed downlink transmission scheme uses power control to provide a significant increase of spectral efficiency compared to a reference scheme, while achieving a low combiner complexity.

For systems of more than two cells, we can apply the results presented

in this paper by clustering groups of two cells, over which optimization would be effected. An interesting direction of research would also be to search for distributed algorithms realizing some or all of the coordination gains without the need for centralized control.

Appendix - Reference Schemes

In this appendix we provide the describing equations of some reference schemes used for benchmarking the proposed up- and downlink schemes.

6.1 Average Spectral Efficiency and Number of Combined Branches

Consider a two-cell scenario with downlink transmission and MS-GSC diversity combining, allowing to combine a maximum of L_c from L available branches, but without power control. Then, extending the results of [17], we find that the average spectral efficiency is given by

$$\eta = N - \frac{1}{2}\sum_{n=1}^{N}\left(F_{\gamma_1^c}^{\mathrm{MSC}(\gamma_{\mathrm{T}_N})}(\gamma_{\mathrm{T}_n}) + F_{\gamma_2^c}^{\mathrm{MSC}(\gamma_{\mathrm{T}_N})}(\gamma_{\mathrm{T}_n})\right). \tag{F.45}$$

Similarly, the average per-cell number of combined branches is found as

$$\begin{aligned}\overline{B}_c = 1 &+ \frac{1}{2}\sum_{i=1}^{L_\mathrm{c}-1}\left(F_{\gamma_1^c}^{L/i-\mathrm{GSC}}(\gamma_{\mathrm{T}_N}) + F_{\gamma_2^c}^{L/i-\mathrm{GSC}}(\gamma_{\mathrm{T}_N})\right)\\ &- \frac{L_\mathrm{c}}{2}\left(F_{\gamma_1^c}^{L/L_\mathrm{c}-\mathrm{GSC}}(\gamma_{\mathrm{T}_1}) + F_{\gamma_2^c}^{L/L_\mathrm{c}-\mathrm{GSC}}(\gamma_{\mathrm{T}_1})\right).\end{aligned} \tag{F.46}$$

6.2 Transmit Power

To evaluate the transmit power consumption of the proposed schemes, we will find the following two reference schemes useful. First, the *on/off power control* scheme which transmits with full power in a cell as long as the pre-adaptation SNIR level is above γ_{T_1}, yielding an average per-cell transmit power $\overline{P}_{\mathrm{On/off}}$ of

$$\overline{P}_{\mathrm{On/off}} = \frac{P_{\max}}{2}\left(\int_{\gamma_{\mathrm{T}_1}}^{\infty} f_{\gamma_1^c}(\gamma_1^c)\,\mathrm{d}\gamma_1^c + \int_{\gamma_{\mathrm{T}_1}}^{\infty} f_{\gamma_2^c}(\gamma_2^c)\,\mathrm{d}\gamma_2^c\right). \tag{F.47}$$

Second, we will compare the proposed scheme to an extended version of the single-cell continuous power control scheme given in [10], where the

extension is to use the scheme in each cell without centralized coordination. Given pre-adaptation SNIRs above γ_{T_1}, constellations n, k are selected, and by using power control the following power level are obtained

$$P_1^* = \frac{\gamma_{\mathrm{T}_n}(\sigma_1^2 + P_{\max} G_{21})}{G_{11}}, \quad P_2^* = \frac{\gamma_{\mathrm{T}_k}(\sigma_2^2 + P_{\max} G_{12})}{G_{22}}. \tag{F.48}$$

Using (F.48), we can then derive the average transmit power $\overline{P}_{\text{Ex. s-c}}$ as follows:

$$\overline{P}_{\text{Ex. s-c}} = \frac{1}{2} \sum_{n=1}^{N} \Big(\int_{\gamma_{\mathrm{T}_n}}^{\gamma_{\mathrm{T}_{n+1}}} P_1^* f_{\gamma_1^c}(\gamma_1^c)\, \mathrm{d}\gamma_1^c + \int_{\gamma_{\mathrm{T}_n}}^{\gamma_{\mathrm{T}_{n+1}}} P_2^* f_{\gamma_2^c}(\gamma_2^c)\, \mathrm{d}\gamma_2^c \Big). \tag{F.49}$$

References

[1] M.-S. Alouini and A. J. Goldsmith, "Adaptive modulation over Nakagami fading channels," *Kluwer J. Wireless Communications*, vol. 13, pp. 119–143, May 2000.

[2] K. J. Hole, H. Holm, and G. E. Øien, "Adaptive multidimensional coded modulation over flat fading channels," *IEEE Journal on Selected Areas in Communications*, vol. 18, no. 7, pp. 1153–1158, July 2000.

[3] A. Gjendemsjø, G. E. Øien, and P. Orten, "Optimal discrete-level power control for adaptive coded modulation schemes with capacity-approaching component codes," in *Proc. IEEE International Conference on Communications*, Istanbul, Turkey, June 2006, pp. 5047–5052.

[4] D. Gesbert, S. G. Kiani, A. Gjendemsjø, and G. E. Øien, "Adaptation, coordination and distributed resource allocation in interference-limited wireless networks," *Proc. of the IEEE, Special Issue on Adaptive Transmission*, (Invited Paper), to appear Dec. 2007. [Online]. Available: http://www.iet.ntnu.no/~gjendems/publications/

[5] T. Eng, N. Kong, and L. B. Milstein, "Comparison of diversity combining techniques for Rayleigh fading channels," *IEEE Transactions on Communications*, vol. 44, pp. 1117–1129, Sept. 1996.

[6] M.-S. Alouini and M. K. Simon, "An MGF-based performance analysis of generalized selection combining over Rayleigh fading channels," *IEEE Transactions on Communications*, vol. 48, no. 3, pp. 401–415, March 2000.

[7] M. K. Simon and M.-S. Alouini, *Digital Communication over Fading Channels*, 2nd ed. Wiley-IEEE Press, 2005.

[8] N. Belhaj, M.-S. Alouini, and K. A. Qaraqe, "Minimum selection GSC with down-link power control," in *Proc. IEEE Vehicular Technology Conference*, Melbourne, Australia, May 2006, pp. 1821–1825.

[9] S. S. Nam, M.-S. Alouini, and K. A. Qaraqe, "Diversity combining with up-link power control," in *Proc. IEEE International Symposium on Personal, Indoor and Mobile Radio Communications*, Helsinki, Finland, Sept. 2006, pp. 1–5.

[10] A. Gjendemsjø, H.-C. Yang, G. E. Øien, and M.-S. Alouini, "Minimum selection GSC with adaptive modulation and post-combining power control," in *Proc. IEEE Wireless Communications and Networking Conference*, Hong Kong, China, March 2007, pp. 2006 –2011.

[11] J. H. Winters, "Optimum combining in digital mobile radio with cochannel interference," *IEEE Journal on Selected Areas in Communications*, vol. SAC-2, no. 4, pp. 528–539, July 1984.

[12] S. W. Kim, D. S. Ha, and J. Reed, "Minimum selection GSC and adaptive low-power RAKE combining scheme," in *Proc. IEEE International Symposium on Circuits and Systems*, Bangkok, Thailand, May 2003, pp. 357–360.

[13] P. Gupta, N. Bansal, and R. K. Mallik, "Analysis of minimum selection H-S/MRC in Rayleigh fading," *IEEE Transactions on Communications*, vol. 53, no. 5, pp. 780–784, May 2005.

[14] R. K. Mallik, P. Gupta, and Q. T. Zhang, "Minimum selection GSC in independent Rayleigh fading," *IEEE Transactions on Vehicular Technology*, vol. 54, no. 3, pp. 1013–1021, May 2005.

[15] H.-C. Yang, "New results on ordered statistics and analysis of minimum-selection generalized selection combining (GSC)," *IEEE Transactions on Wireless Communications*, vol. 5, no. 7, pp. 1876–1885, July 2006.

[16] M. Andrews, K. Kumaran, K. Ramanan, A. Stoylar, P. Whiting, and R. Vijayakumar, "Providing quality of service over a shared wireless link," *IEEE Communications Magazine*, vol. 39, no. 2, pp. 150–154, Feb. 2001.

[17] H.-C. Yang, N. Belhaj, and M.-S. Alouini, "Performance analysis of joint adaptive modulation and diversity combining over fading channels," *IEEE Transactions on Communications*, vol. 55, no. 3, pp. 520–528, March 2007.

[18] Spatial Channel Model AHG, "Spatial channel model text description," 3GPP-3GPP2, Tech. Rep., 2003.